ELECTRONIC SUPPORTING INFORMATION

The effect of alcohols as vehicles on the percutaneous absorption and skin retention of ibuprofen modified with L-valine alkyl esters

Paula Ossowicz[a], Joanna Klebeko[a], Ewa Janus[a], Anna Nowak[b], Wiktoria Duchnik[b], Łukasz Kucharski[b], and Adam Klimowicz[b]*

[a] West Pomeranian University of Technology, Szczecin, Faculty of Chemical Technology and Engineering, Department of Chemical Organic Technology and Polymeric Materials, Piastów Ave. 42, 71-065 Szczecin, Poland
[b] Pomeranian Medical University in Szczecin, Department of Cosmetic and Pharmaceutical Chemistry, Powstańców

**Corresponding author at: West Pomeranian University of Technology, Piastów Ave. 42, 71-065 Szczecin, Poland, Tel: +48914494801. E-mail: possowicz@zut.edu.pl;*

Number of pages: 58

Number of figures: 65

Number of tables: 7

Table of Contents

SPECTRAL ANALYSIS, IDENTIFICATION & CHARACTERISATION OF COMPOUNDS

L-VALINE ALKYL ESTER HYDROCHLORIDES

Table S1. Amounts of substrates and yields of synthesis of L-valine alkyl ester hydrochlorides (ValOR·HCl)

No.	Compound	Substrate		Product		
		Amino acid [g]	TMSCl [mL]	L-ValOR·HCl [g]	Yield [%]	State
1	ValOMe·HCl	5.17	11.20	7.29	98	white solid
2	ValOHept·HCl	5.34	11.56	10.47	91	white solid
3	ValOOkt·HCl	5.47	11.85	11.06	89	white solid

ValOMe·HCl– L-valine methyl ester hydrochloride

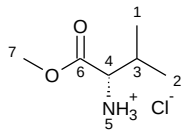

Compound was obtained according general procedure and the reaction yielded 7.29 g of ValOMe·HCl (98.5%) as white solid. **^{1}H NMR** (400 MHz, $CDCl_3$) δ in ppm: 8.82 (s, 3H, H5); 3.99 (d, 1H, $J_{4,3}$=4.9 Hz, H4); 3.83 (s, 3H, H7); 2.46-2.50 (m, 1H, H3); 1.14 (dd, 6H, H2, H1); **^{13}C NMR** (100 MHz, $CDCl_3$) δ in ppm: 168.92 (C6); 58.64 (C4); 52.93 (C7); 29.87 (C3); 18.45 (C2) 18.29 (C1); **FT-IR**: ν (ATR): 2969; 2886; 2675; 1739; 1699; 1679; 1592; 1504; 1465; 1437; 1399; 1378; 1355; 1293; 1241; 1158; 1140; 1070; 1020; 975; 928; 880; 770; 753; 664; 520; 480; 426 cm^{-1}; **UV-Vis** (EtOH): λ_{max}= 202.4 nm; **Elemental analysis:** Calc. (%) for $C_6H_{14}NO_2Cl$ (167.640 g/mol) C (42.99), H (8.42), N (8.36), O (19.09), Found C (42.90), H -(8.38), N (8.35), O (19.09); $\mathbf{T_m}$=164.8-172.4ºC; $[\boldsymbol{\alpha}]_{\boldsymbol{D}}^{\mathbf{20}}$ = +24.628 (c=0.605 g/100 cm^3 EtOH).

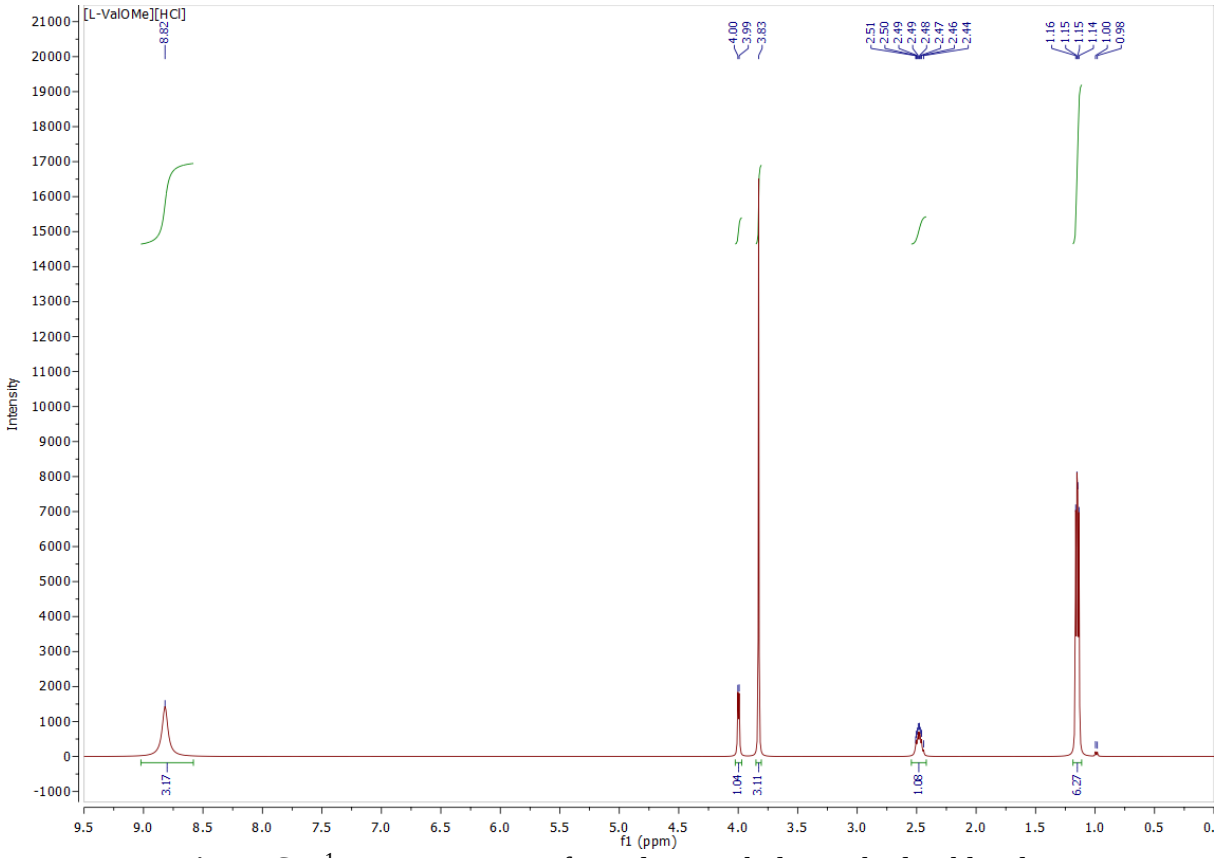

Figure S1. ^{1}H NMR spectra of L-valine methyl ester hydrochloride

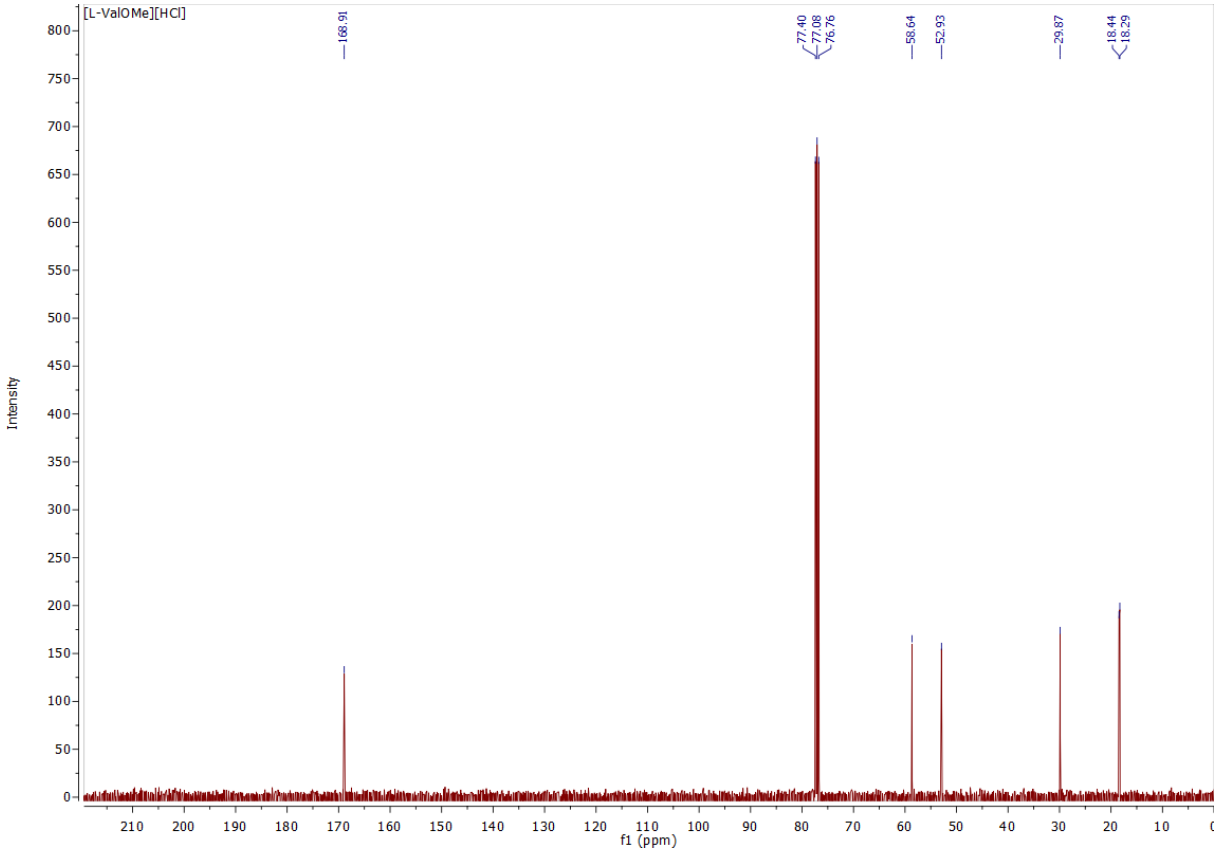

Figure S2.^{13}C NMR spectra of L-valine methyl ester hydrochloride

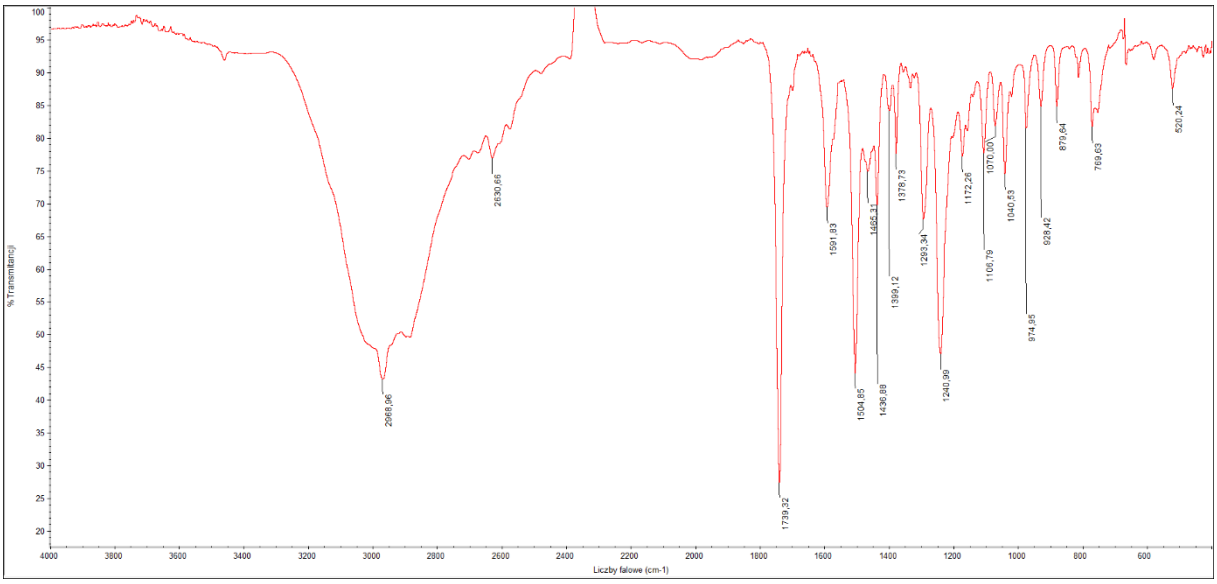

Figure S3. FTIR spectra of L-valine methyl ester hydrochloride

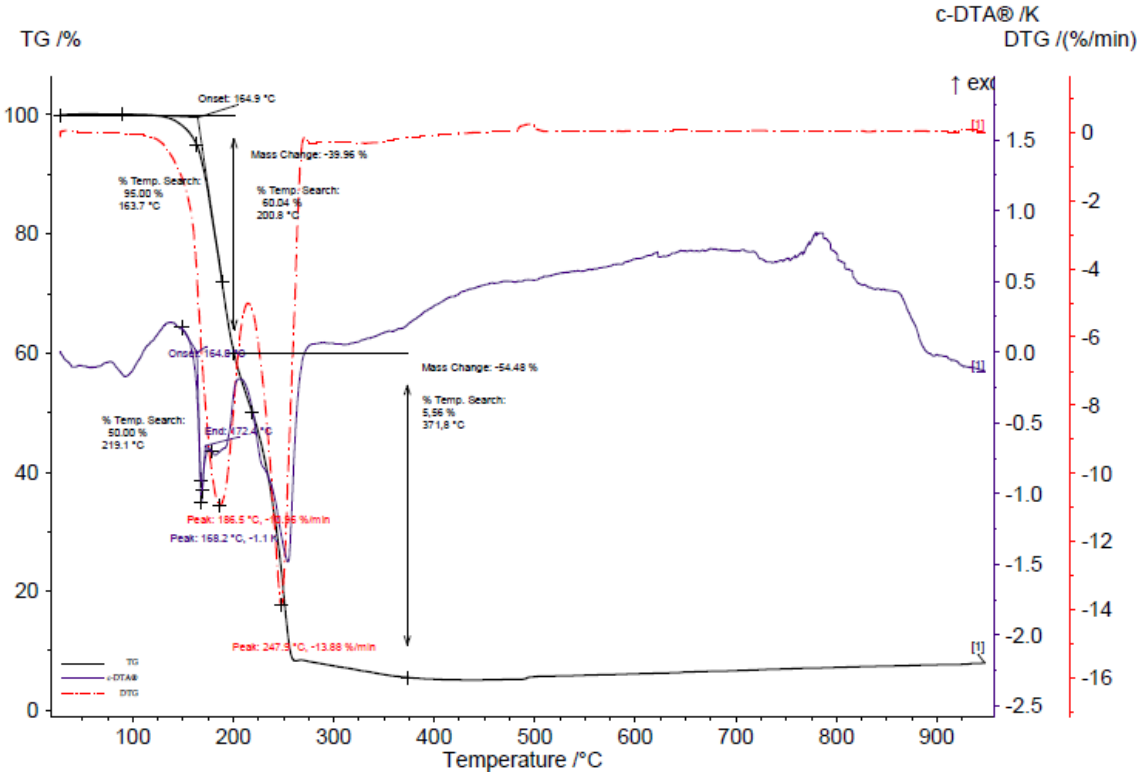

Figure S4. The TG, DTG and c-DTA curves of L-valine methyl ester hydrochloride

ValOHept·HCl – L-valine heptyl ester hydrochloride

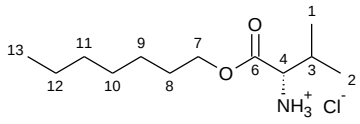

The compound was obtained according to general procedure and the reaction yielded 10.47 g of ValOHept·HCl (91.0%) as yellow solid. **^{1}H NMR** (400 MHz, $CDCl_3$) δ in ppm: 8.76 (s, 3H, H5); 4.13-4.27 (m, 2H, H7); 3.96 (d, 1H, $J_{4,3}$=3.9 Hz, H4); 2.44-2.52 (m, 1H, H3); 1.60-1.71 (m, 2H, H8); 1.28-1.38 (m, 8H, H9, H10, H11, H12); 1.15 (dt, 6H, H13, H2); 0.88 (t, 3H, H1 $J_{1,3}$=6.9); **^{13}C NMR** (100 MHz, CDCl3) δ in ppm: 168.50 (C6); 66.42 (C4); 58.52 (C7); 31.65 (C3); 29.88 (C8); 28.81 (C9); 28.38 (C10); 25.73 (C11); 22.54 (C12); 18.41 (C2); 18.23 (C1); 14.02 (C13); **FT-IR**: ν (ATR): 2952; 2924; 2898; 2856; 2703; 2675; 2611; 2577; 2038; 1731; 1695; 1586; 1574; 1508; 1465; 1417; 1397; 1378; 1352; 1340; 1325; 1288; 1274; 1252; 1232; 1210; 1170; 1107; 1042; 996; 985; 963; 923; 904; 864; 844; 808; 760; 722; 703; 665; 536; 514; 473; 436; 411 cm^{-1}; **UV-Vis** (EtOH): λ_{max}= 204.9 nm; **Elemental analysis:** Calc. (%) for $C_{12}H_{26}NO_2Cl$ (251.796 g/mol) C (57.24), H (10.41), N (5.63), O (12.71), Found C (57.60), H (10.38), N (5.64), O (13.29); $[\boldsymbol{\alpha}]_{\boldsymbol{D}}^{\boldsymbol{20}}$ = +9.933 (c=0.594 g/100 cm^3 EtOH).

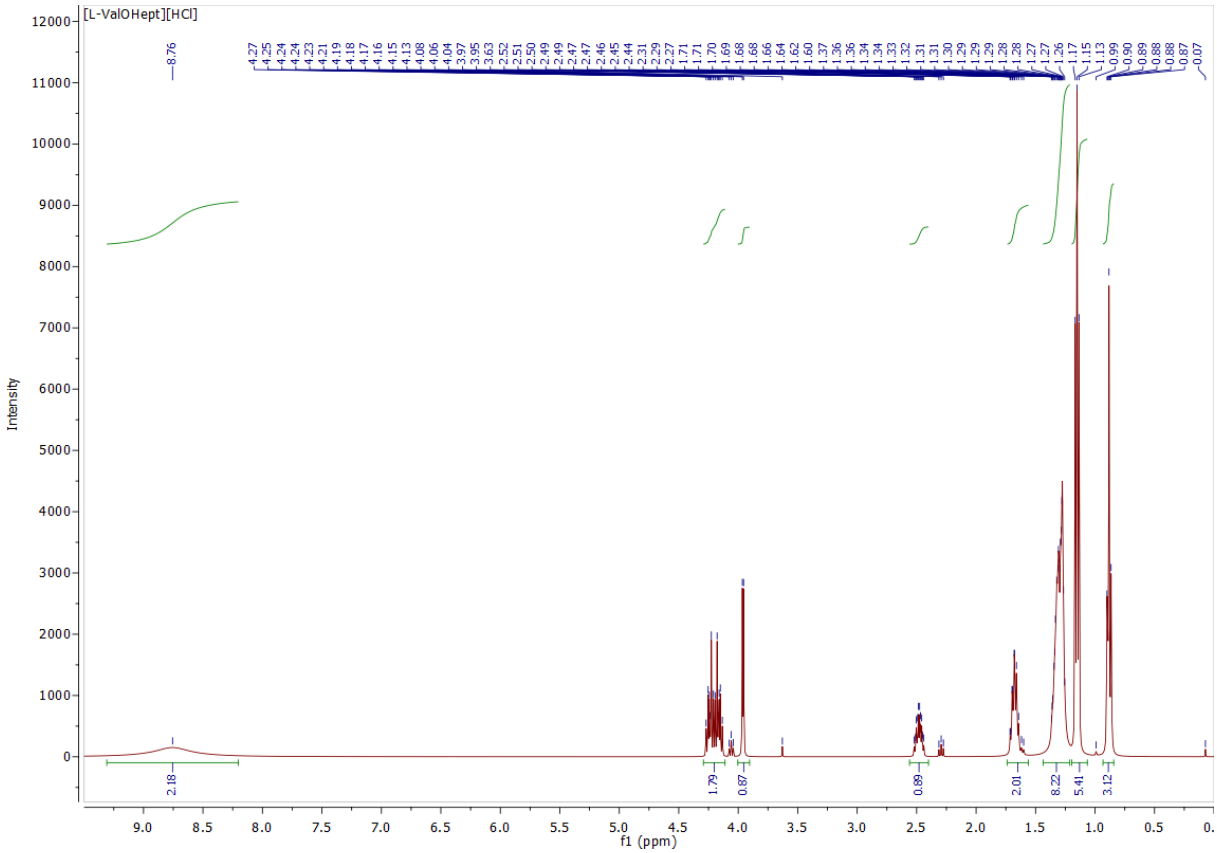

Figure S5. ^{1}H NMR spectra of L-valine heptyl ester hydrochloride

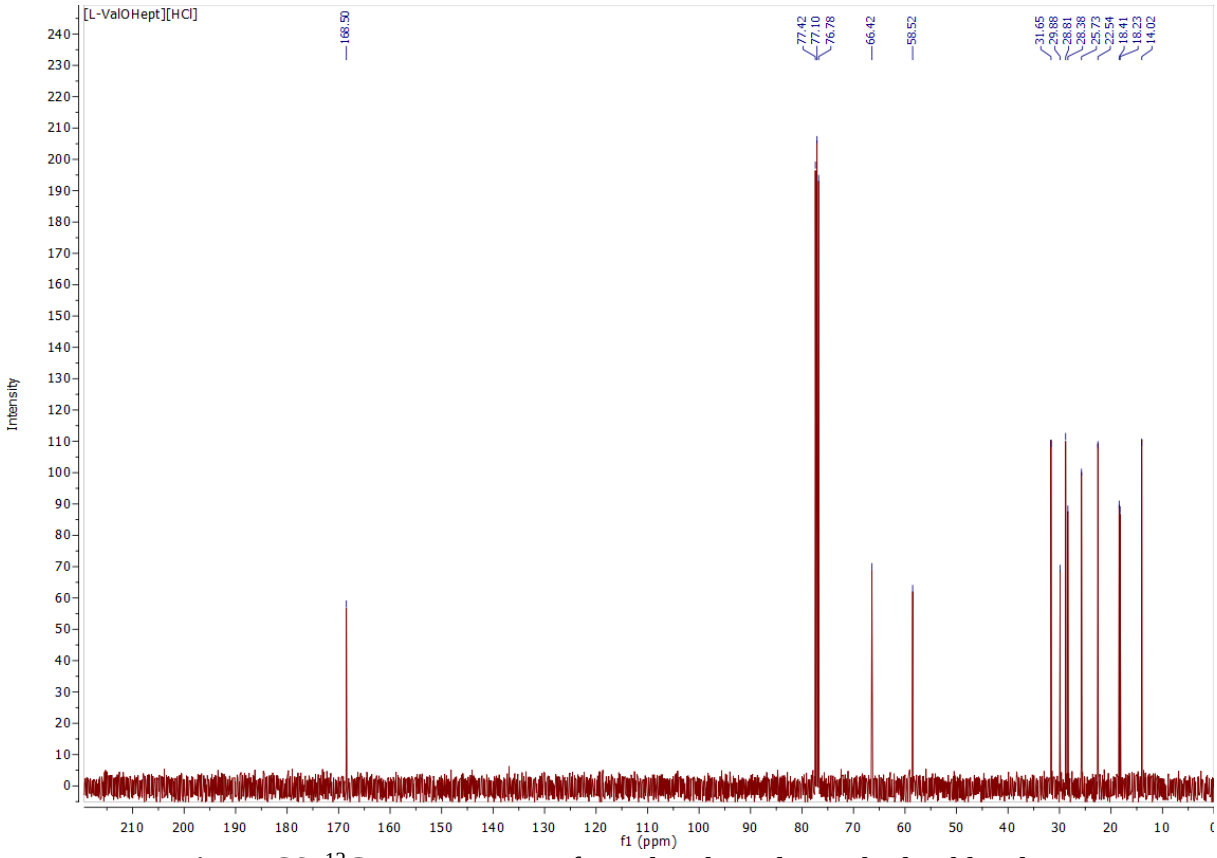

Figure S6. ^{13}C NMR spectra of L-valine heptyl ester hydrochloride

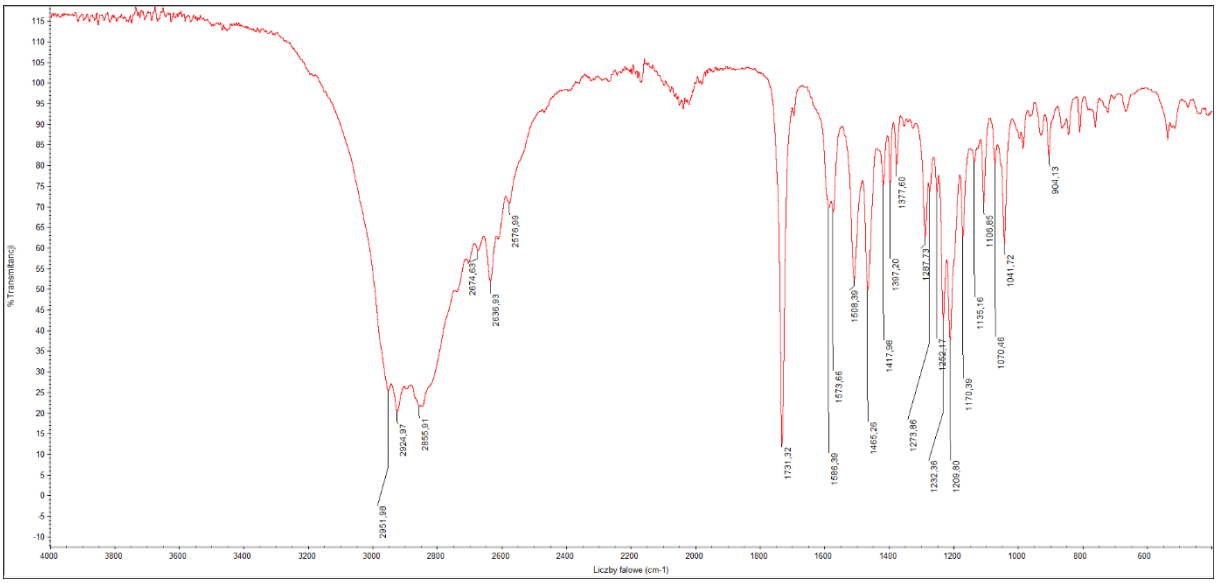

Figure S7. FTIR spectra of L-valine heptyl ester hydrochloride

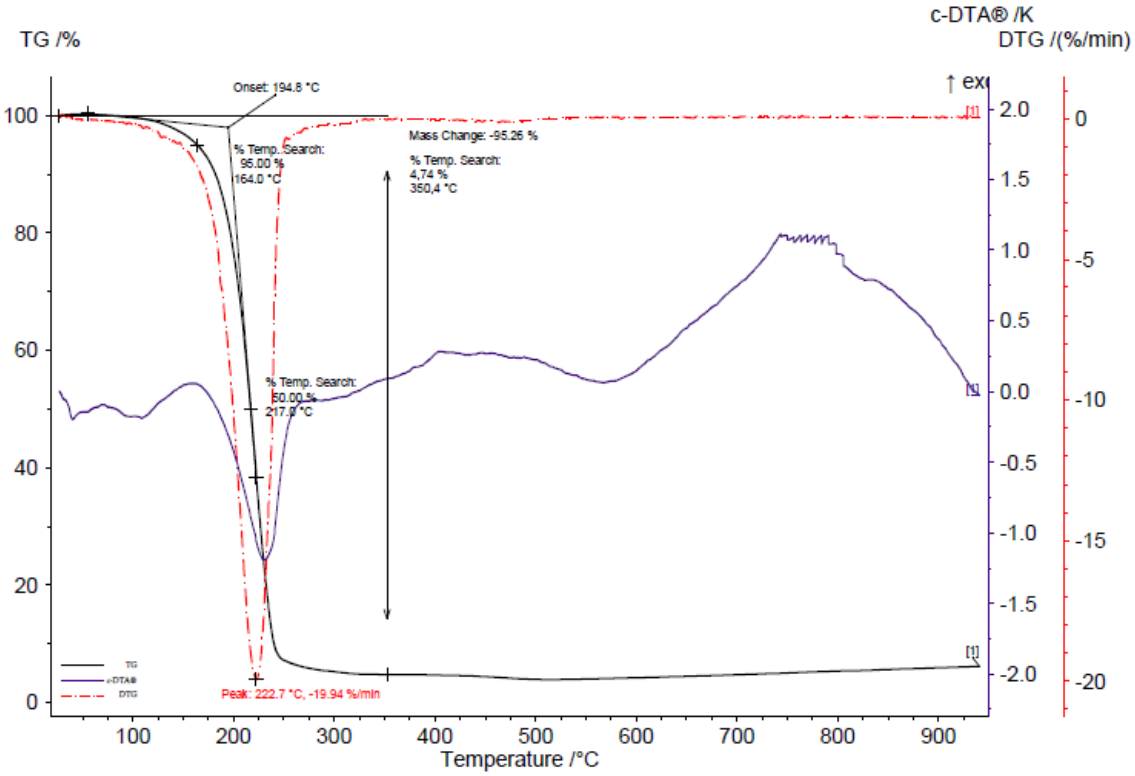

Figure S8. The TG, DTG and c-DTA curves of L-valine heptyl hydrochloride

ValOOct·HCl – L-valine octyl ester hydrochloride

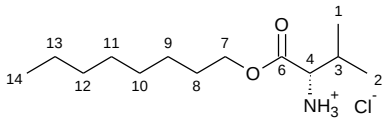

The compound was obtained according to general procedure and the reaction yielded 11.06 g of ValOOct·HCl (89.2%) as white solid. **^{1}H NMR** (400 MHz, $CDCl_3$) δ in ppm: 8.42 (s, 3H, H5); 4.13-4.27 (m, 2H, H7); 3.95 (d, 1H, $J_{4,3}$=3.9 Hz, H4); 2.46-2.52 (m, 1H, H3); 1.64-1.71 (m, 2H, H8); 1.27-1.36 (m, 10H, H9, H10, H11, H12); 1.15(dt, 6H, H2, H13); 0.88 (t, 3H, $J_{1,3}$=6.9 Hz, H1); **^{13}C NMR** (100 MHz, $CDCl_3$) δ in ppm: 168.53 (C6); 66.41 (C4); 58.53 (C7); 31.74 (C3); 29.90 (C8); 29.13 (C9); 29.10 (C10); 28.38 (C11); 25.78 (C12); 22.60 (C13); 18.41 (C2); 18.25 (C1); 14.07 (C14); **FT-IR**: ν (ATR): 2952; 2925; 2853; 2638; 2042; 1733; 1697; 1587; 1572; 1512; 1466; 1417; 1397; 1353; 1287; 1225; 1207; 1170; 1135; 1107; 1071; 1041; 990; 958; 939; 911; 878; 807; 777; 723; 666; 537; 519; 473; 443; 422; 411 cm^{-1}; **UV-Vis** (EtOH): λ_{max}= 211.8 nm; **Elemental analysis:** Calc. (%) for $C_{13}H_{28}NO_2Cl$ (265.823 g/mol) C (58.74), H (10.62), N (5.27), O (12.04), Found C (58.79), H (10.67), N (5.60), O (12.00); **T_m**=70.9-80.4ºC; $[\alpha]_D^{20}$ = +12.035 (c=0.565 g/100 cm^3 EtOH).

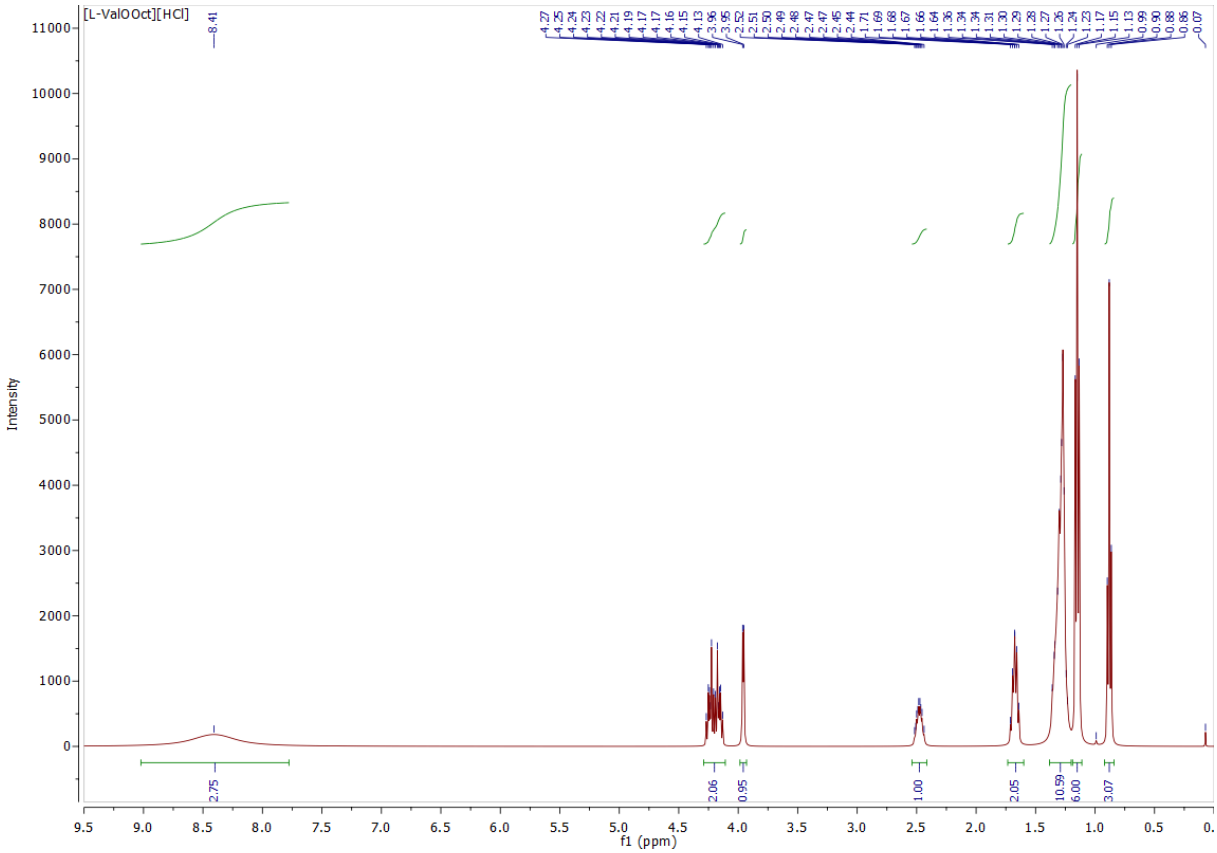

Figure S9. ^{1}H NMR spectra of L-valine octyl ester hydrochloride

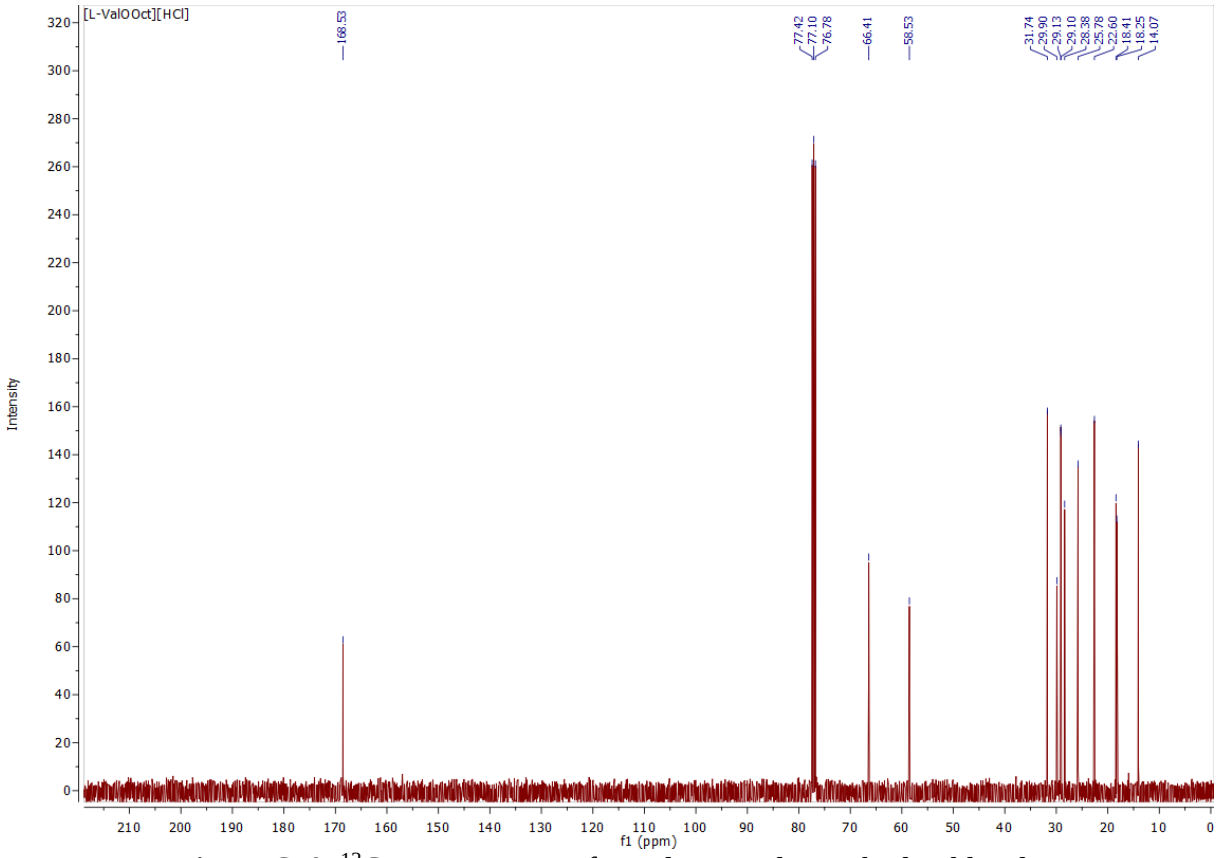

Figure S10. ^{13}C NMR spectra of L-valine octyl ester hydrochloride

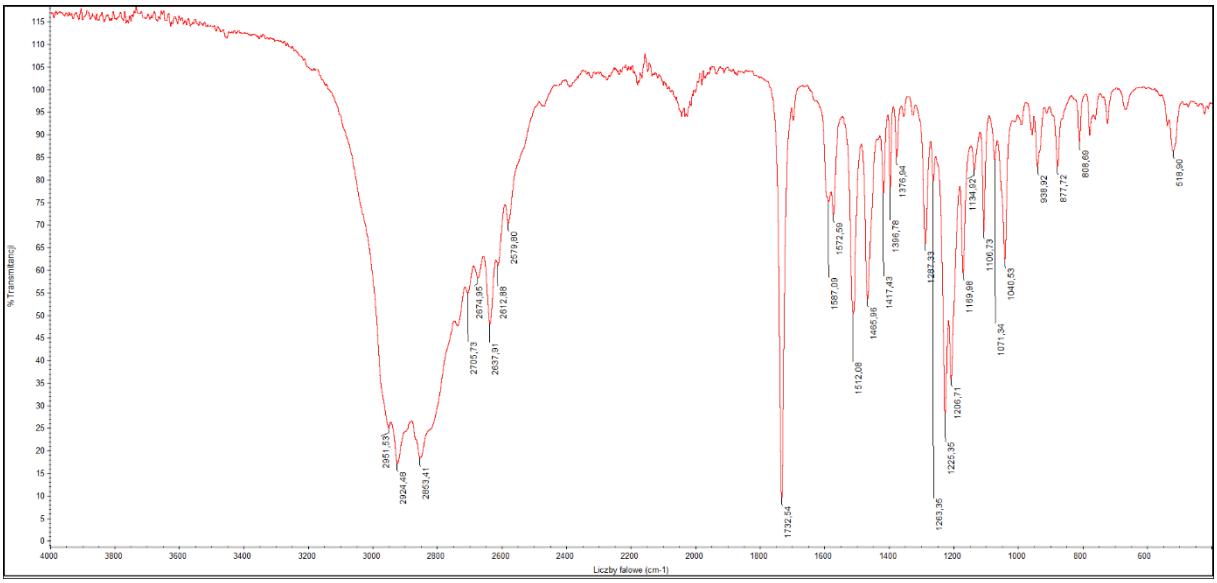

Figure S11. FTIR spectra of L-valine octyl ester hydrochloride

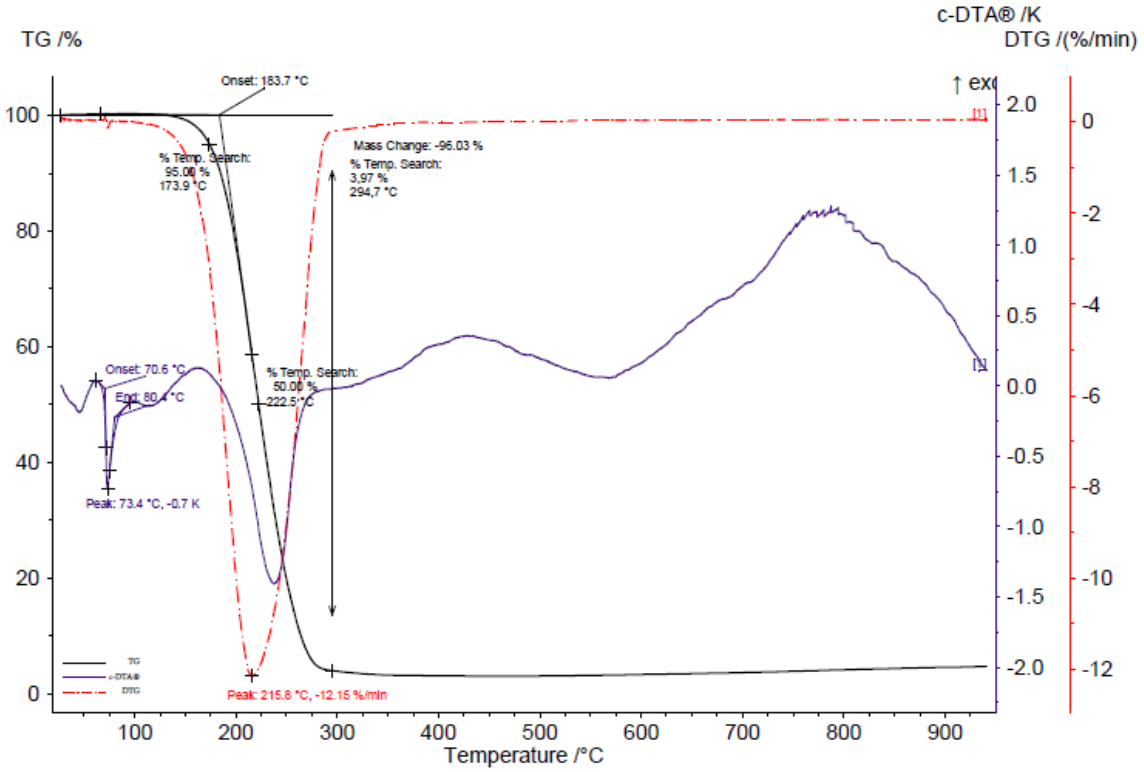

Figure S12. The TG, DTG and c-DTA curves of L-valine octyl hydrochloride

L-VALINE ALKYL ESTER

Table S2. Amounts of substrates and yields of synthesis of L-valine alkyl esters (L-ValOR)

No.	Compound	Substrate		Product		
		L-ValOR·HCl [g]	25% $NH_3 \cdot H_2O$ [mL]	L-ValOR [g]	Yield [%]	State
1	ValOMe	1.17	3.02	0.76	84	yellow liquid
2	ValOHept	1.08	1.86	0.68	74	yellow liquid
3	ValOOkt	1.27	1.94	0.80	73	yellow liquid

[ValOMe]– L-valine methyl ester

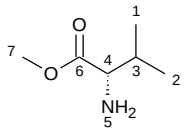

The compound was obtained according to general procedure and the reaction yielded 0.76 g of ValOMe (83.5%) as a yellow liquid. **^{1}H NMR** (400 MHz, $CDCl_3$) δ in ppm: 3.72 (s, 3H, H7); 3.30 (d, 1H, $J_{4,3}$=4.9 Hz, H4); 1.99-2.04 (m, 1H, H3); 1.52 (s, 2H, H5); 0.98 (d, 3H, $J_{2,3}$=6.9 Hz, H2); 0.91 (d, 3H, $J_{1,3}$=6.8 Hz, H1); **^{13}C NMR** (100 MHz, $CDCl_3$) δ in ppm: 175.89 (C6); 59.78 (C4); 51.53 (C7); 32.01 (C3); 19.12 (C2) 17.06 (C1); **FT-IR**: ν (ATR): 3439; 3429; 2960; 2934; 2874; 1731; 1604; 1466; 1436; 1388; 1369; 1339; 1280; 1225; 1194; 1170; 1083; 1050; 903; 842; 817; 765; 752; 719 cm^{-1}; **UV-Vis** (EtOH): λ_{max}= 203.9 nm; $[\boldsymbol{\alpha}]_{\boldsymbol{D}}^{\boldsymbol{20}}$ = +52.000 (c=0.550 g/100 cm^3 EtOH).

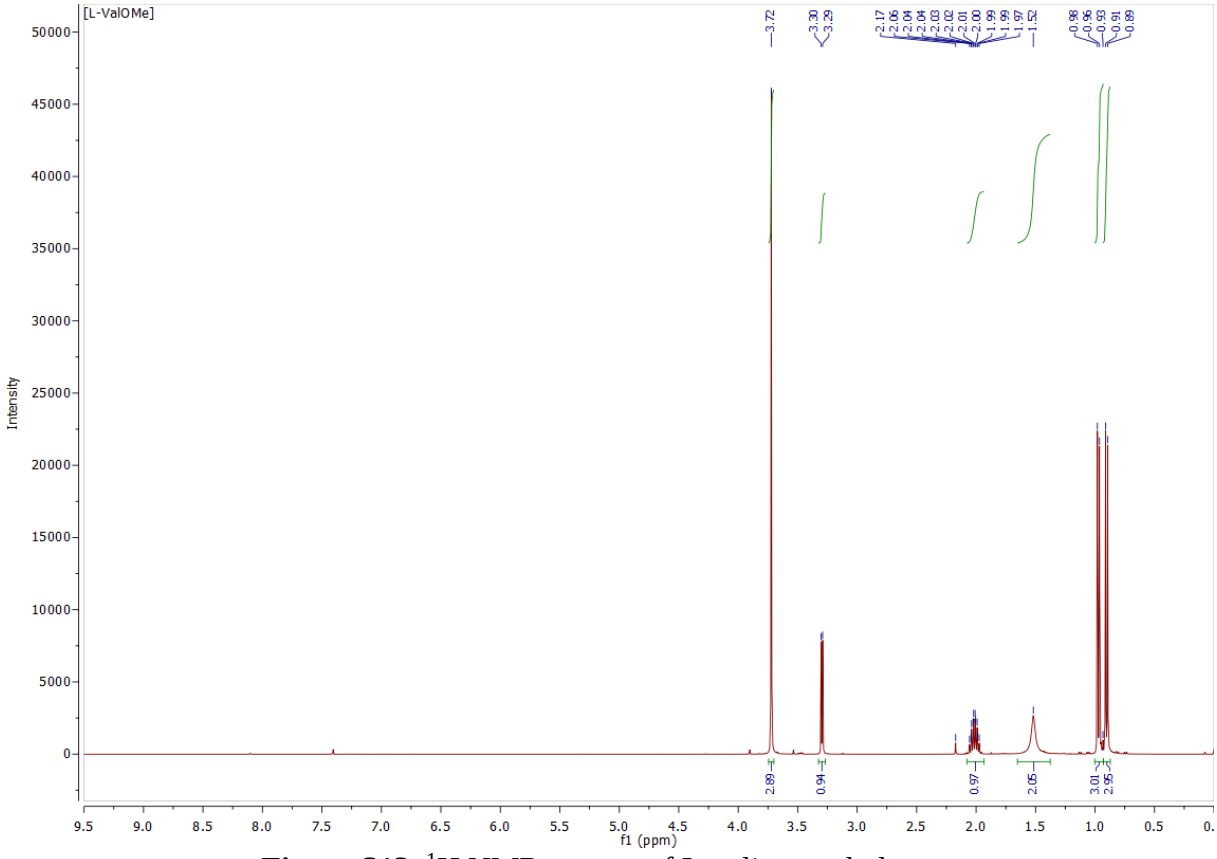

Figure S13. ^{1}H NMR spectra of L-valine methyl ester

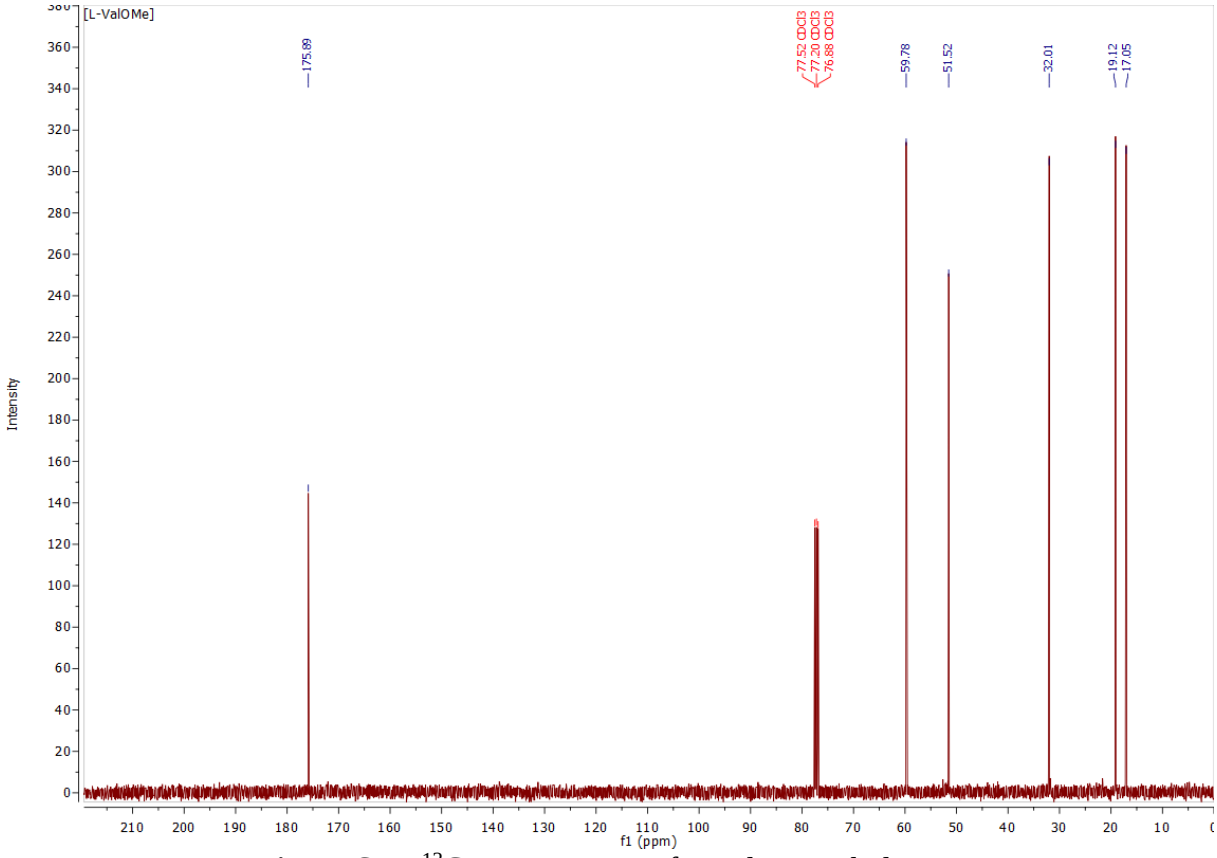

Figure S14. ^{13}C NMR spectra of L-valine methyl ester

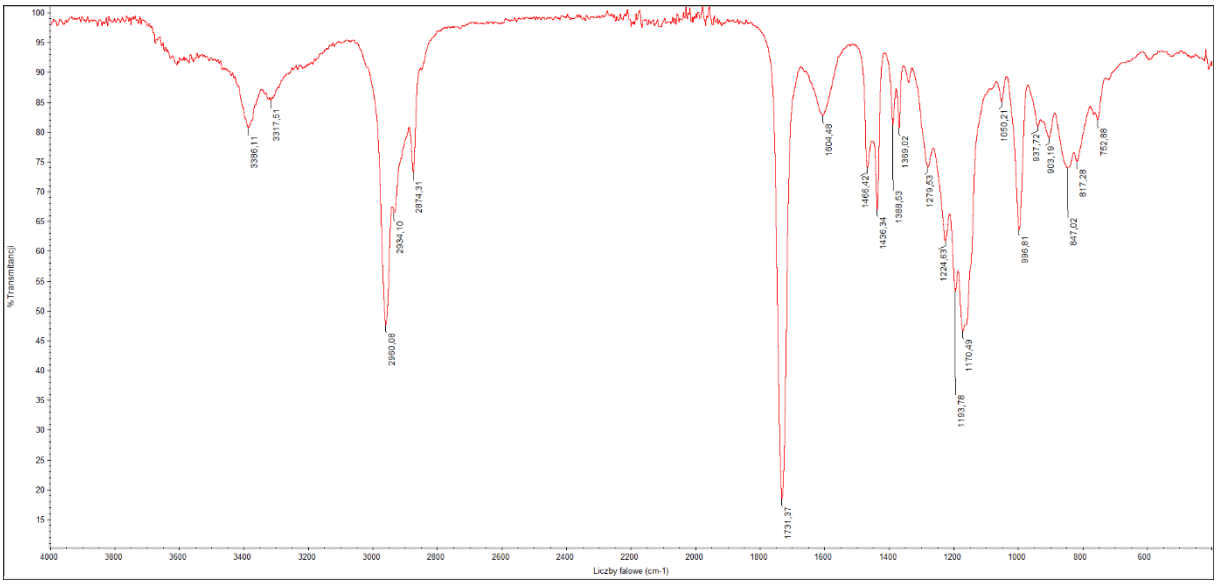

Figure S15. FTIR spectra of L-valine methyl ester

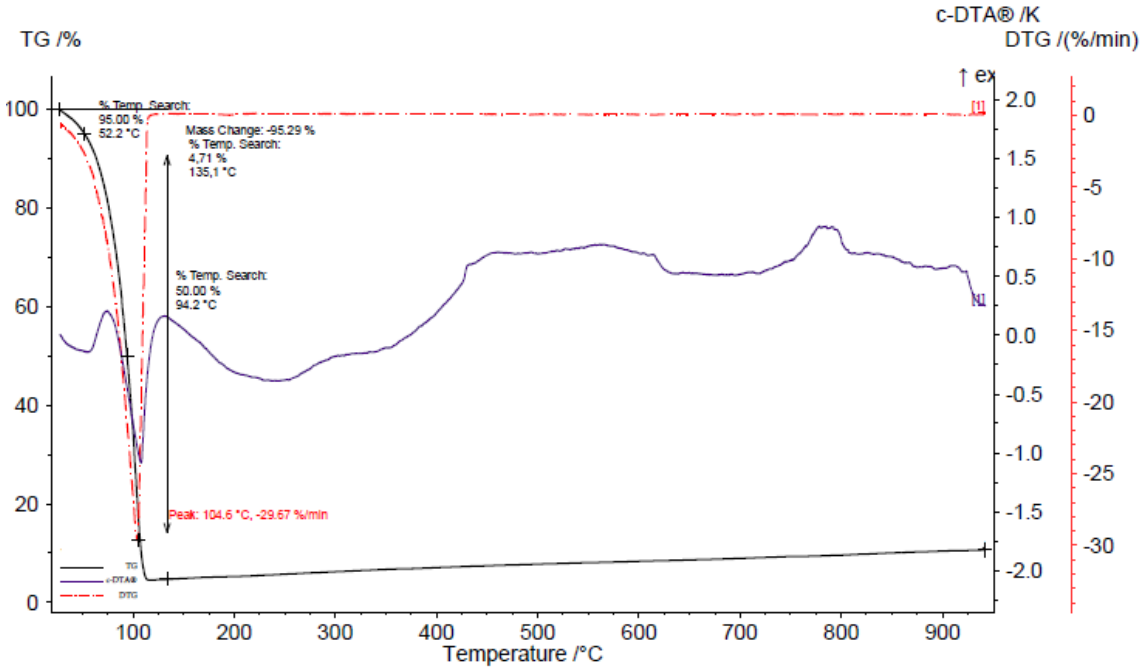

Figure S16. The TG, DTG and c-DTA curves of L-valine methyl ester

[ValOHept] – L-valine heptyl ester

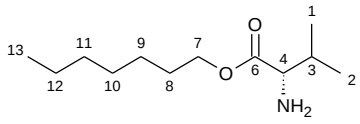

The compound was obtained according to general procedure and the reaction yielded 0.68 g of ValOHept (74.1%) as a yellow liquid. **^{1}H NMR** (400 MHz, $CDCl_3$) δ in ppm: 3.98-4.09 (m, 2H, H7); 3.19 (d, 1H, $J_{4,3}$=4.0 Hz, H4); 1.92-1.97 (m, 1H, H3); 1.55-1.60 (m, 2H, H8); 1.47 (s, 2H, H5); 1.14-1.31 (m, 8H, H9, H10, H11, H12) 0.89 (d, 3H, H2, $J_{1,3}$=6.9); 0.79-0.83 (m, 6H, H14, H1); **^{13}C NMR** (100 MHz, $CDCl_3$) δ in ppm: 175.50 (C6); 64.66 (C4); 59.78 (C7); 31.98 (C3); 31.56 (C8); 28.73 (C9); 28.49 (C10); 25.74 (C11); 22.42 (C12); 19.15 (C2); 16.99 (C1); 13.89 (C13); **FT-IR**: ν (ATR): 3392; 3328; 2957; 2927; 2871; 2858; 1731; 1608; 1467; 1388; 1379; 1368; 1338; 1277; 1225; 1172; 1049; 990; 954; 928; 906; 848; 725; cm^{-1}; **UV-Vis** (EtOH): λ_{max}= 205.7 nm; $[\boldsymbol{\alpha}]_{\boldsymbol{D}}^{\boldsymbol{20}}$ = +15.750 (c=0.800 g/100 cm^3 EtOH).

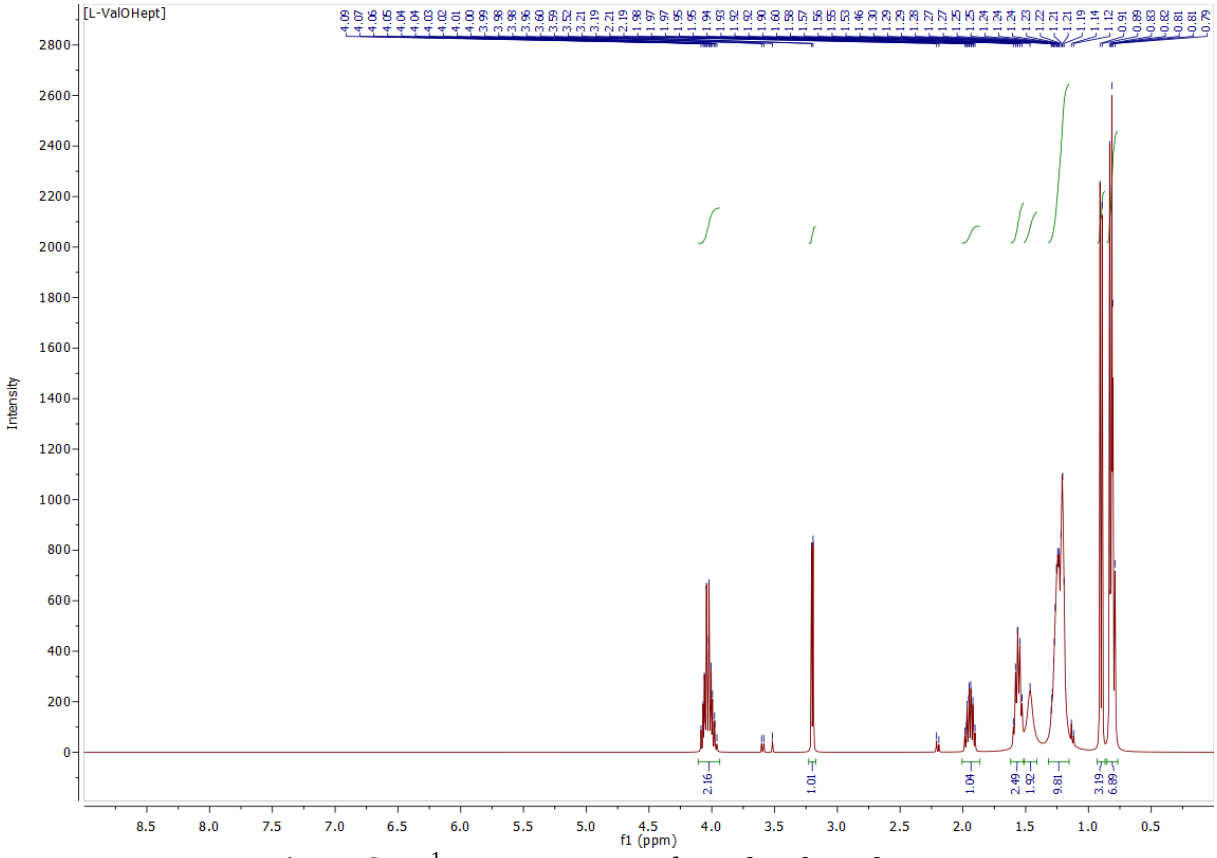

Figure S17. ^{1}H NMR spectra of L-valine heptyl ester

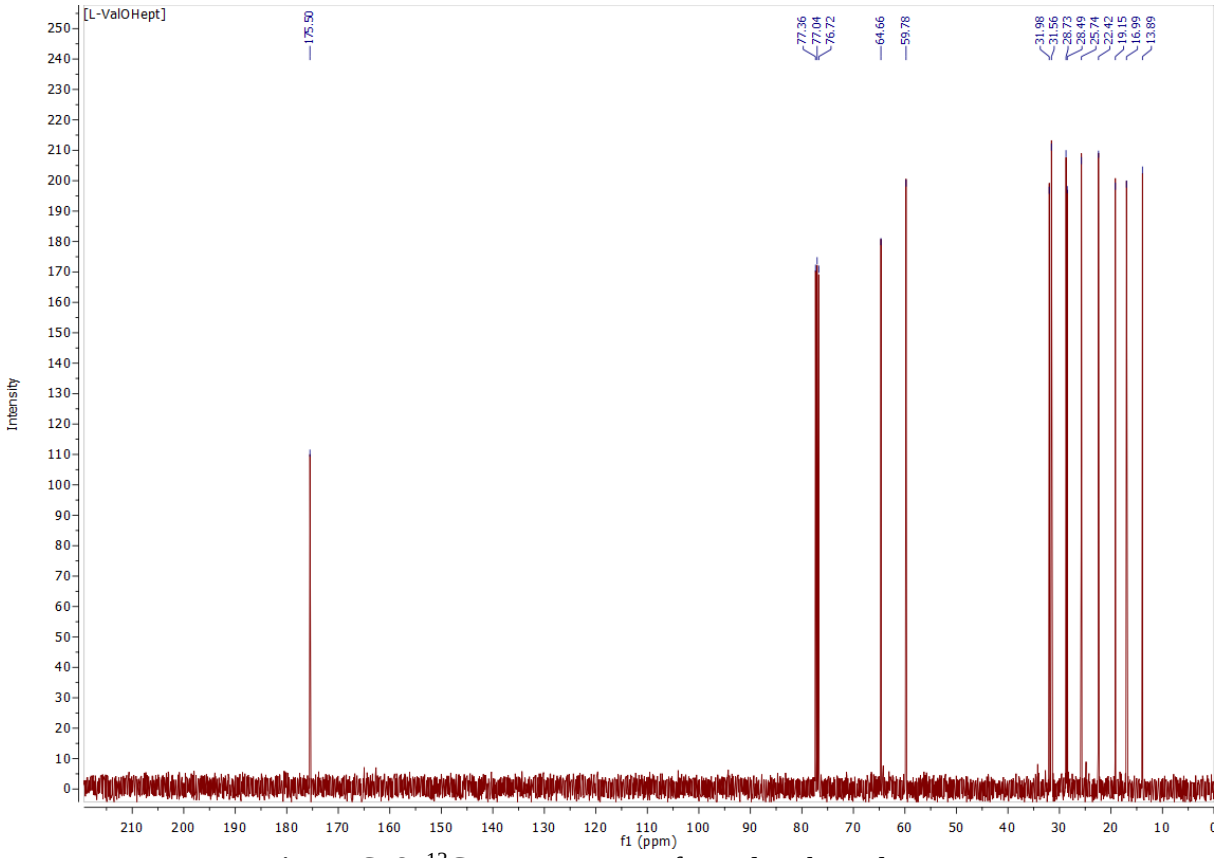

Figure S18. ^{13}C NMR spectra of L-valine heptyl ester

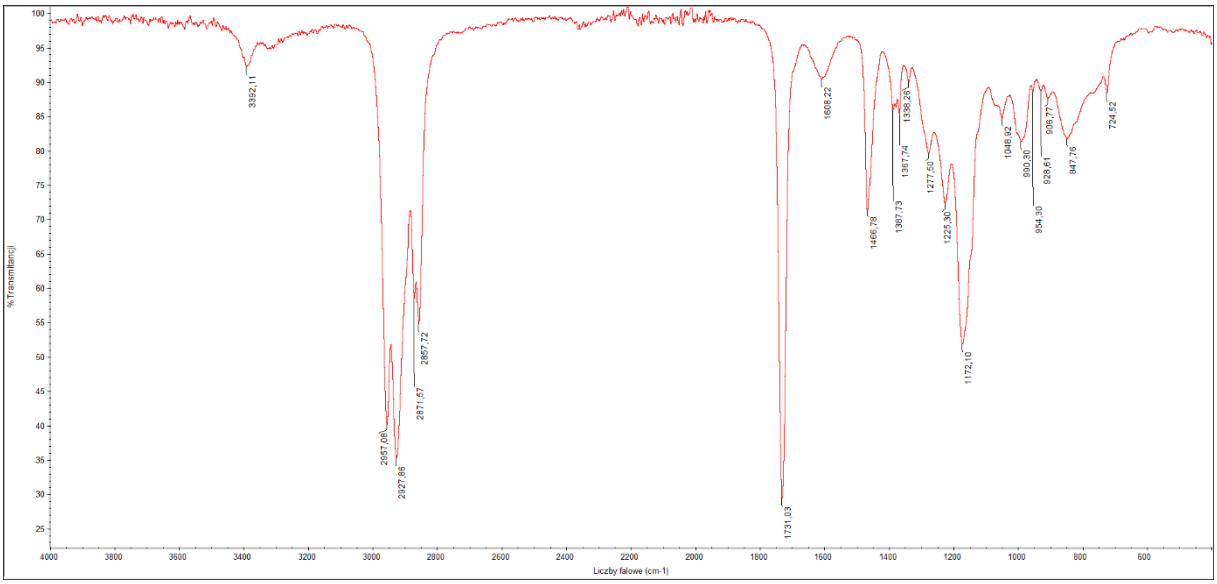

Figure S19. FTIR spectra of L-valine heptyl ester

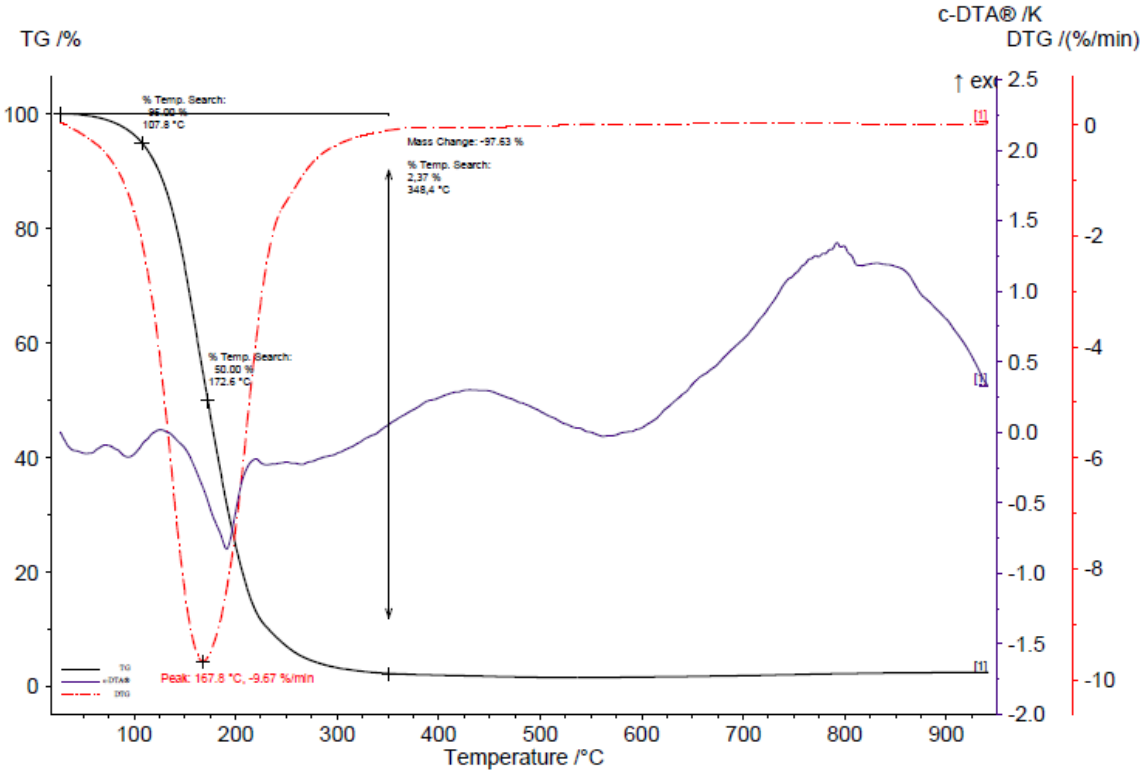

Figure S20. The TG, DTG and c-DTA curves of L-valine heptyl ester

[ValOOct] – L-valine octyl ester

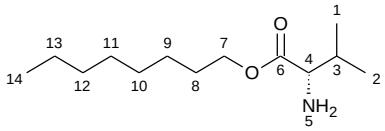

The compound was obtained according to general procedure and the reaction yielded 0.80 g of ValOOct (73.0%) as a yellow liquid. **^{1}H NMR** (400 MHz, $CDCl_3$) δ in ppm: 3.90-4.01 (m, 2H, H7); 3.12 (d, 1H, $J_{4,3}$=5.0 Hz, H4); 1.83-1.91 (m, 1H, H3); 1.45-1.52 (m, 4H, H8, H5); 1.03-1.22 (m, 10H, H9, H10, H11, H12, H13) 0.82 (d, 3H, H2, $J_{1,3}$=6.9); 0.71-0.76 (m, 6H, H14, H1); **^{13}C NMR** (100 MHz, $CDCl_3$) δ in ppm: 175.38 (C6); 64.53 (C4); 59.68 (C7); 31.90 (C3); 31.55 (C8); 28.95 (C9); 28.42 (C10); 22.40 (C11); 19.03 (C2); 16.90 (C1); 13.82 (C14); **FT-IR**: ν (ATR): 3389; 3327; 2957; 927; 2856; 2856; 1731; 1607; 1467; 1388; 1379; 1368; 1338; 1280; 1223; 1172; 1074; 1048; 982; 955; 982; 955; 908; 844; 770; 725; cm^{-1}; **UV-Vis** (EtOH): λ_{max}= 204.4 nm; $[\boldsymbol{\alpha}]_{\boldsymbol{D}}^{\mathbf{20}}$ = +18.127 (c=1.164 g/100 cm^3 EtOH).

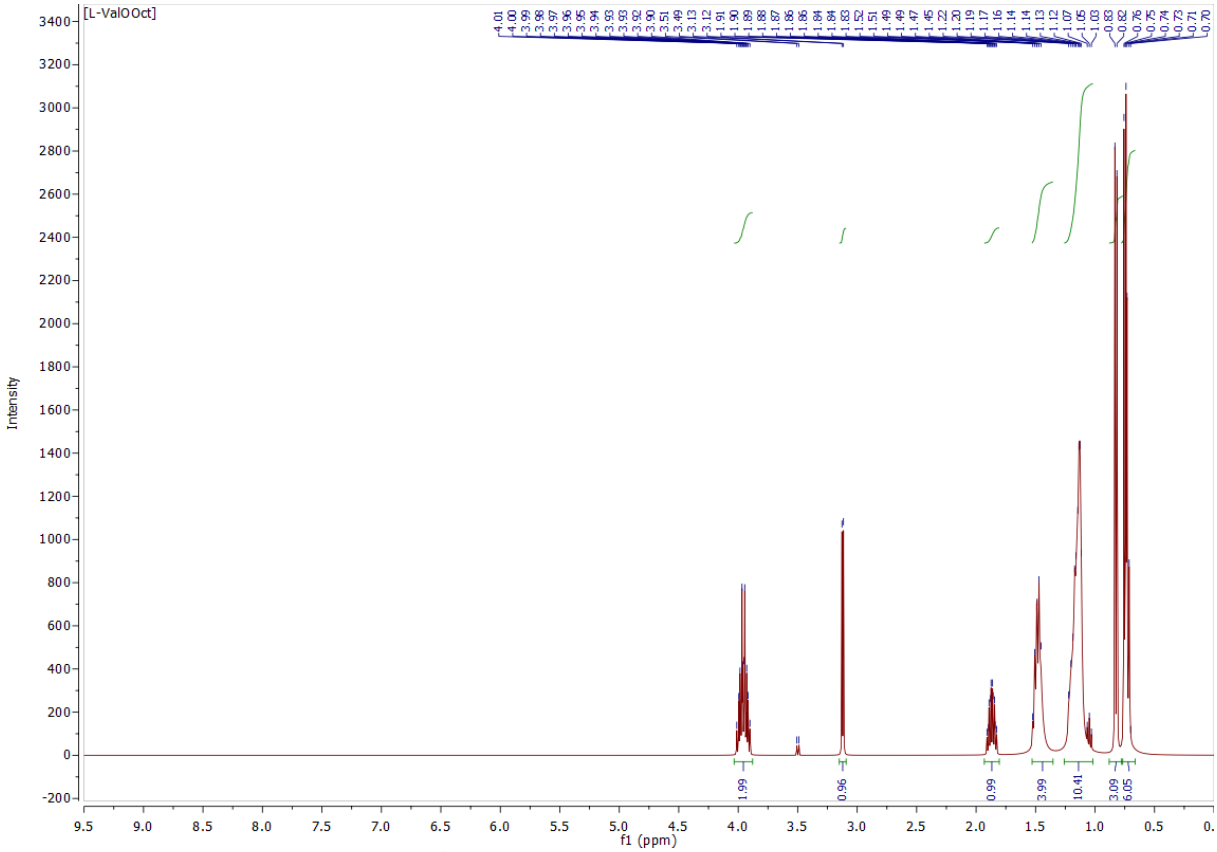

Figure S21. ^{1}H NMR spectra of L-valine octyl ester

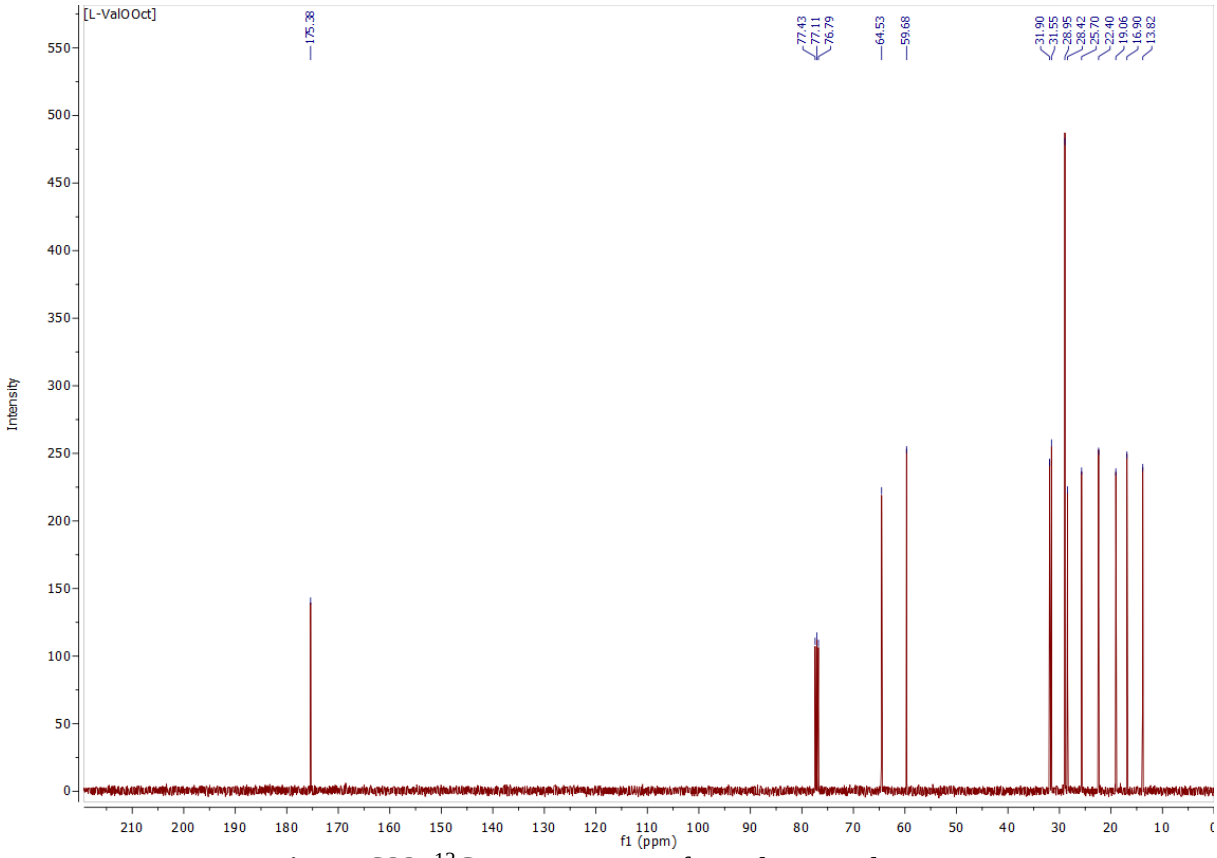

Figure S22. ^{13}C NMR spectra of L-valine octyl ester

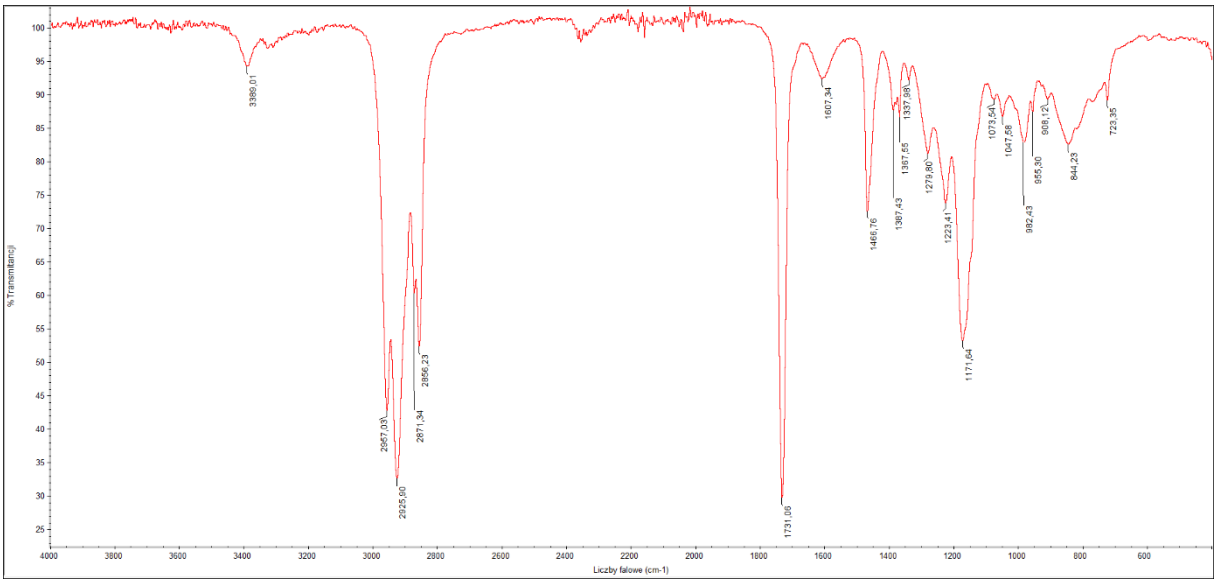

Figure S23. FTIR spectra of L-valine octyl ester

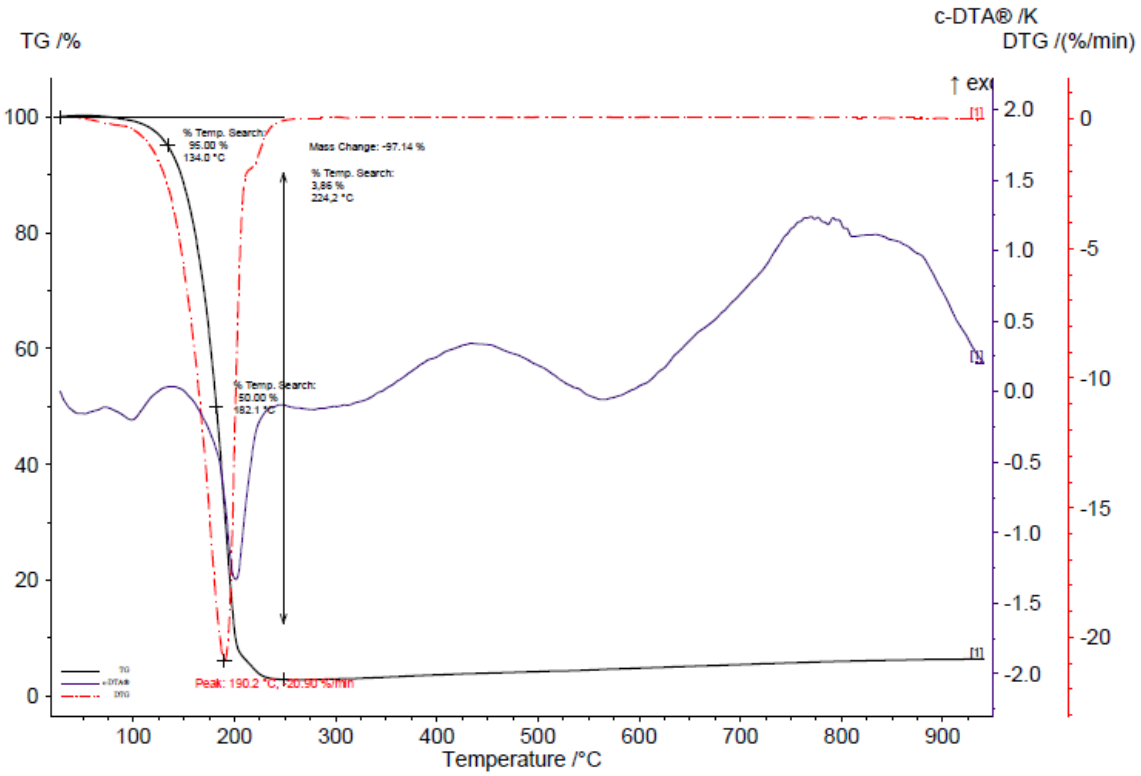

Figure S24. The TG, DTG and c-DTA curves of L-valine octyl ester

L-VALINE ALKYL ESTER IBUPROFENATE

Table S3. Yields of synthesis of L-valine alkyl esters ibuprofenate ([L-ValOR][IBU])

No.	Compound	Substrate		Product		
		L-ValOR [g]	Ibuprofen [g]	[L-ValOR][IBU] [g]	Yield [%]	State
1	[L-ValOMe][IBU]	0.60	0.94	1.51	97.6	white solid
2	[L-ValOHept][IBU]	0.65	0.62	1.17	92.0	white solid
3	[L-ValOOkt][IBU]	0.57	0.51	1.06	98.0	white solid

[ValOMe][IBU] – L-valine methyl ester ibuprofenate

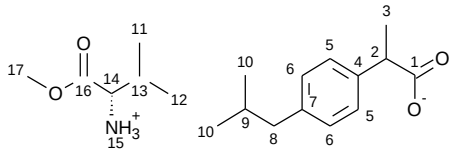

The compound was obtained according to general procedure and the reaction yielded 1.46 g of [ValOMe][IBU](97.6%) as white solid. **^{1}H NMR** (400 MHz, $CDCl_3$) δ in ppm: 7.18 (d, 2H, $J_{5,6}$=8.1 Hz, H5); 7.05 (d, 2H, $J_{6,5}$=8.1 Hz, H6); 5.08 (s, 3H, H15); 3.71 (s, 3H, H17); 3.63-3.69 (q, 1H, H2); 3.38 (d, 1H, $J_{14,13}$=4.6 Hz, H14); 2.43 (d, 2H, $J_{8,9}$=7.1 Hz, H8); 2.01-2.09 (m, 1H, H13); 1.79-1.87 (m, 1H, H9); 1.46 (d, 3H, $J_{3,2}$=7.1 Hz, H3); 0.94 (d, 3H, H11); 0.83-0.94 (m, 12H, H10, H11, H12); **^{13}C NMR** (100 MHz, $CDCl_3$) δ in ppm: 179.31 (C1); 175.01 (C16); 140.50 (C7); 137.89 (C4); 129.30 (C5); 127.26 (C6); 59.26 (C14); 51.95 (C14); 45.30 (C8); 45.06 (C2); 31.76 (C13); 30.20 (C9); 22.41 (C10); 18.96 (C12); 18.37 (C3); 17.27 (C11); **FT-IR**: ν (ATR): 2964; 2929; 2867; 1740; 1599; 1548; 1511; 1464; 1452; 1384; 1357; 1331; 1286; 1262; 1226; 1203; 1173; 1111; 1075; 1057; 986; 978; 882; 770; 727; 693; 528 cm^{-1}; **UV-Vis** (EtOH): λ_{max}=228.7 nm; **Elemental analysis:** Calc. (%) for $C_{20}H_{33}NO_4$ (337.458 g/mol) C (67.63), H (9.26), N (4.15), O (18.96), Found C (67.63), H (9.26), N (4.11), O (18.18); **T_m**=81.5-96.2ºC; $[\alpha]_D^{20}$ = +14.933 (c=0.529 g/100 cm^3 EtOH).

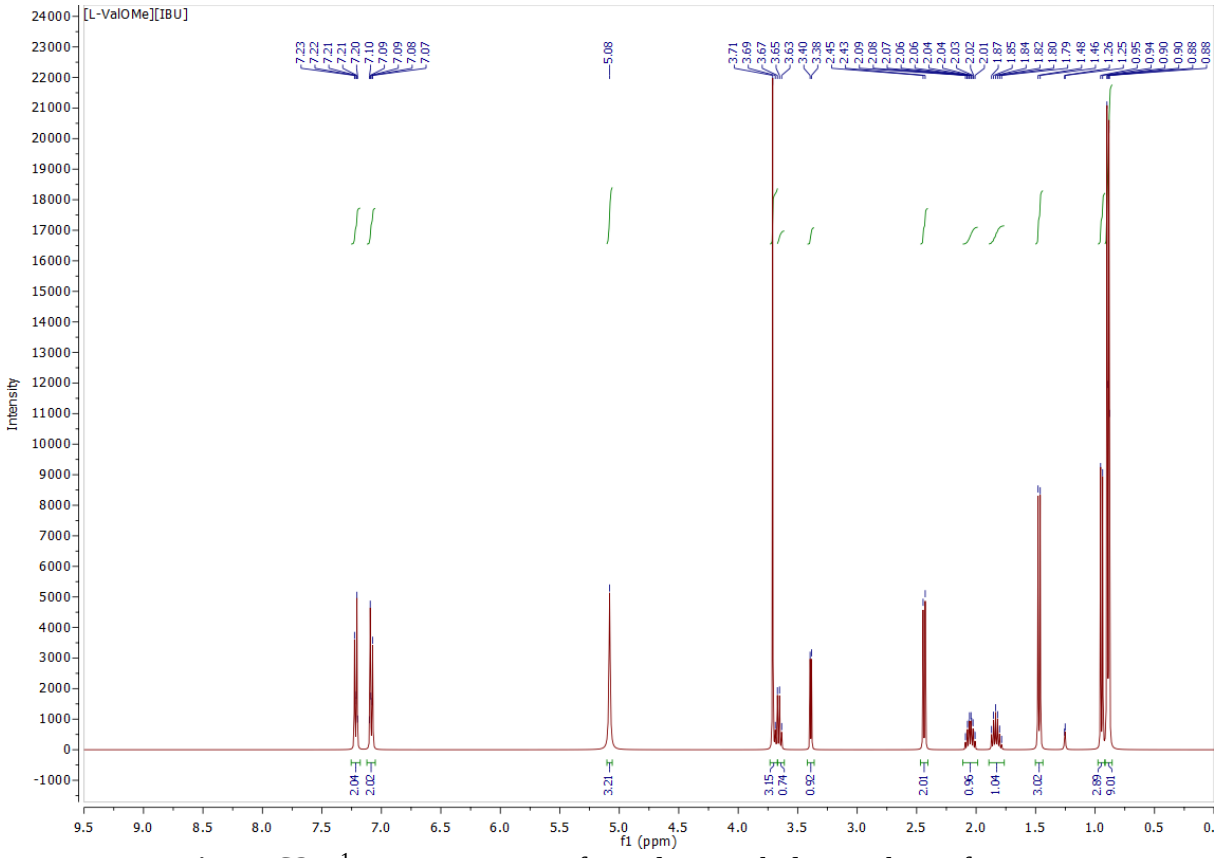

Figure S25. ^{1}H NMR spectra of L-valine methyl ester ibuprofenate

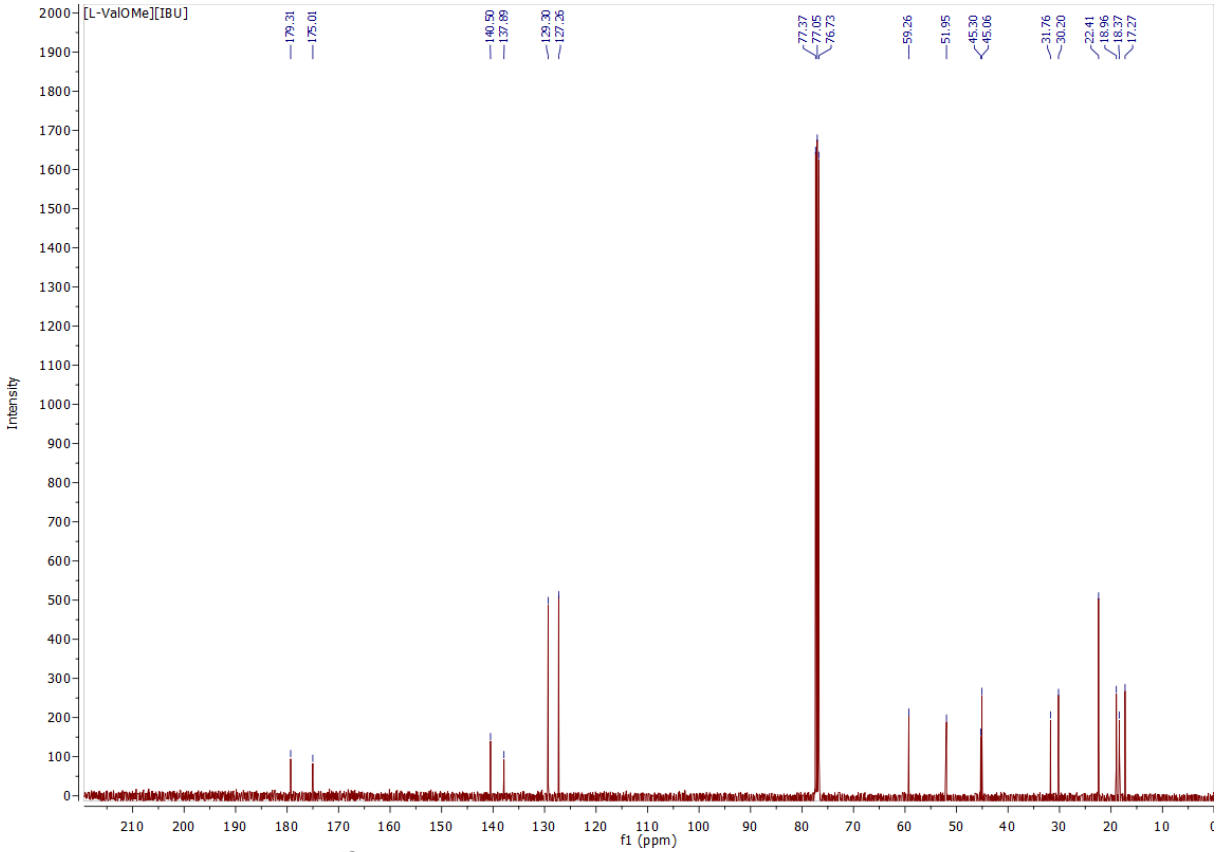

Figure S26. ^{13}C NMR spectra of L-valine methyl ester ibuprofenate

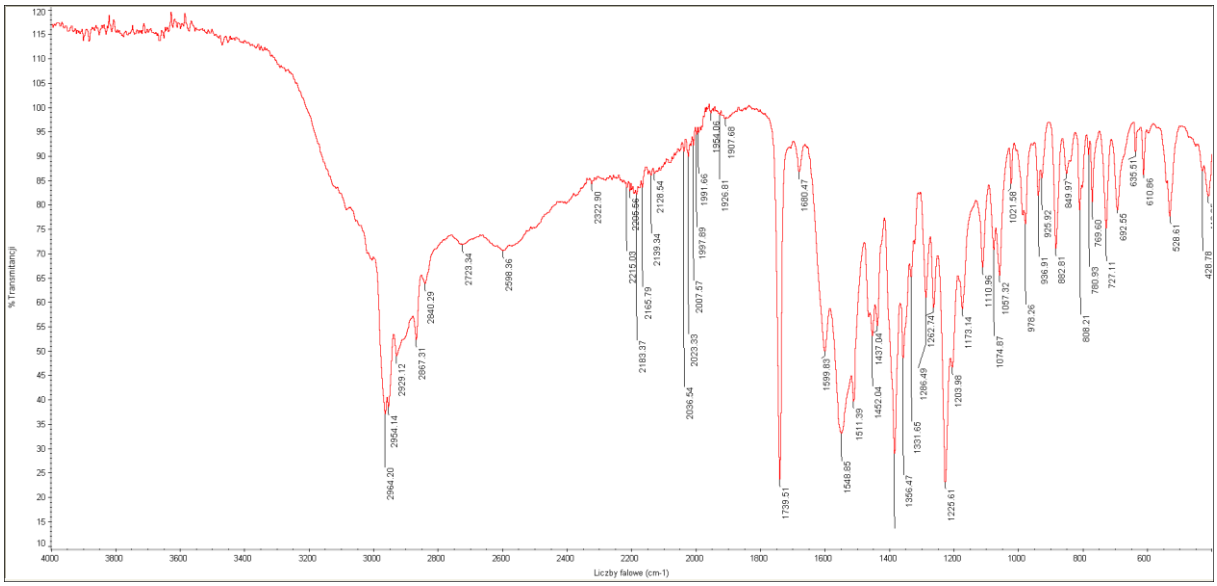

Figure S27. FT-IR spectra of L-valine methyl ester ibuprofenate

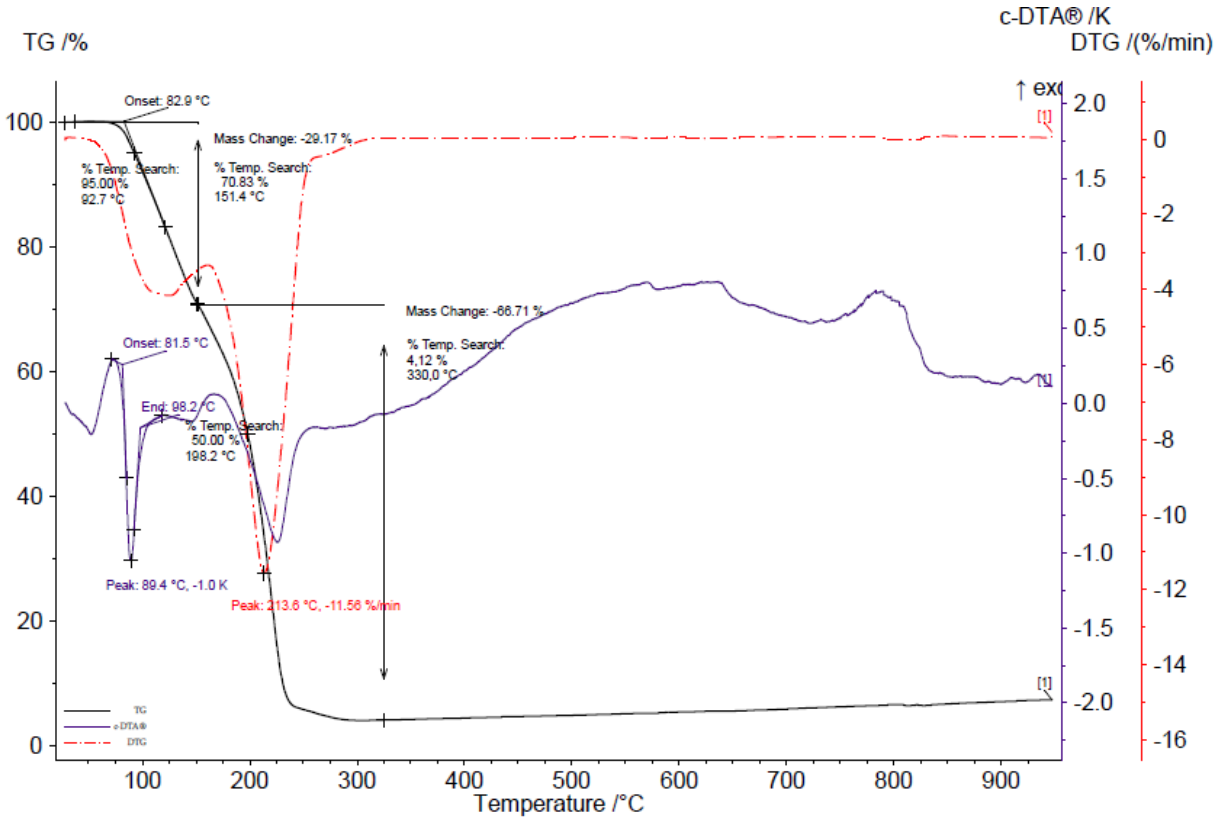

Figure S28. The TG, DTG and c-DTA curves of L-valine methyl ester ibuprofenate

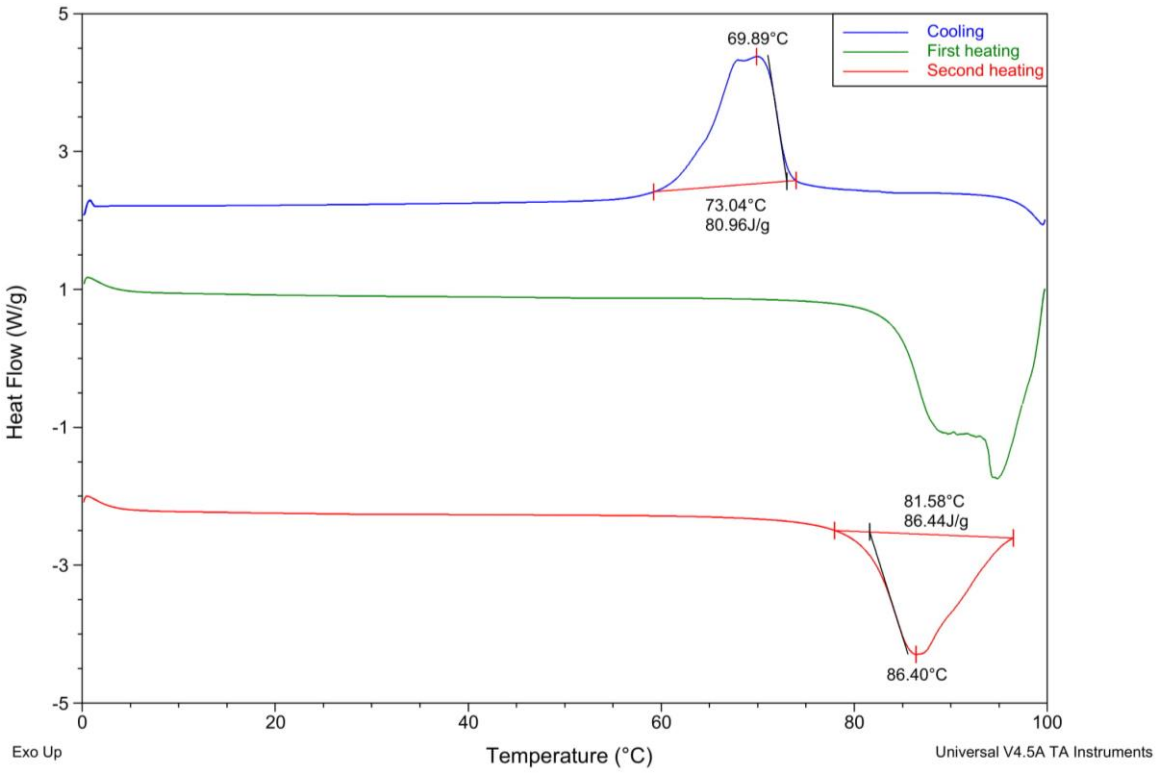

Figure S29. The DSC curves of L-valine methyl ester ibuprofenate

[ValOHept][IBU] – L-valine heptyl ester ibuprofenate

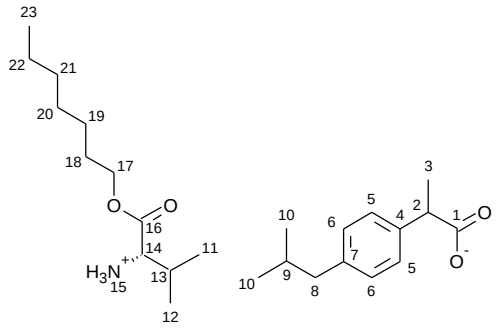

The compound was obtained according to general procedure and the reaction yielded 1.4 g of [L-ValOHept][IBU] (92.0%) as white solid**. ^{1}H NMR** (400 MHz, $CDCl_3$) δ in ppm: 7.20 (d, 2H, $J_{5,6}$=8.1 Hz, H5); 7.06 (d, 2H, $J_{6,5}$=8.0 Hz, H6); 5.82 (s, 3H, H15); 4.06-4.14 (m, 2H, H17); 3.61-3.66 (m, 1H, H2); 3.39 (d, 1H, $J_{14,13}$=4.5 Hz, H14); 2.42 (d, 2H, $J_{8,9}$=7.1 Hz, H8); 2.03-2.08 (m, 1H, H13); 1.80-1.85 (m, 1H, H9); 1.59-1.64 (m, 2H, H18); 1.44 (d, 3H, $J_{3,2}$=7.1 Hz, H3); 1.26-1.33 (m, 9H, H19, H20, H21, H22); 0.87-0.94(m, 15H, H10, H11, H12, H23); **^{13}C NMR** (100 MHz, $CDCl_3$) δ in ppm: 179.22 (C1); 174.20 (C16); 140.28 (C7); 138.32 (C4); 129.23 (C5); 127.26 (C6); 65.24 (C17); 59.07 (C14); 45.57 (C8); 45.07 (C2); 31.71(C13); 31.56 (C18); 30.20 (C9); 28.87 (C19); 28.58 (C20); 25.86 (C21); 22.59 (C22); 22.42 (C10); 18.84 (C12); 18.49 (C3); 17.27 (C11); 14.07 (C23); **FT-IR**: ν (ATR): 2959; 2927; 2863; 2727; 2160; 1737; 1677; 1600; 1583; 1545; 1510; 1465; 1416; 1388; 1358; 1320; 1288; 1255; 1224; 1212; 1175; 1116; 1060; 1022; 1003; 936; 882; 848; 810; 786; 725; 694; 636 cm^{-1}; **UV-Vis** (EtOH): λ_{max}=219.5 nm; **Elemental analysis:** Calc. (%) for $C_{25}H_{43}NO_4$ (421.619 g/mol) C (71.72), H (10.23), N (3.32), O (15.18), Found C (71.22), H (10.30), N (3.04), O (15.14); **T_m**=57.5-72.2ºC; $[\boldsymbol{\alpha}]_{\boldsymbol{D}}^{\boldsymbol{20}}$ = +7.678 (c=0.533 g/100 cm^3 EtOH).

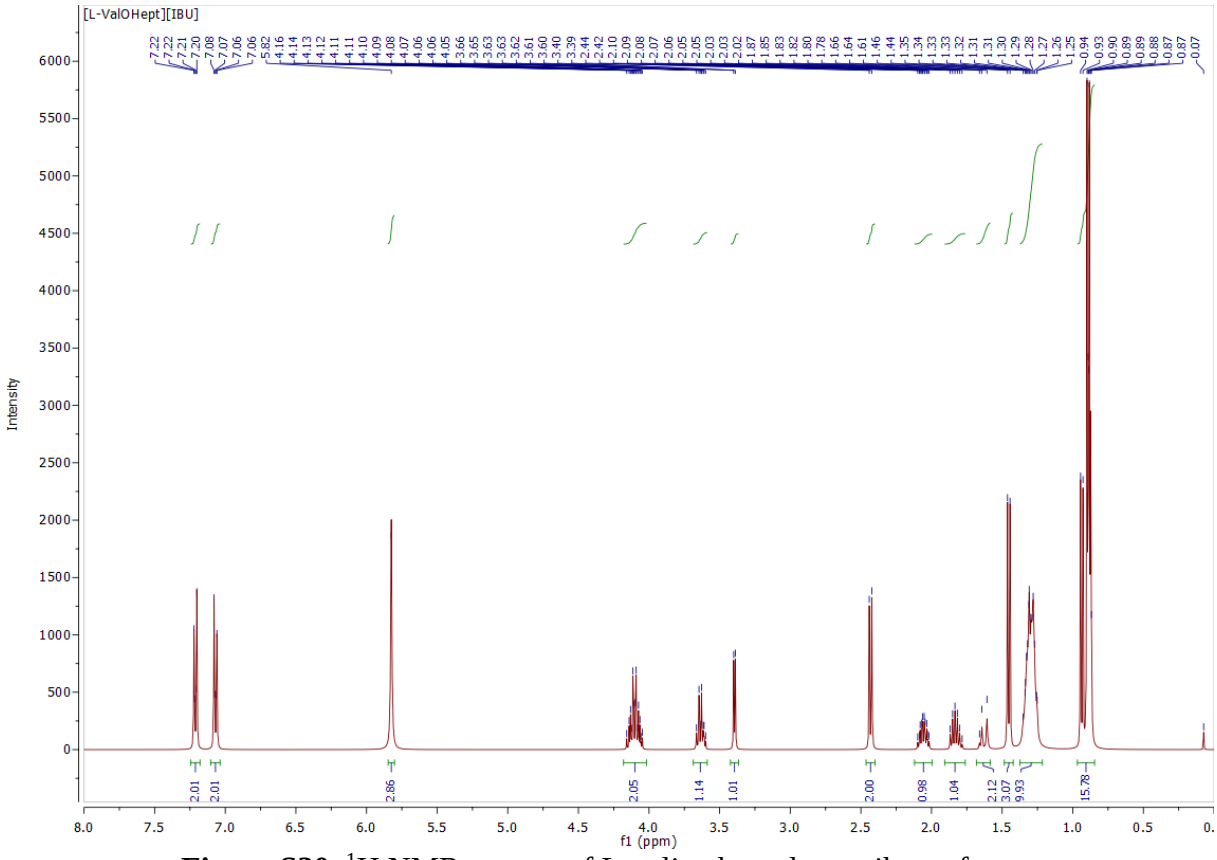

Figure S30. ^{1}H NMR spectra of L-valine heptyl ester ibuprofenate

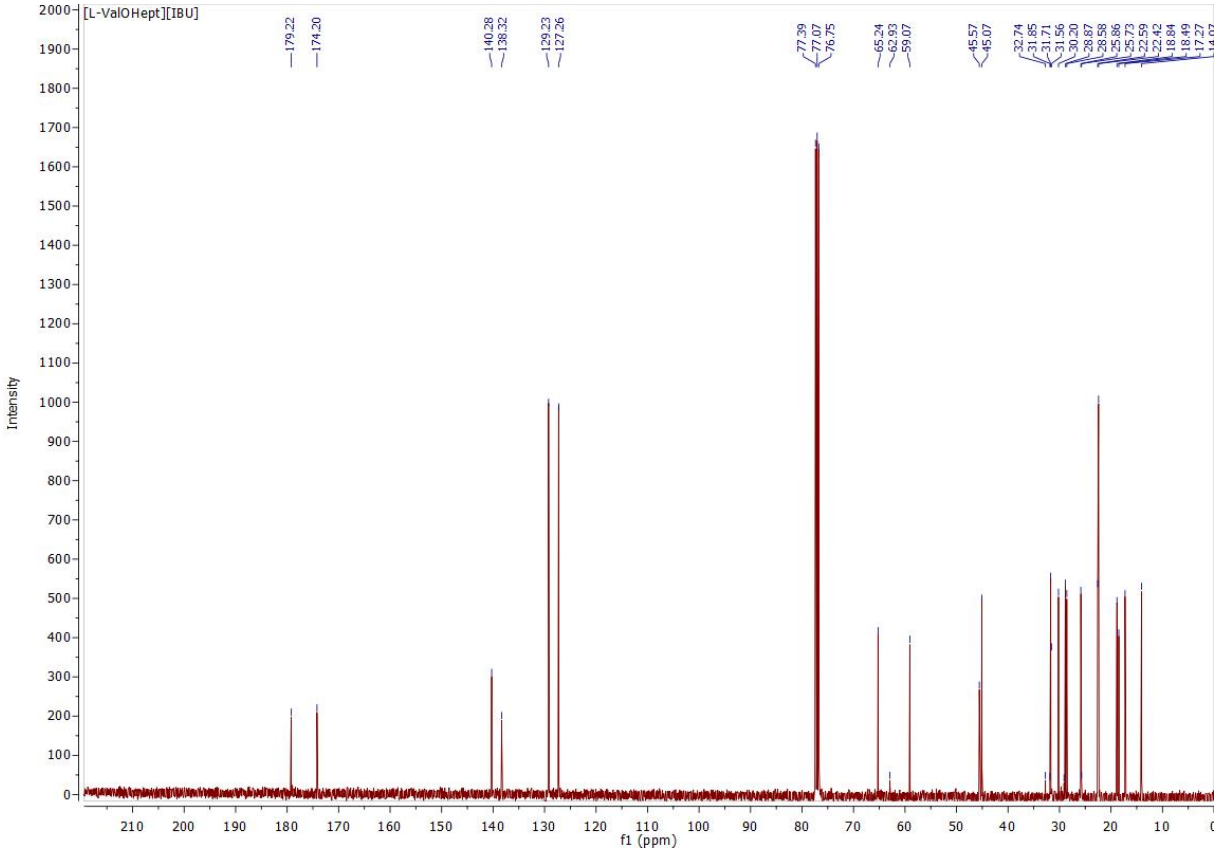

Figure S31. ^{13}C NMR spectra of L-valine heptyl ester ibuprofenate

Figure S32. FT-IR spectra of L-valine heptyl ester ibuprofenate

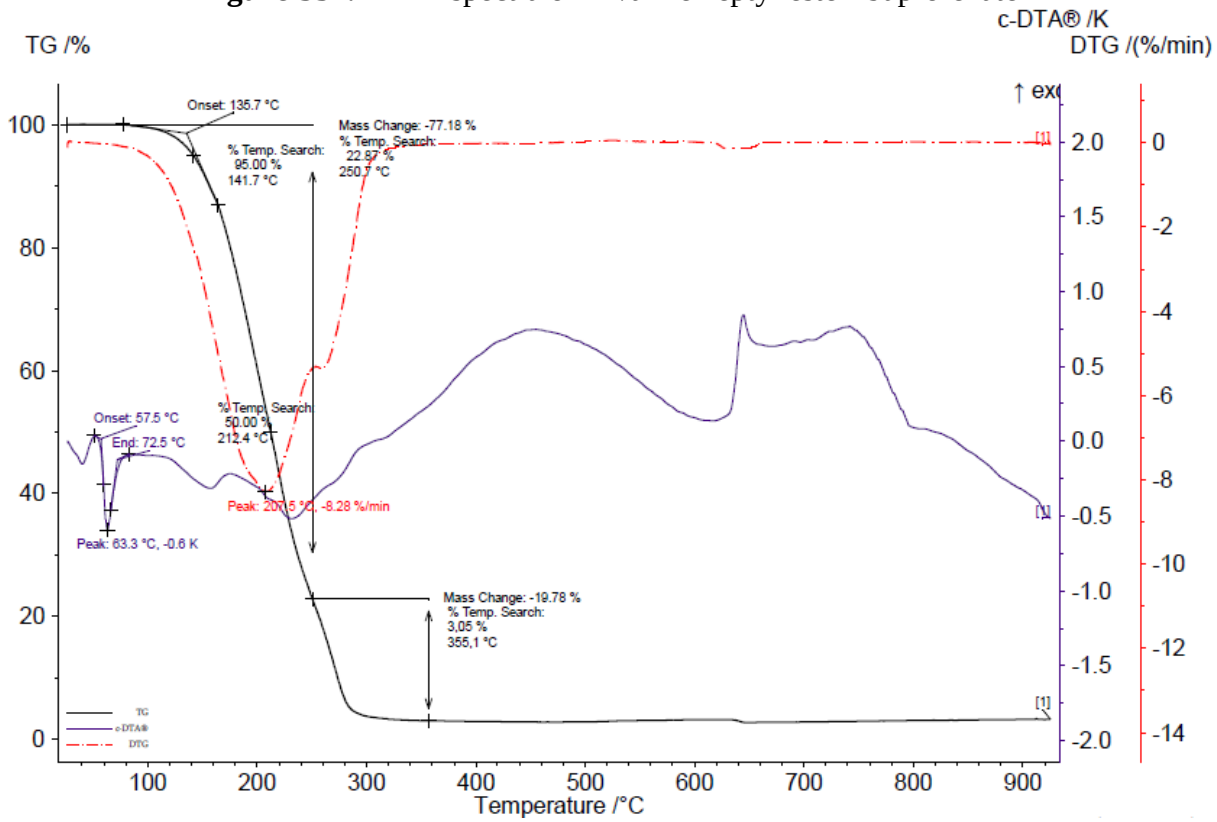

Figure S33. The TG, DTG and c-DTA curves of L-valine heptyl ester ibuprofenate

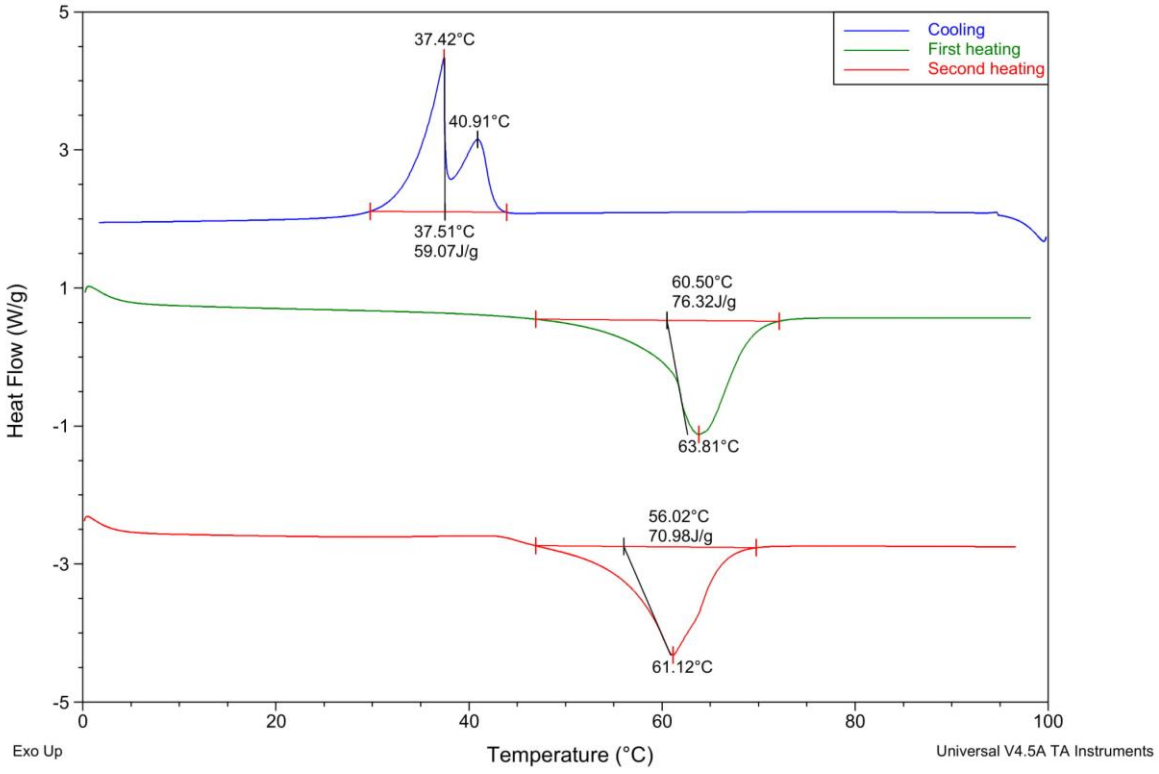

Figure S34. The DSC curves of L-valine heptyl ester ibuprofenate

[ValOOct][IBU] – L-valine octyl ester ibuprofenate

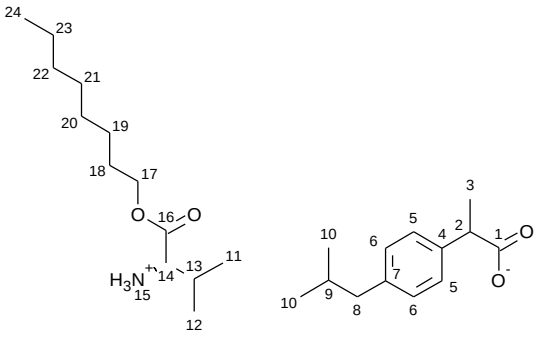

The compound was obtained according to general procedure and the reaction yielded 0.6 g of [L-ValOOct][IBU] (98.0%) as white solid. **^{1}H NMR** (400 MHz, CDCl3) δ in ppm: 7.20 (d, 2H, J5,6=8.91 Hz, H5); 7.05 (d, 2H, $J_{6,5}$=8.0 Hz, H6); 6.03 (s, 3H, H15); 4.06-4.14 (m, 2H, H17); 3.60- 3.65 (q, 1H, H2); 3.39 (d, 1H, $J_{14,13}$=4.5 Hz, H14); 2.42 (d, 2H, $J_{8,9}$=7.2 Hz, H8); 2.03-2.08 (m, 1H, H13); 1.80-1.87 (m, 1H, H9); 1.59-1.64 (m, 2H, H18); 1.43 (d, 3H, $J_{3,2}$=7.1 Hz, H3); 1.27-1.30 (m, 11H, H19, H20, H21, H22, H23); 0.87-0.94 (m, 15H, H10, H11, H12, H24); **^{13}C NMR** (100 MHz, CDCl3) δ in ppm: 179.22 (C1); 173.98 (C16); 140.17 (C7); 138.52 (C4); 129.19 (C5); 127.27 (C6); 65.27 (C17); 59.00 (C14); 45.71 (C8); 45.08 (C2); 31.79 (C13); 31.48 (C18); 30.20 (C9); 29.17 (C19); 28.57 (C20); 25.89 (C21); 22.65 (C22); 22.42 (C10); 18.78 (C12); 18.55 (C3); 17.30 (C11); 14.11 (C11); **FT-IR:** ν (ATR): 2955; 2923; 2855; 2722; 2162; 1739; 1678; 1603; 1510; 1464; 1417; 1388; 1359; 1320; 1288; 1259; 1223;

1209; 1176; 1115; 1082; 1058; 1022; 1004; 940; 882; 848; 812; 786; 726; 693; 637cm^{-1}; **UV-Vis** (EtOH): λ_{max}=219.8 nm; **Elemental analysis:** Calc. (%) for $C_{24}H_{41}NO_4$ (435.645 g/mol) C (71.68), H (10.41), N (3.21), O (14.69), Found C (71.64), H (10.43), N (3.08), O (14.63); $\mathbf{T_m}$=58.2-70.9ºC; $[\boldsymbol{\alpha}]_{\mathbf{D}}^{\mathbf{20}}$ = +8.300 (c=0.506 g/100 cm^3 EtOH).

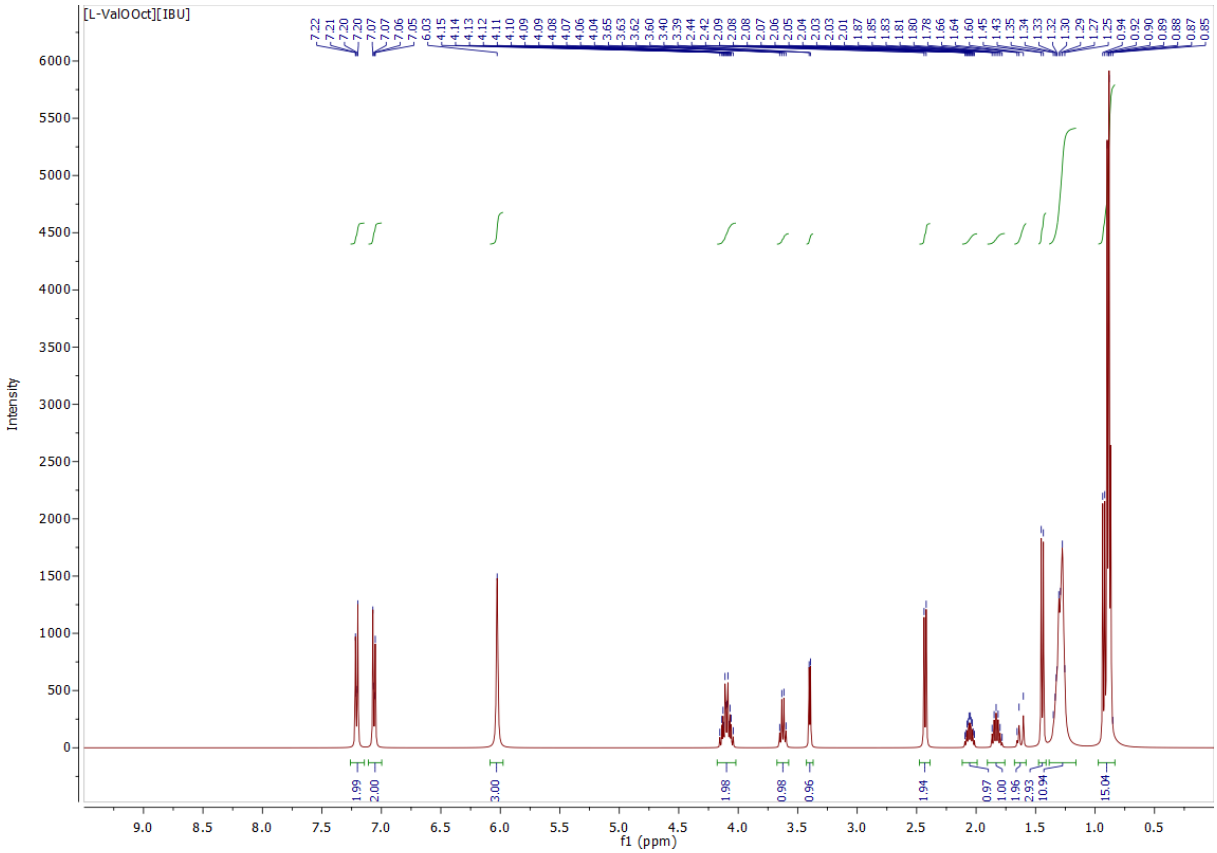

Figure S35. ^{1}H NMR spectra of L-valine octyl ester ibuprofenate

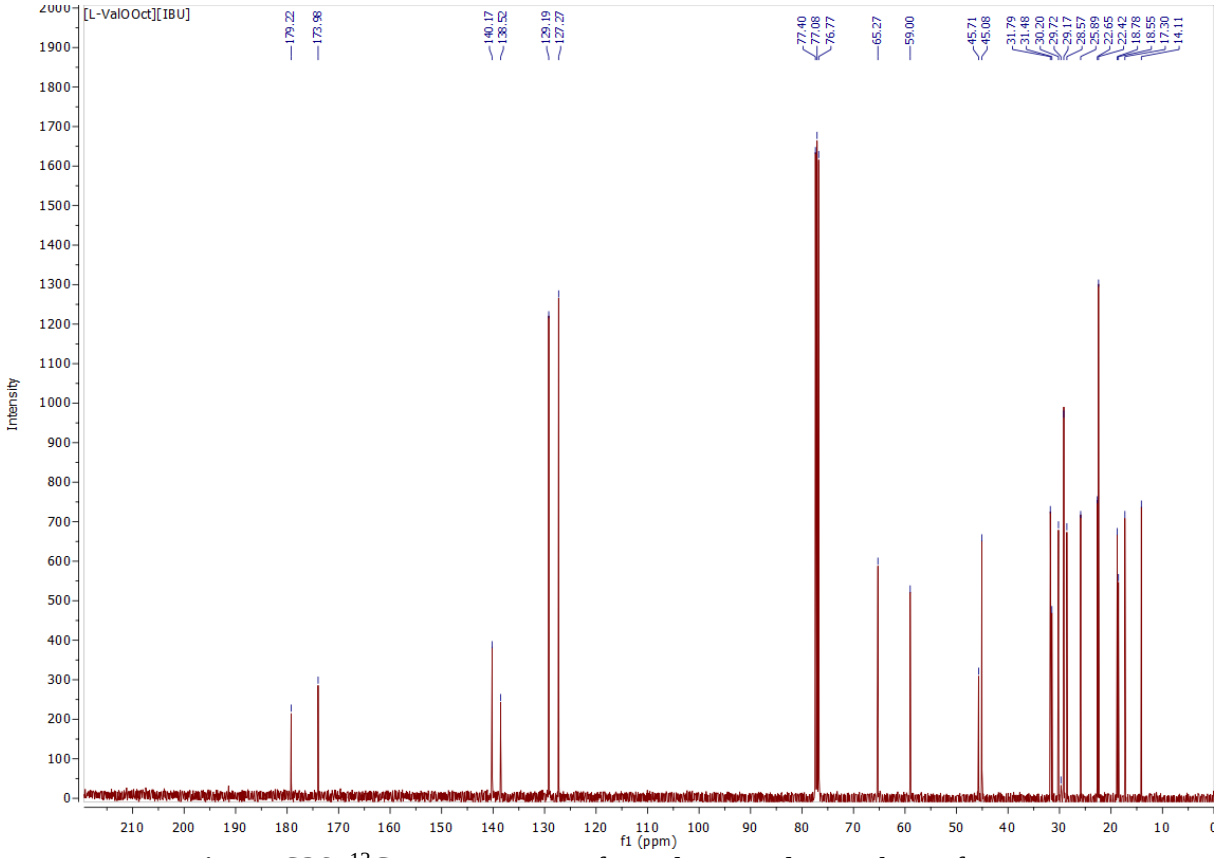

Figure S36. ^{13}C NMR spectra of L-valine octyl ester ibuprofenate

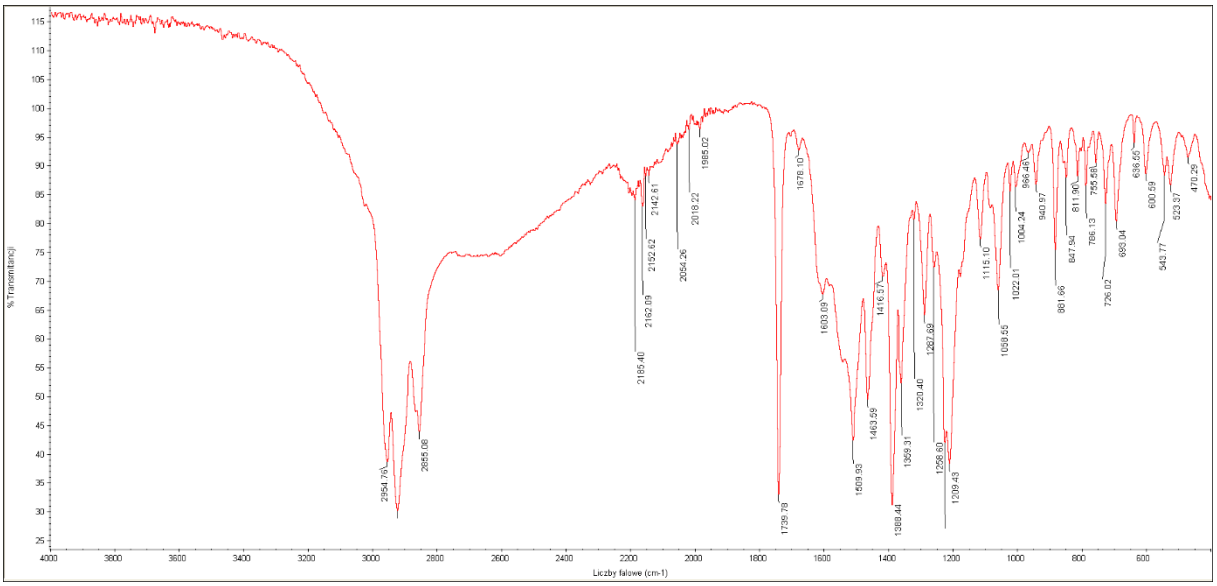

Figure S37. FT-IR spectra of L-valine octyl ester ibuprofenate

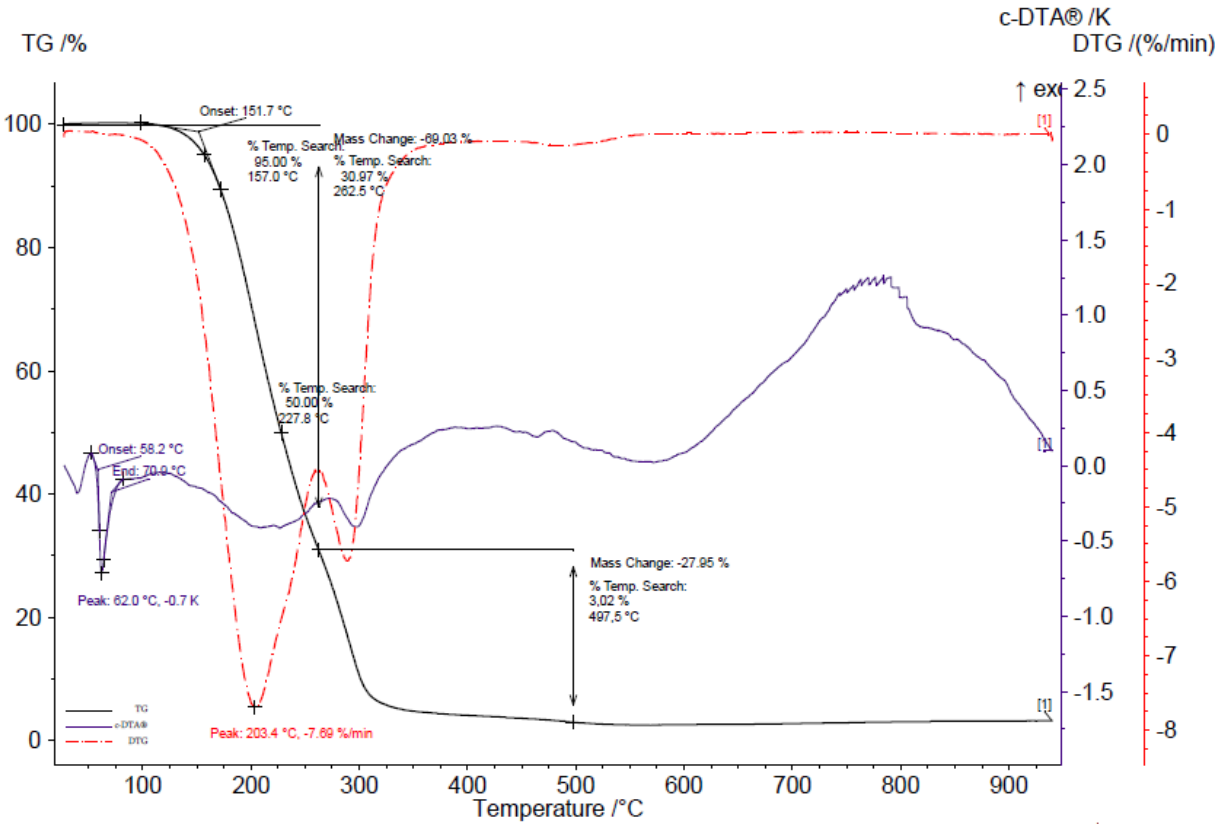

Figure S38. The TG, DTG and c-DTA curves of L-valine octyl ester ibuprofenate

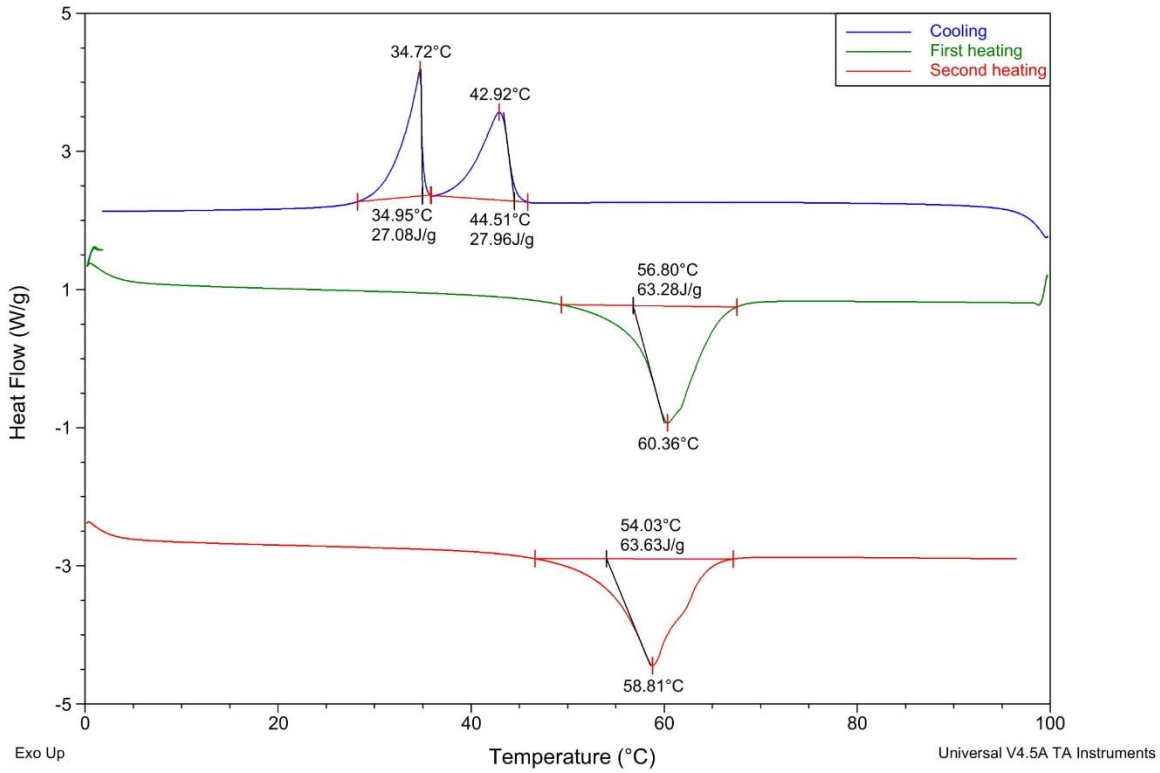

Figure S39. The DSC curves of L-valine octyl ester ibuprofenate

COLLECTED DATA

a)

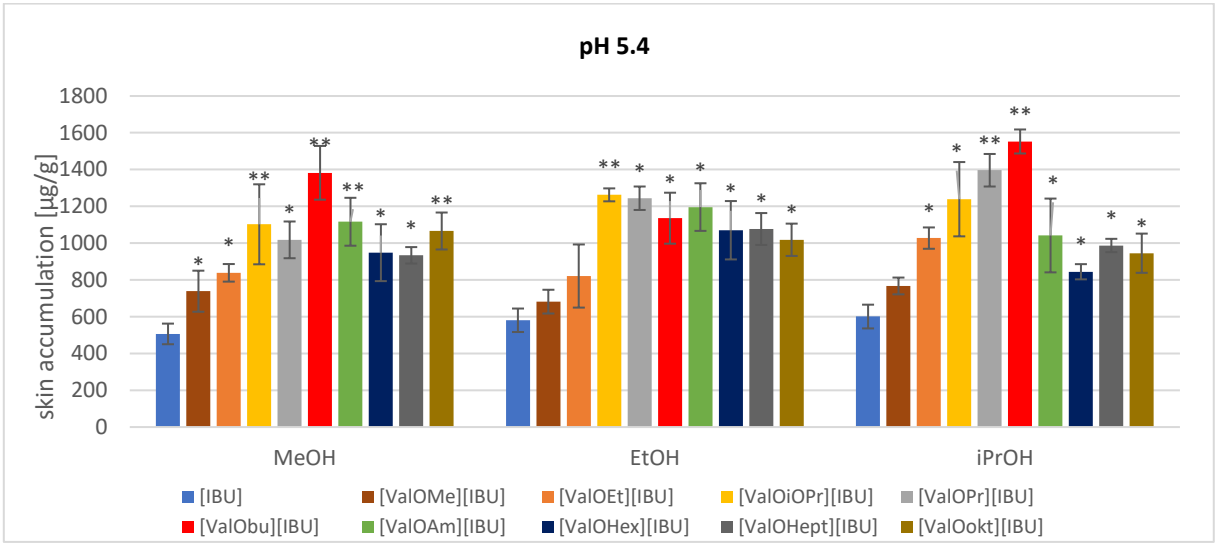

b)

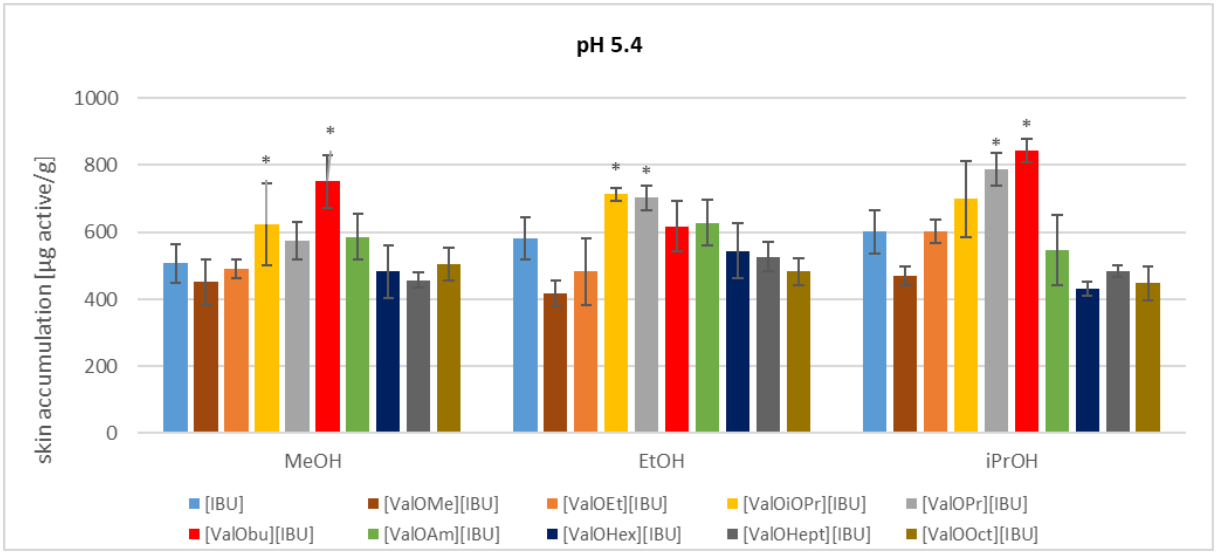

Figure S40. The cumulative mass of compound in skin after 24 hours of permeation (n=3) - acceptor phase with pH 5.4, expressed as µg compound (a) or µg IBU (b) per g skin

a)

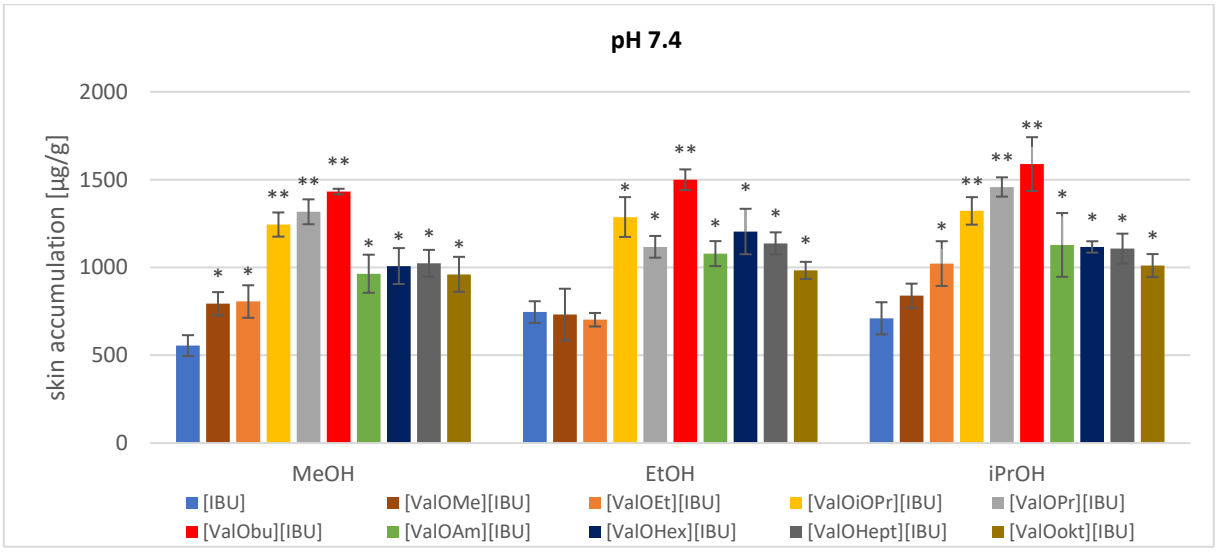

b)

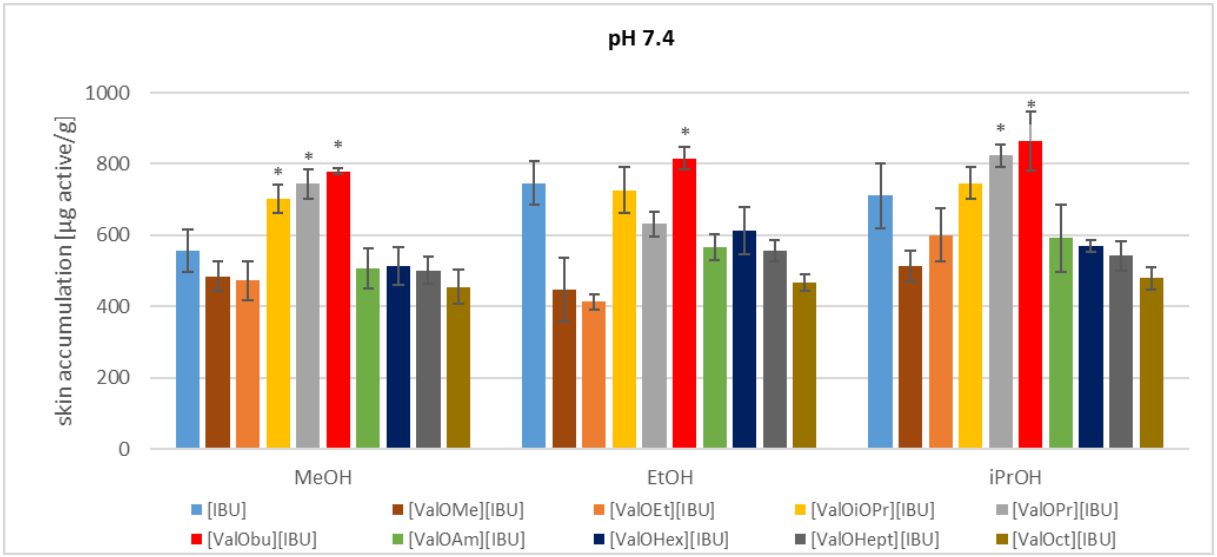

Figure S41. The cumulative mass of compound in skin after 24 hours of permeation (n=3) - acceptor phase with pH 7.4, expressed as µg compound (a) or µg IBU (b) per g skin

Table S4. Statistical differences regarding the cumulative mass of active substance in relation to ibuprofen, taking into account all factors used (a type of alcohol and pH) by the Mann-Whitney test

Compounds	[ValOMe] [IBU]	[ValOEt] [IBU]	[ValOiPr] [IBU]	[ValOPr] [IBU]	[ValOBu] [IBU]	[ValOAm] [IBU]	[ValOHex] [IBU]	[ValOHept] [IBU]	[ValOOct] [IBU]
IBU	z=- 0.616 (p=0.542)	z=4.192 (p=0.000)**	z=-0.933 (p=0.350)	z=-3.306 (p=0.000)**	z=-0.616 (p=0.537)	z=-1.597 (p=0.110)	z=2.167 (p=0.030)	z=4.167 (p=0.000)**	z=5.110 (p=0.000)**

**Value is significantly different from control (ibuprofen) (P<0.001) *Value is significantly different from control (ibuprofen) (P<0.05)

Table S5. Statistical differences between individual alcohols and between acceptor liquids with different pH using the Mann-Whitney test

Alkohol/vehicle	z	p
EtOH *vs* MeOH	2.367	0.0179*
EtOH *vs* iPrOH	-2.130	0.0330*
MeOH *vs* iPrOH	-4.273	0.0000**
pH/ acceptor fluid		
pH 7.4 *vs* pH 5.4	3.1942	0.0014**

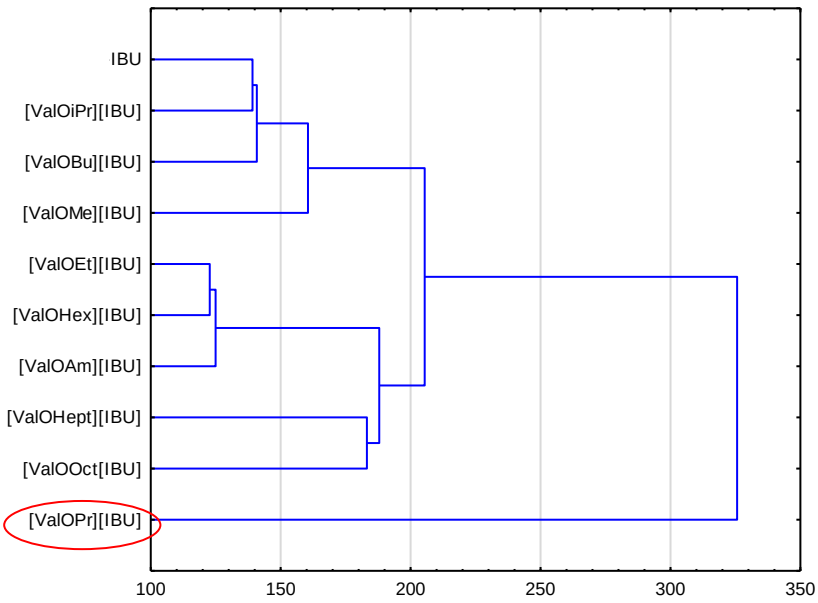

Figure S42. Hierarchical dendrogram of a mean cumulated mass of IBU

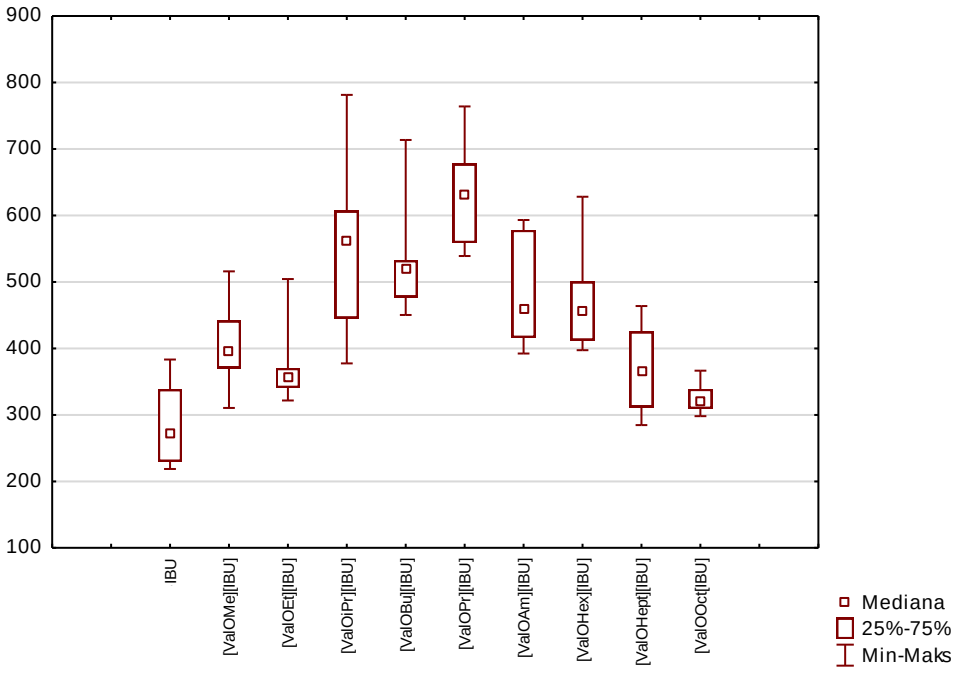

Figure S43. Box and whisker plot of data from a mean cumulative mass of IBU depending on the type of ibuprofen derivative used

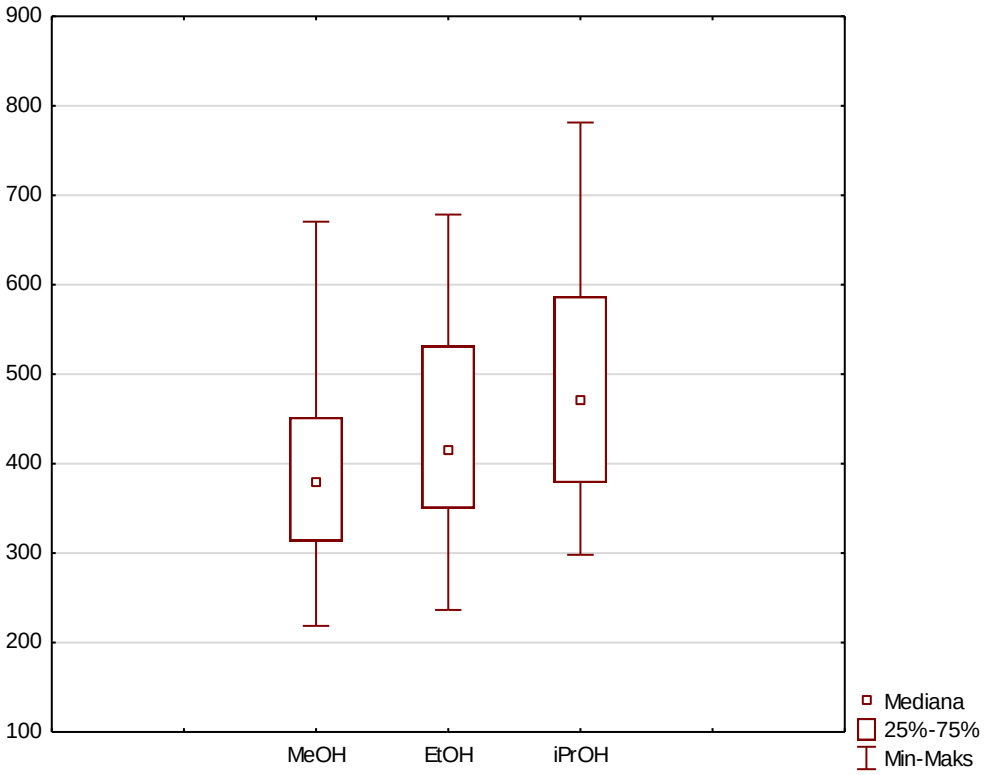

Figure S44. Box and whisker plot of data from a mean cumulative mass of IBU depending on the type vehicles used

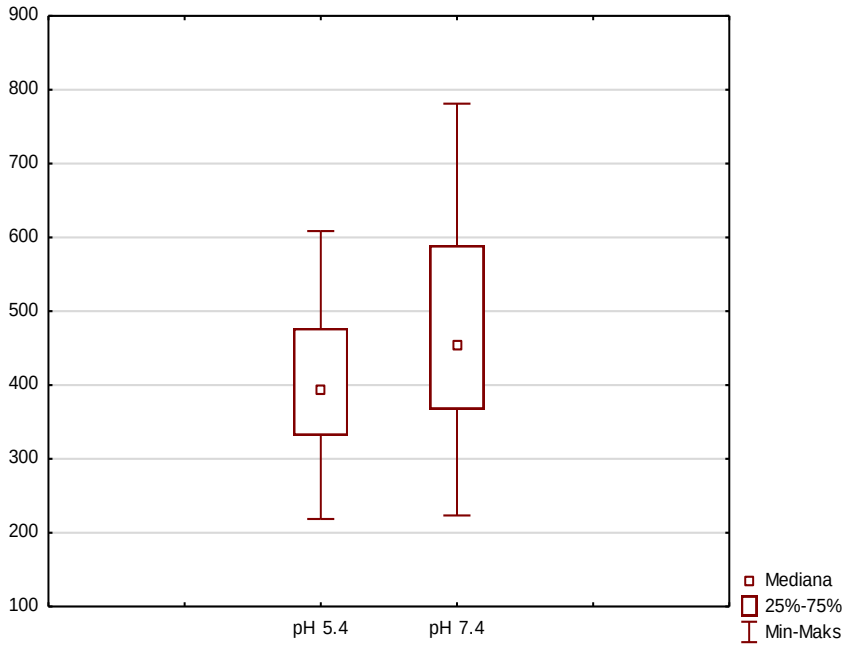

Figure S45. Box and whisker plot of data from a mean cumulative mass of IBU depending on the pH used

Table S6. Skin permeation expressed as % applied dose of IBU, after 24 h permeation of free acid and its salts with L-valine esters from methanolic, ethanolic and isopropanolic solution into acceptor phase at pH 7.4 and 5.4

Compound	Skin permeation, % applied dose of IBU					
	pH 7.4			pH 5.4		
	MeOH	EtOH	iPrOH	MeOH	EtOH	iPrOH
IBU	4.59	6.06[a]	7.60	4.38	4.81	6.72
[ValOMe][IBU]	7.41	8.23	9.50	6.45	7.70	8.69
[ValOEt][IBU]	6.84	7.33[a]	9.59	6.94	6.48	7.38
[ValOiPr][IBU]	10.51	12.09[a]	14.56	7.61	10.51	12.49
[ValOPr][IBU]	13.23	13.55[a]	14.59	12.13	11.10	10.89
[ValOBu][IBU]	9.57	10.66[a]	13.68	9.15	10.31	10.51
[ValOAm][IBU]	9.38	11.79[a]	11.53	7.92	8.06	8.94
[ValOHex][IBU]	8.61	9.81[a]	12.53	8.09	8.50	9.65
[ValOHept][IBU]	6.36	8.57	8.09	5.88	7.14	7.43
[ValOOct[IBU]	6.36	6.85	6.51	6.31	6.42	6.27

a – data reported in (Janus et al., 2020)

Table S7. Skin accumulation expressed as % applied dose of IBU, after 24 h skin permeation of ibuprofen free acid and its salts with L-valine esters from methanolic, ethanolic and isopropanolic solution into acceptor fluid at pH 7.4 and 5.4

Compound	Skin accumulation, % applied dose of IBU					
	pH 7.4			pH 5.4		
	MeOH	EtOH	iPrOH	MeOH	EtOH	iPrOH
IBU	2.62	3.05	3.05	2.27	2.27	3.10
[ValOMe][IBU]	3.17	3.00	3.00	2.97	2.97	3.24
[ValOEt][IBU]	3.61	3.45	3.45	3.62	3.62	4.74
[ValOiPr][IBU]	5.03	5.63	5.63	5.45	5.45	6.52
[ValOPr][IBU]	5.83	5.02	5.02	5.08	5.08	5.92
[ValOBu][IBU]	6.32	6.75	6.75	6.38	6.38	6.43
[ValOAm][IBU]	4.76	4.80	4.80	5.71	5.71	4.95
[ValOHex][IBU]	4.55	4.73	4.73	4.34	4.34	4.56
[ValOHept][IBU]	4.21	4.56	4.56	4.14	4.14	4.12
[ValOOct[IBU]	3.96	4.07	4.07	4.43	4.43	3.92

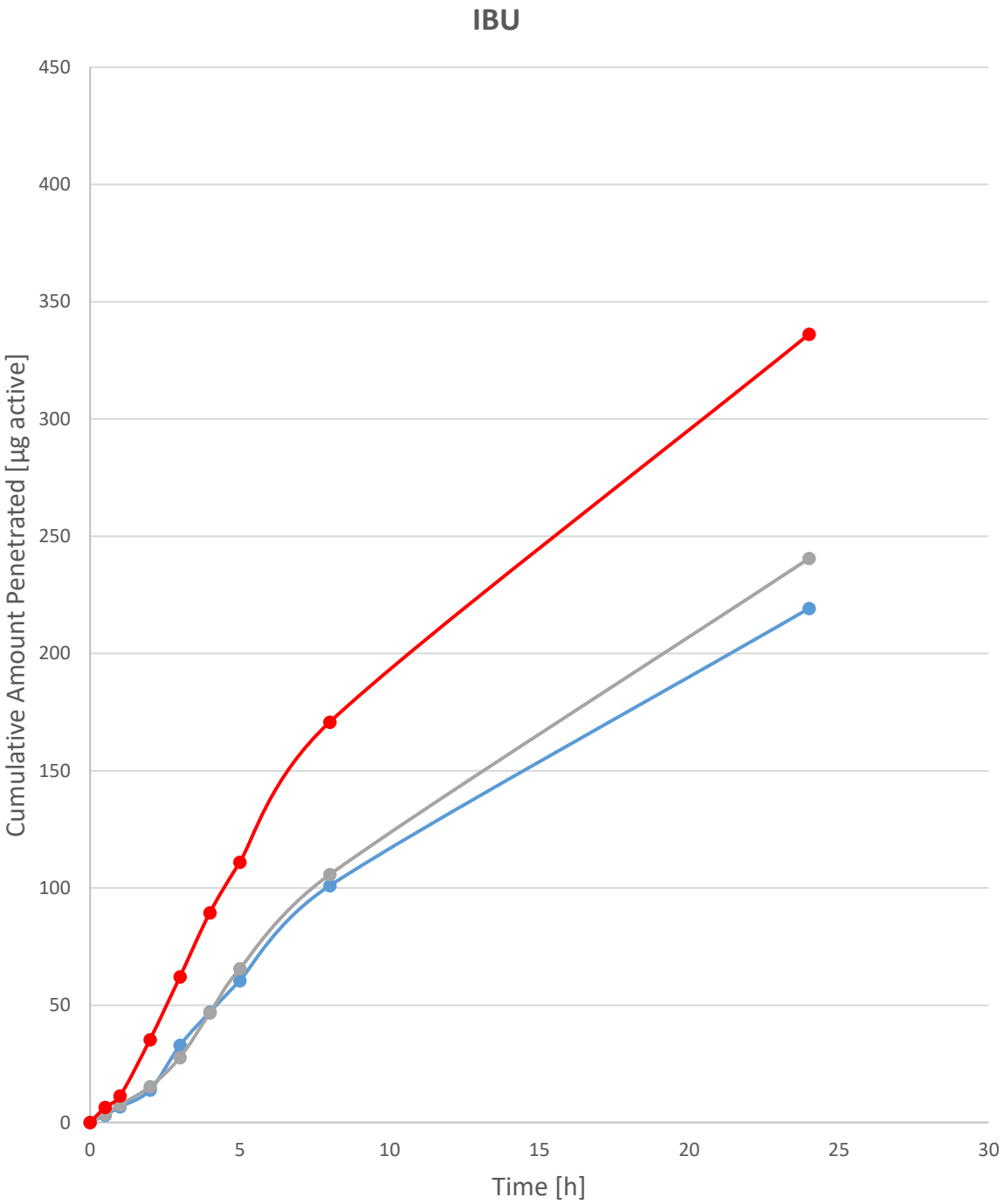

Figure S46. IBU diffusing through pig skin from alcoholic solutions (blue – methanolic; gray – ethanolic; red – isopropanolic) to acceptor phase with pH 5.4

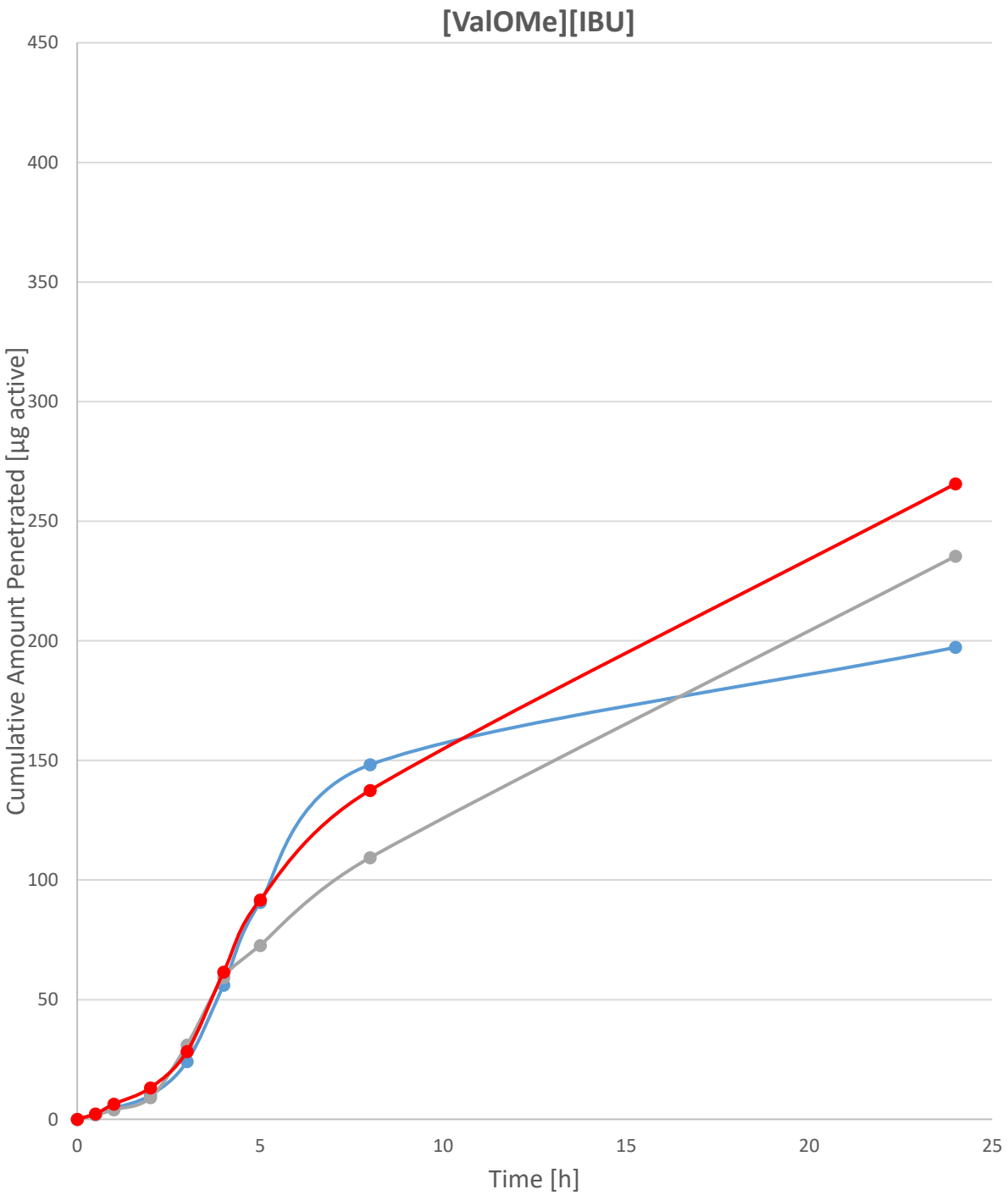

Figure S47. [ValOMe][IBU] diffusing through pig skin from alcoholic solution (blue – methanolic; gray – ethanolic; red – isopropanolic) to acceptor phase with pH 5.4

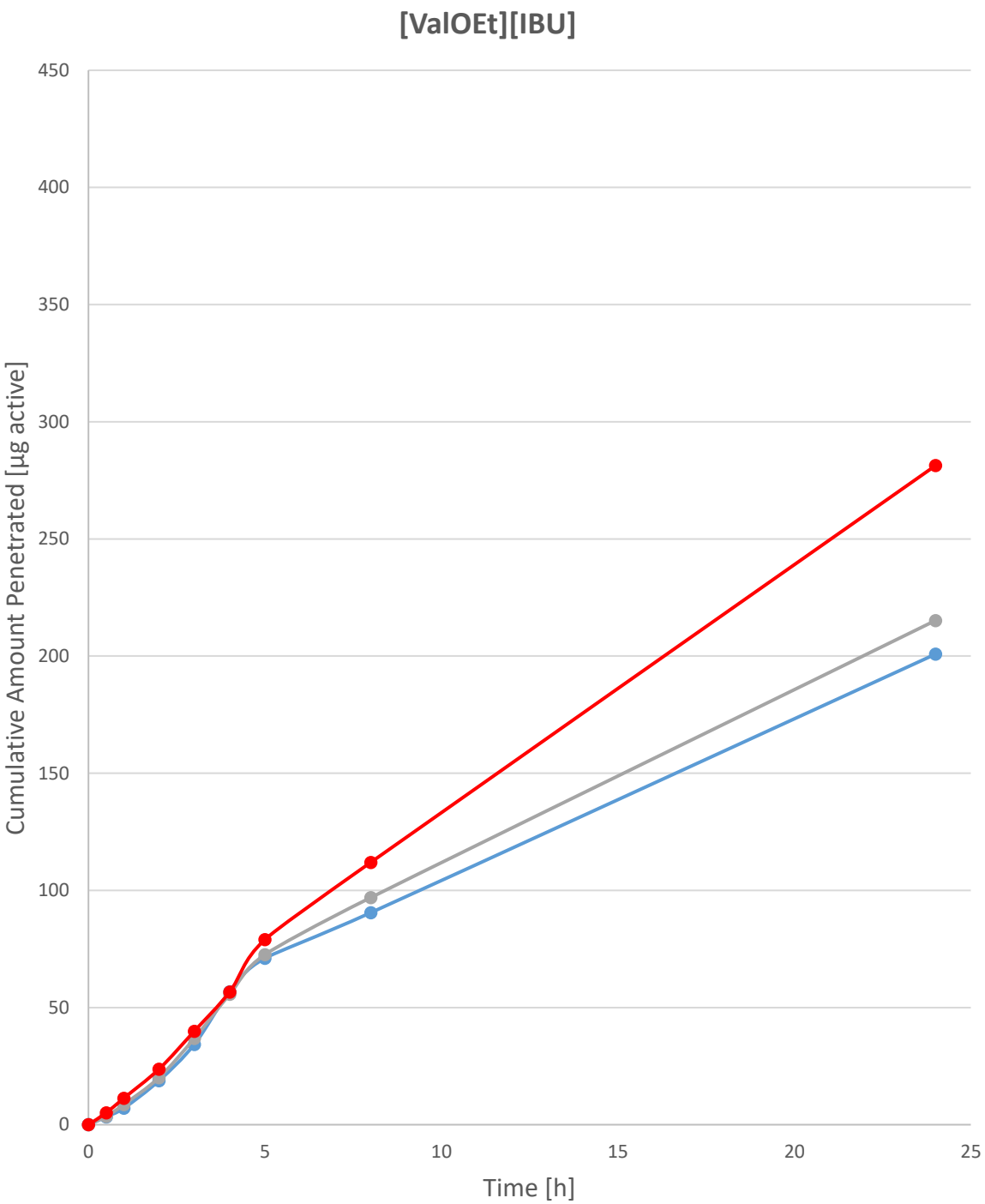

Figure S48. [ValOEt][IBU] diffusing through pig skin from alcoholic solution (blue – methanolic; gray – ethanolic; red – isopropanolic) to acceptor phase with pH 5.4

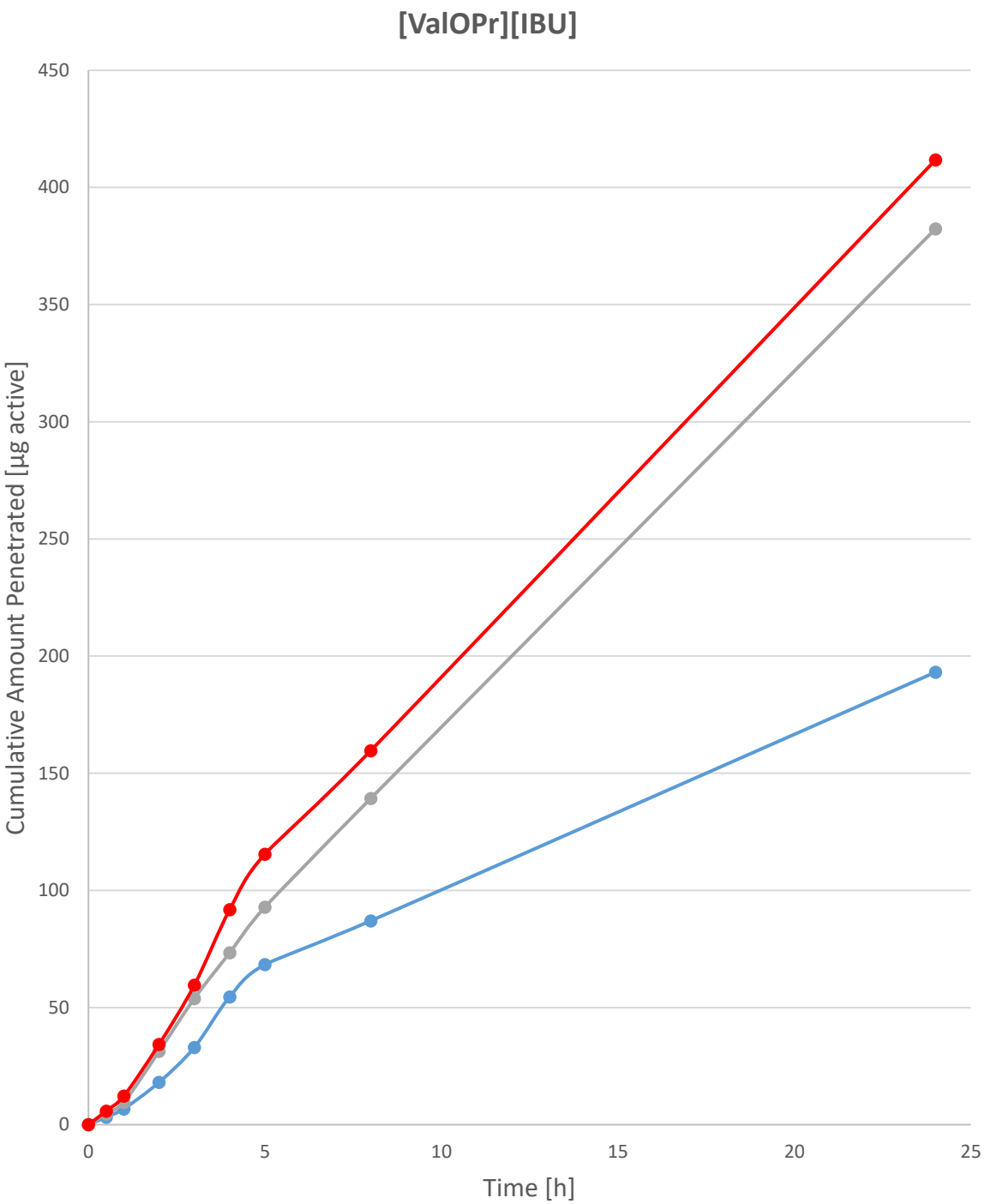

Figure S49. [ValOPr][IBU] diffusing through pig skin from alcoholic solution (blue – methanolic; gray – ethanolic; red – isopropanolic) to acceptor phase with pH 5.4

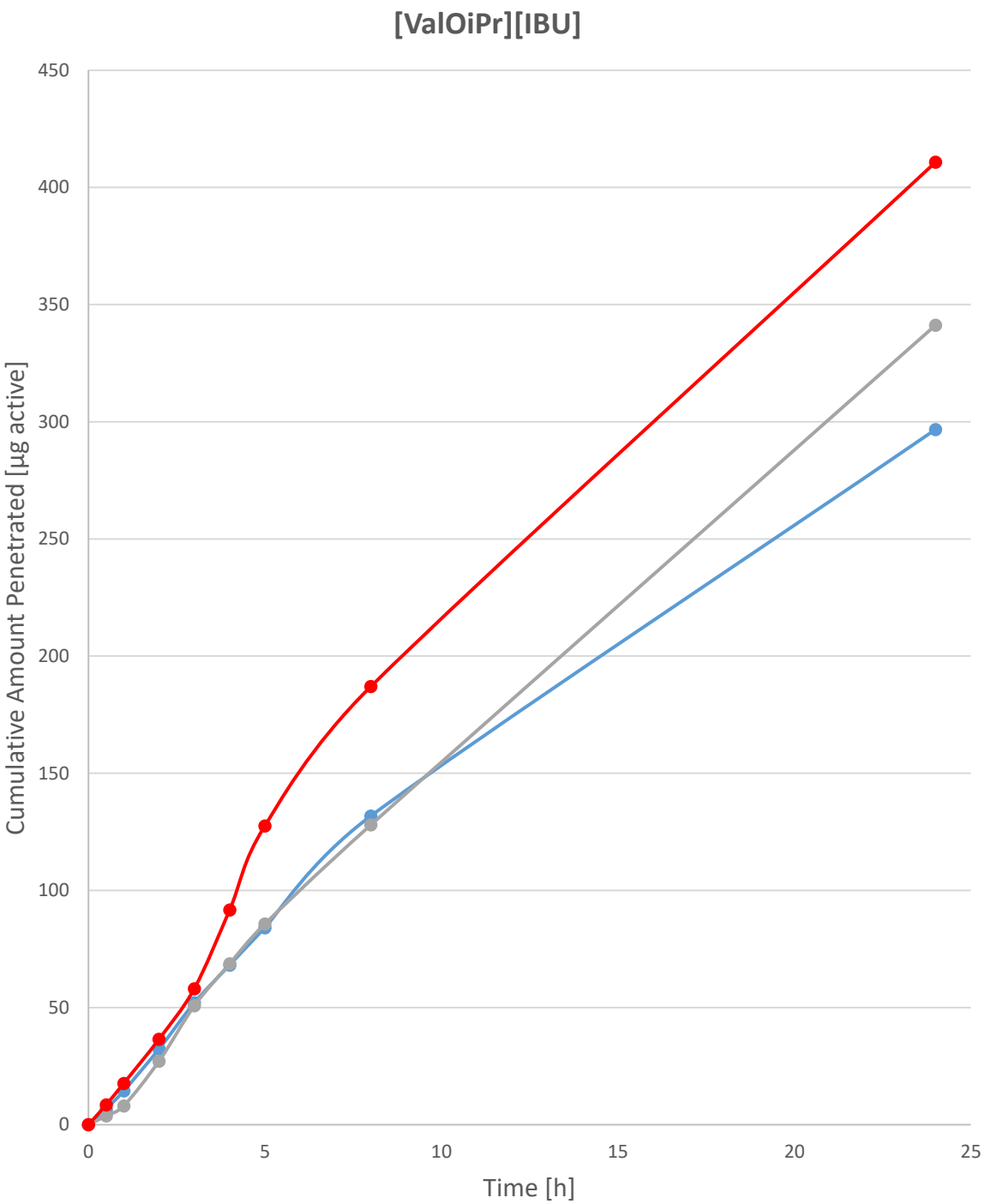

Figure S50. [ValOiPr][IBU] diffusing through pig skin from alcoholic solution (blue – methanolic; gray – ethanolic; red – isopropanolic) to acceptor phase with pH 5.4

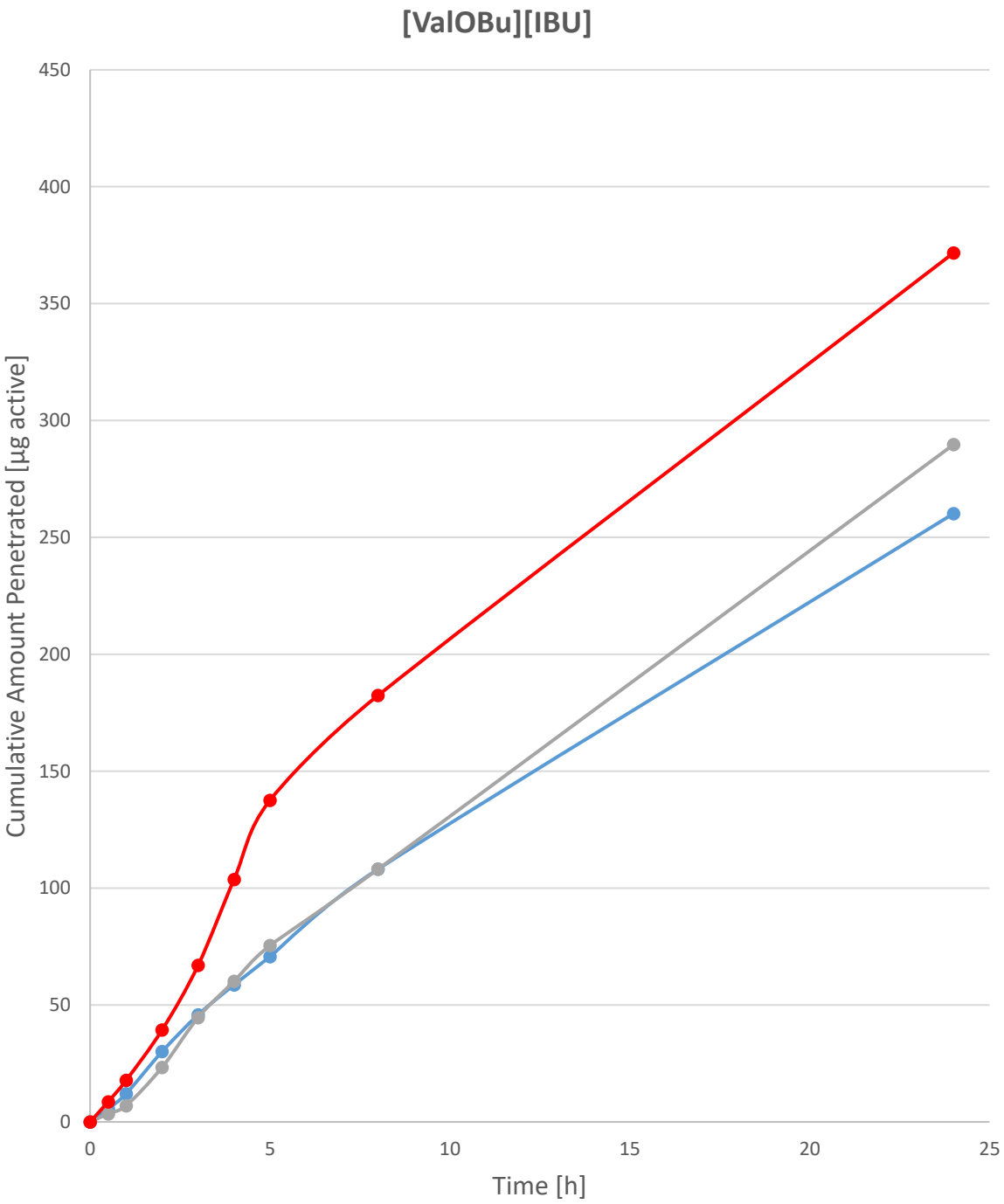

Figure S51. [ValOBu][IBU] diffusing through pig skin from alcoholic solution (blue – methanolic; gray – ethanolic; red – isopropanolic) to acceptor phase with pH 5.4

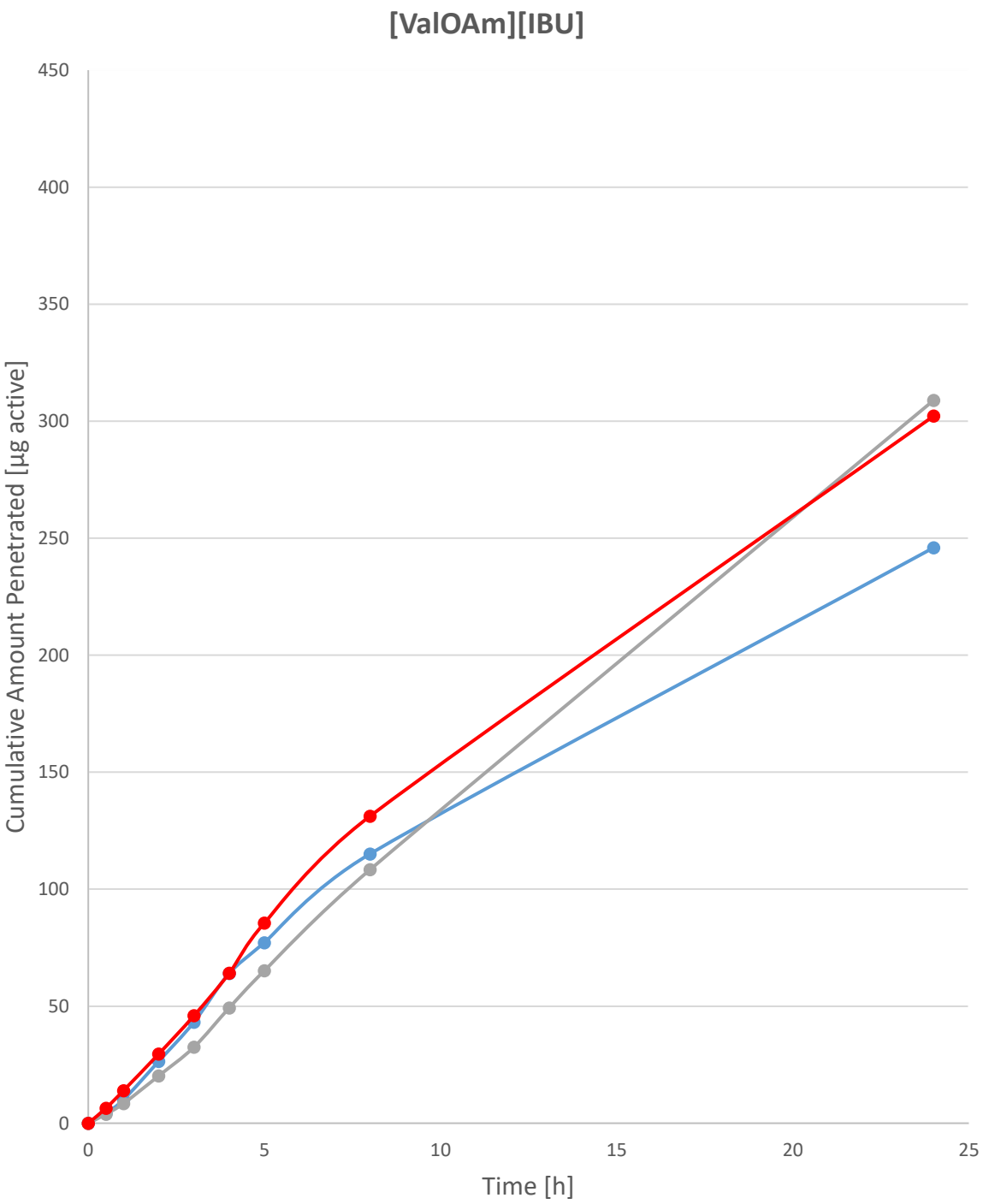

Figure S52. [ValOAm][IBU] diffusing through pig skin from alcoholic solution (blue – methanolic; gray – ethanolic; red – isopropanolic) to acceptor phase with pH 5.4

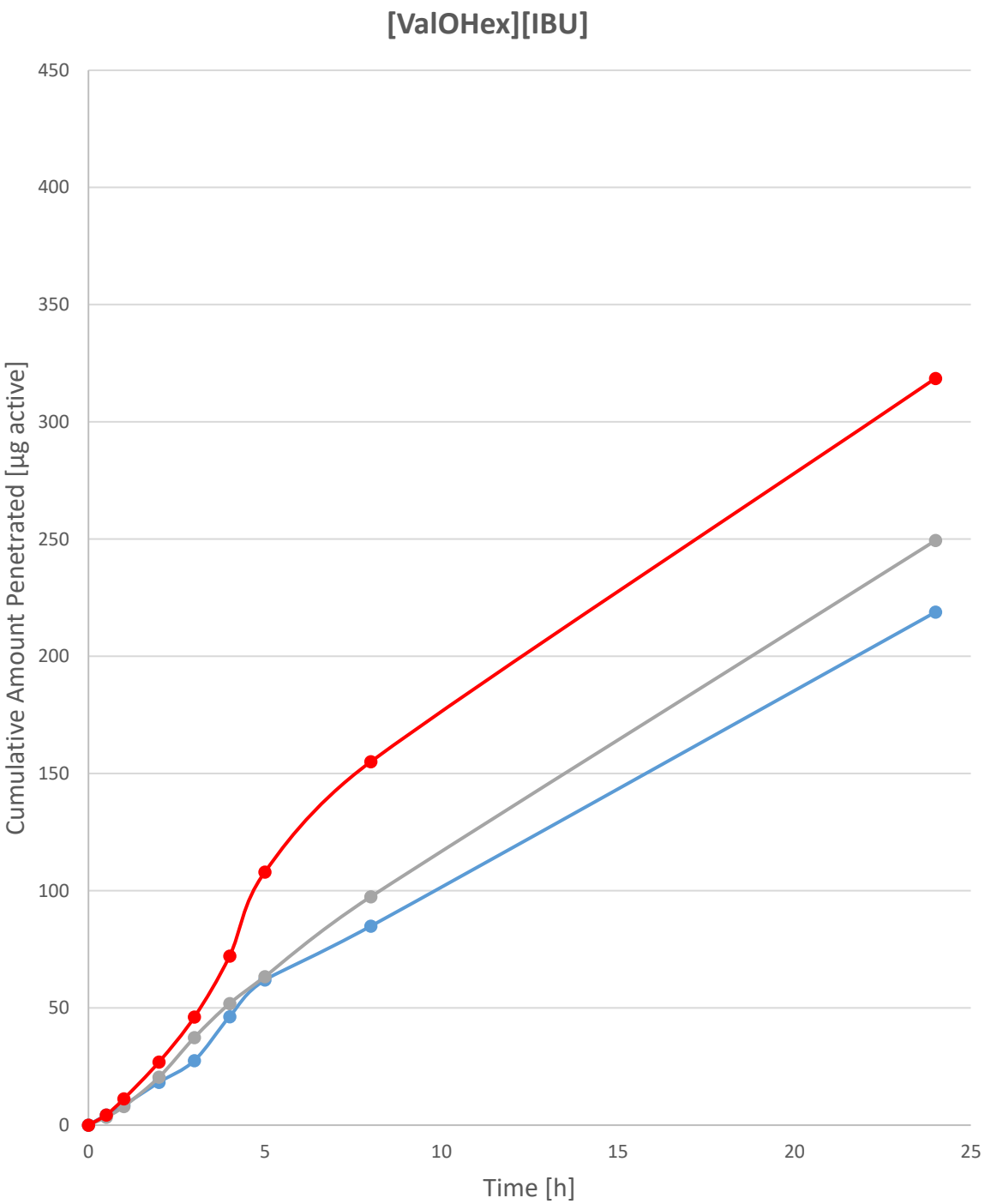

Figure S53. [ValOHex][IBU] diffusing through pig skin from alcoholic solution (blue – methanolic; gray – ethanolic; red – isopropanolic) to acceptor phase with pH 5.4

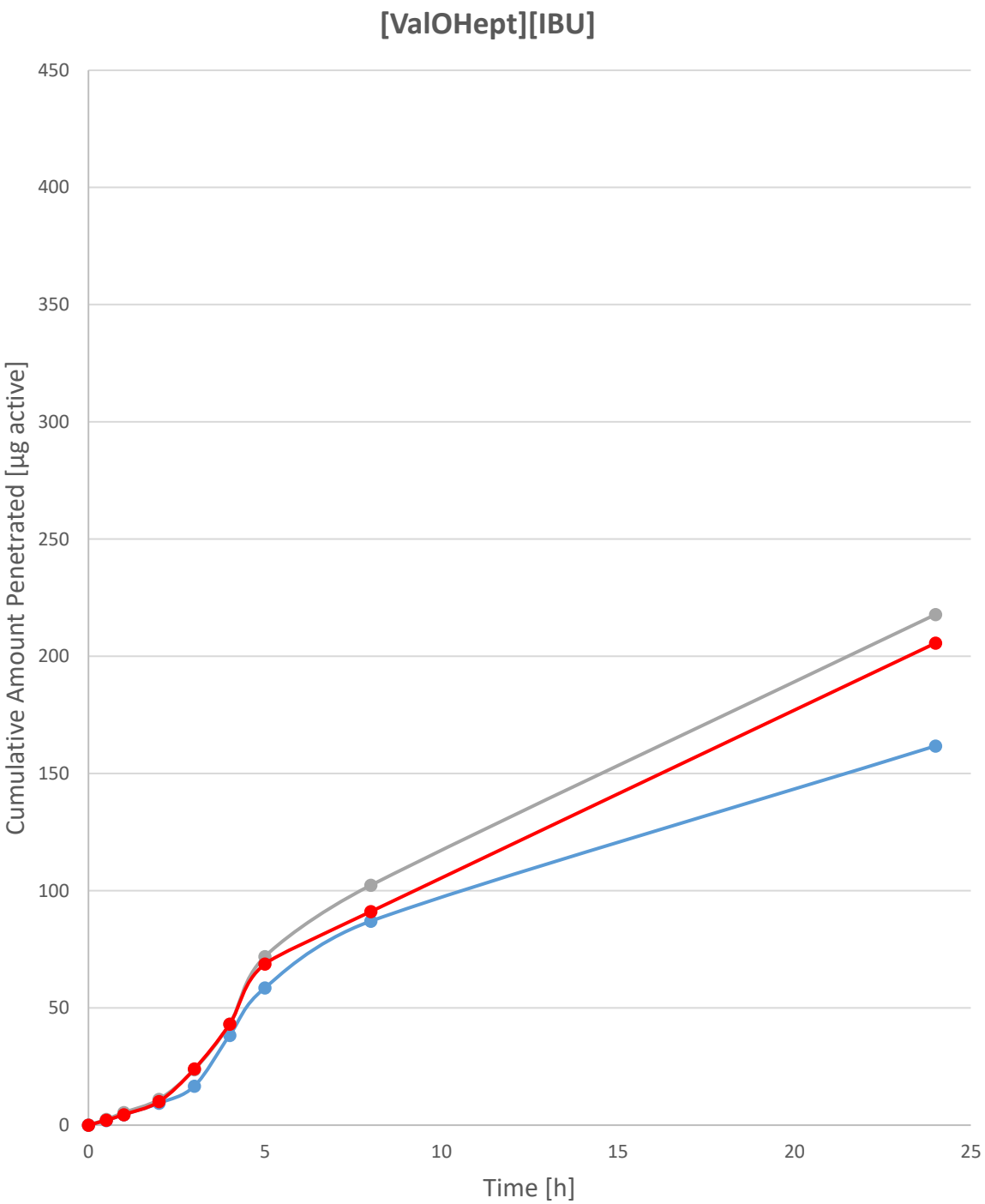

Figure S54. [ValOHept][IBU] diffusing through pig skin from alcoholic solution (blue – methanolic; gray – ethanolic; red – isopropanolic) to acceptor phase with pH 5.4

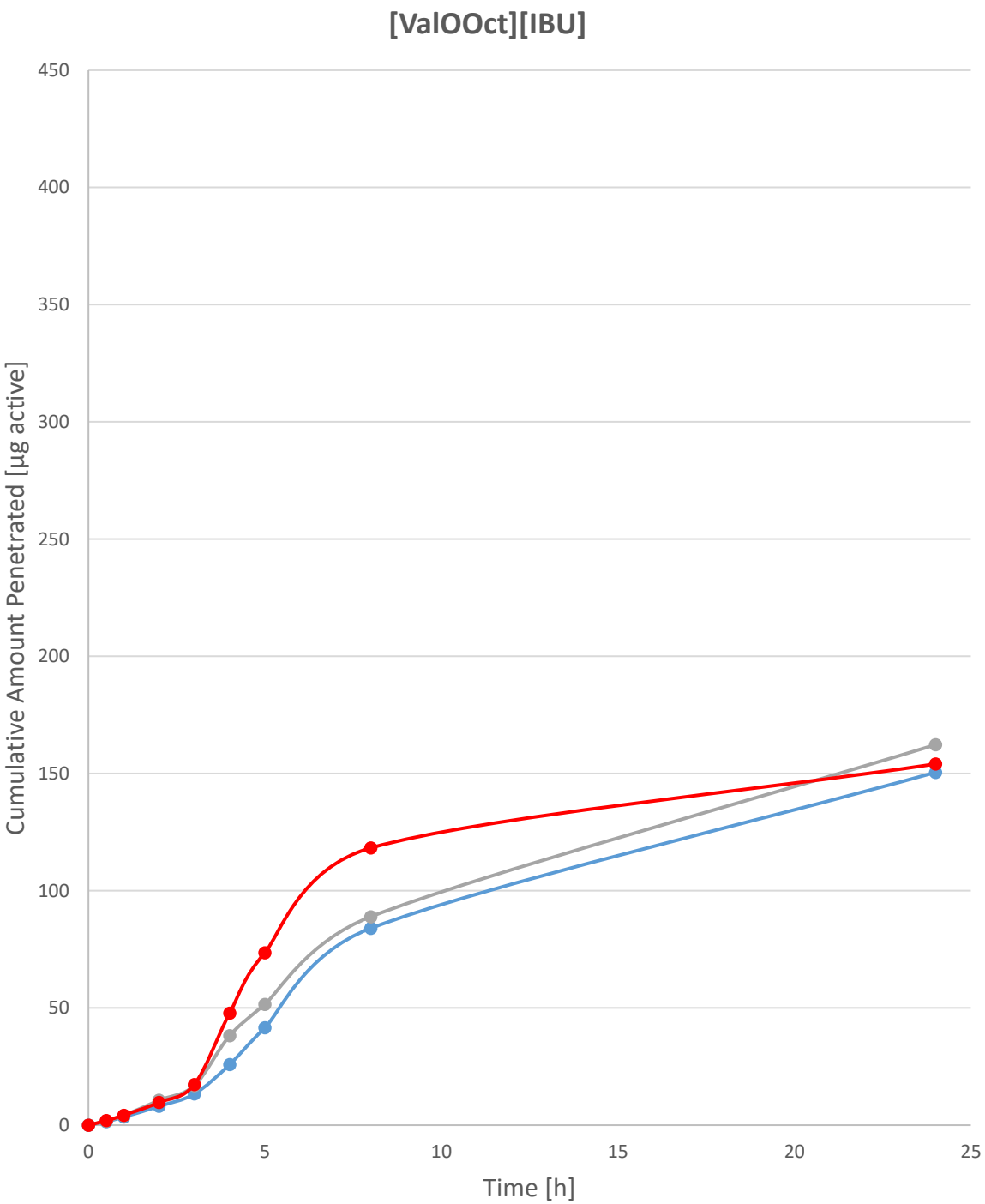

Figure S55. [ValOOct][IBU] diffusing through pig skin from alcoholic solution (blue – methanolic; gray – ethanolic; red – isopropanolic) to acceptor phase with pH 5.4

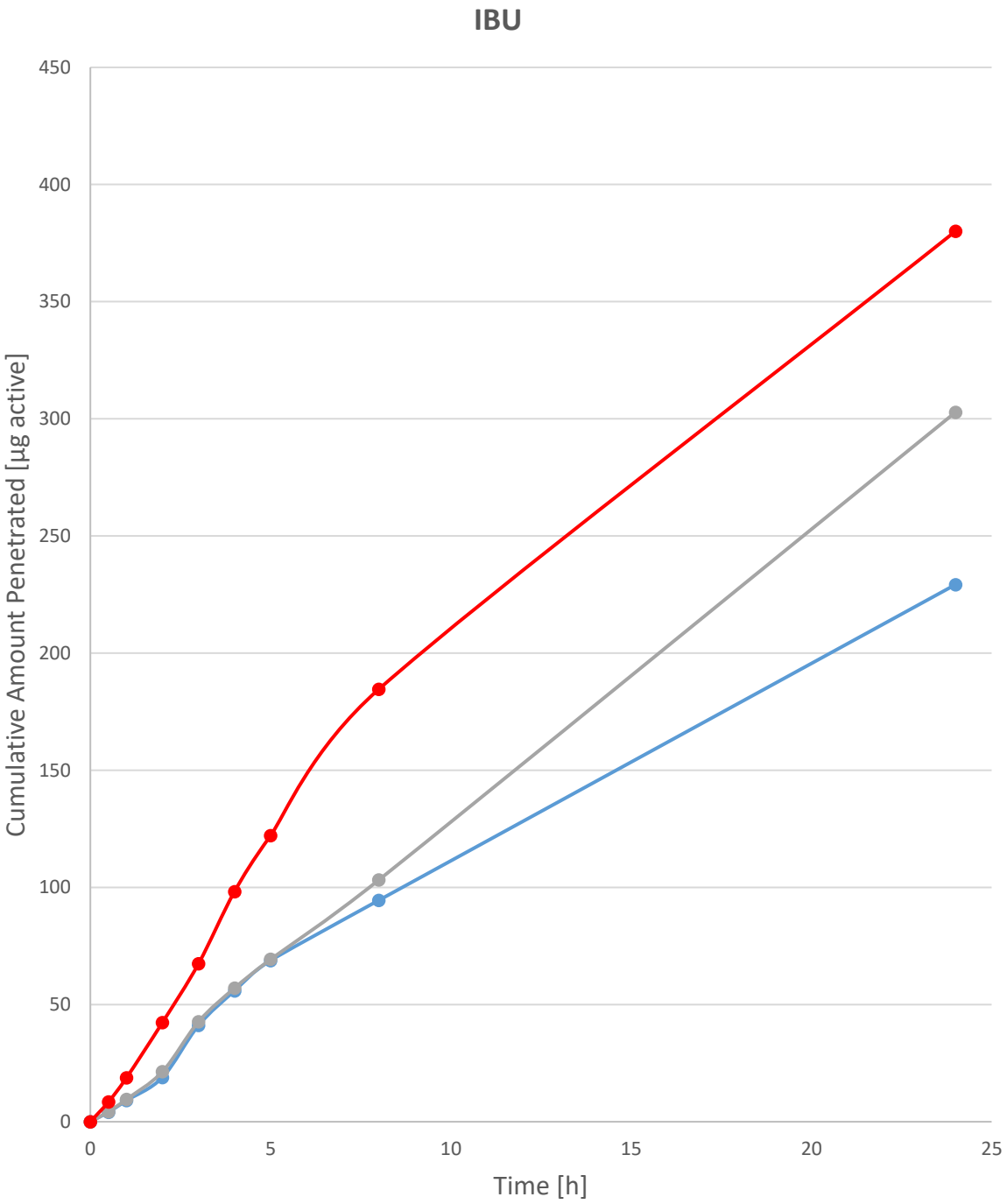

Figure S56. IBU diffusing through pig skin from alcoholic solution (blue – methanolic; gray – ethanolic; red – isopropanolic) to acceptor phase with pH 7.4

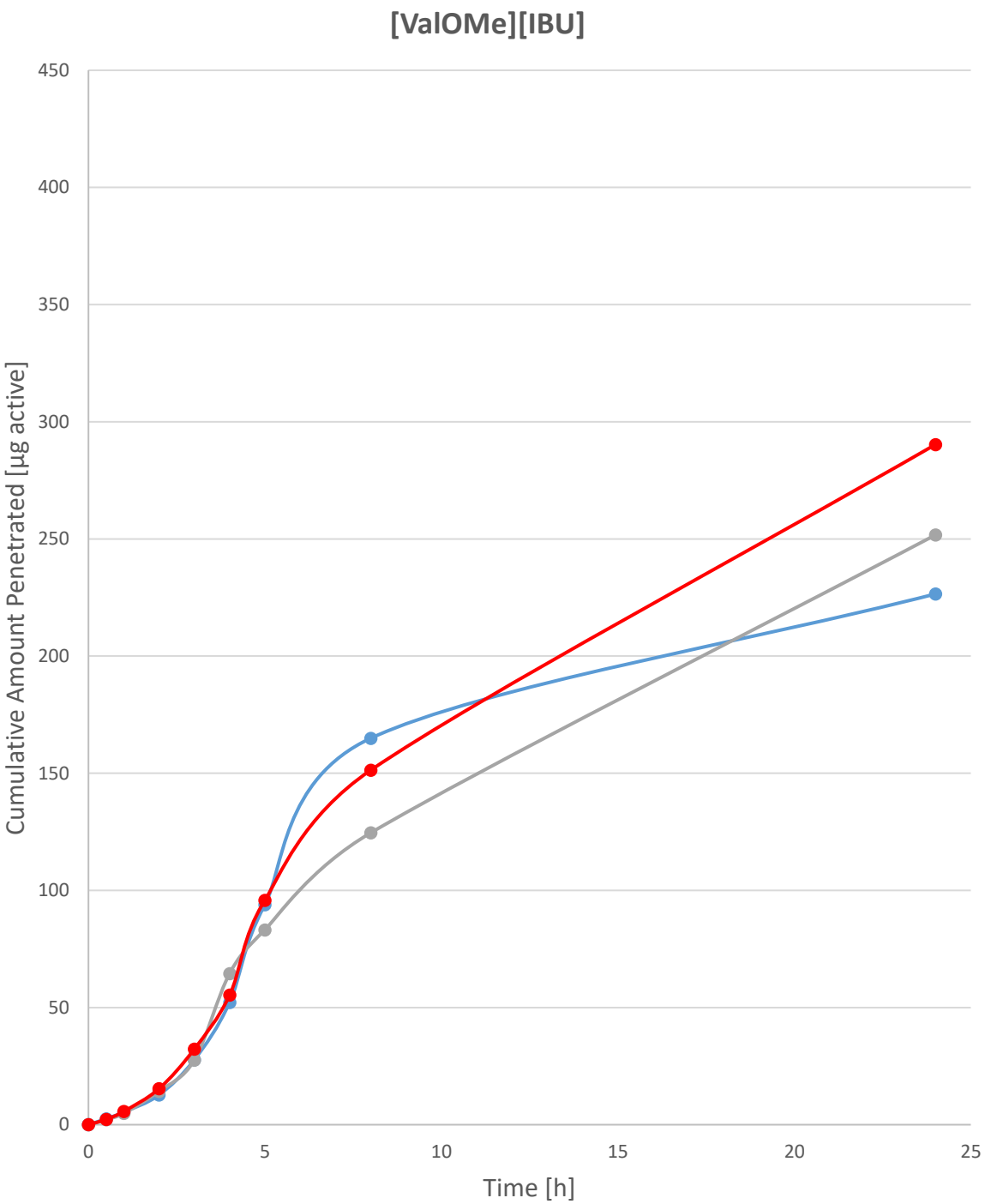

Figure S57. [ValOMe][IBU] diffusing through pig skin from alcoholic solution (blue – methanolic; gray – ethanolic; red – isopropanolic) to acceptor phase with pH 7.4

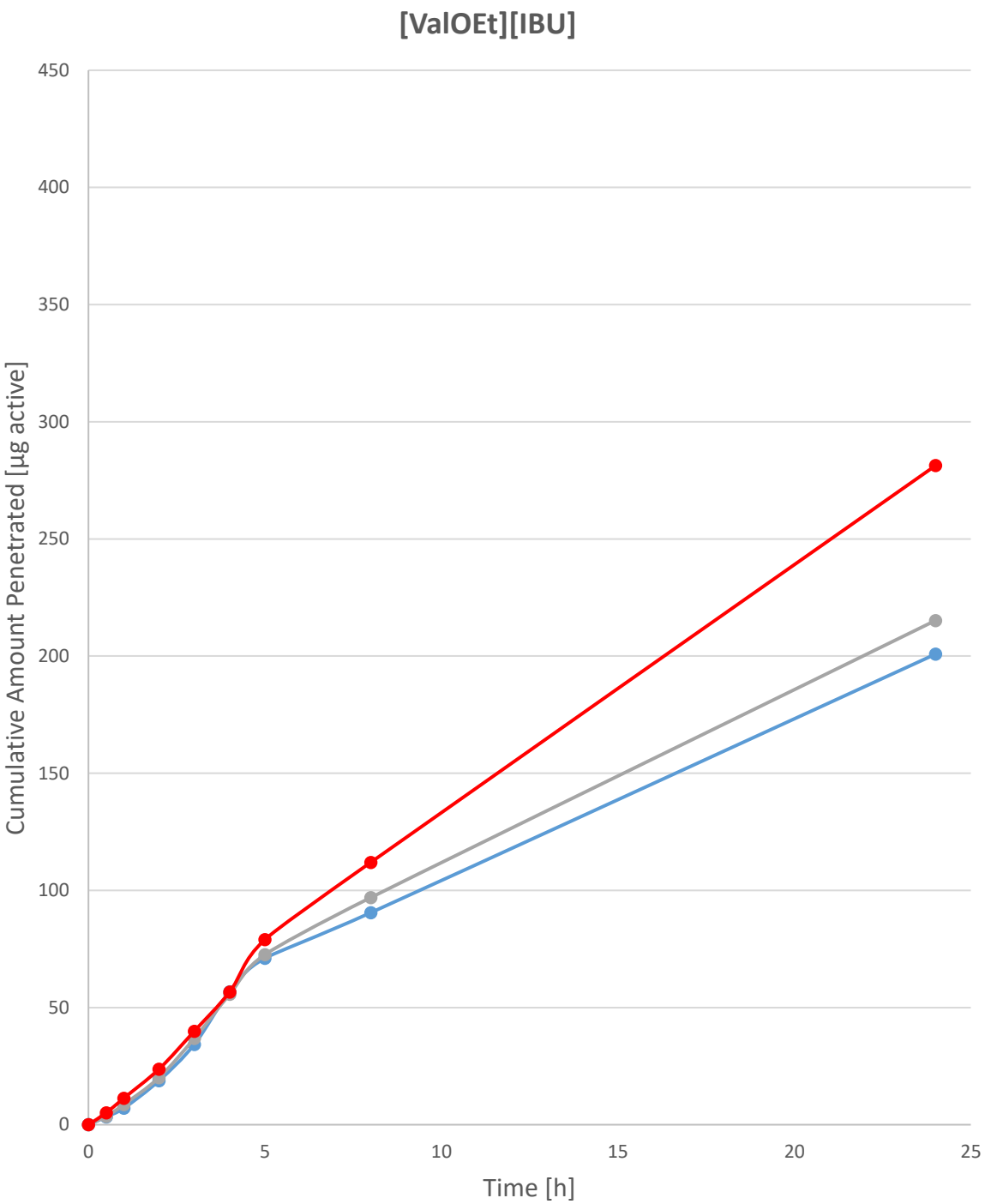

Figure S58. [ValOEt][IBU] diffusing through pig skin from alcoholic solution (blue – methanolic; gray – ethanolic; red – isopropanolic) to acceptor phase with pH 7.4

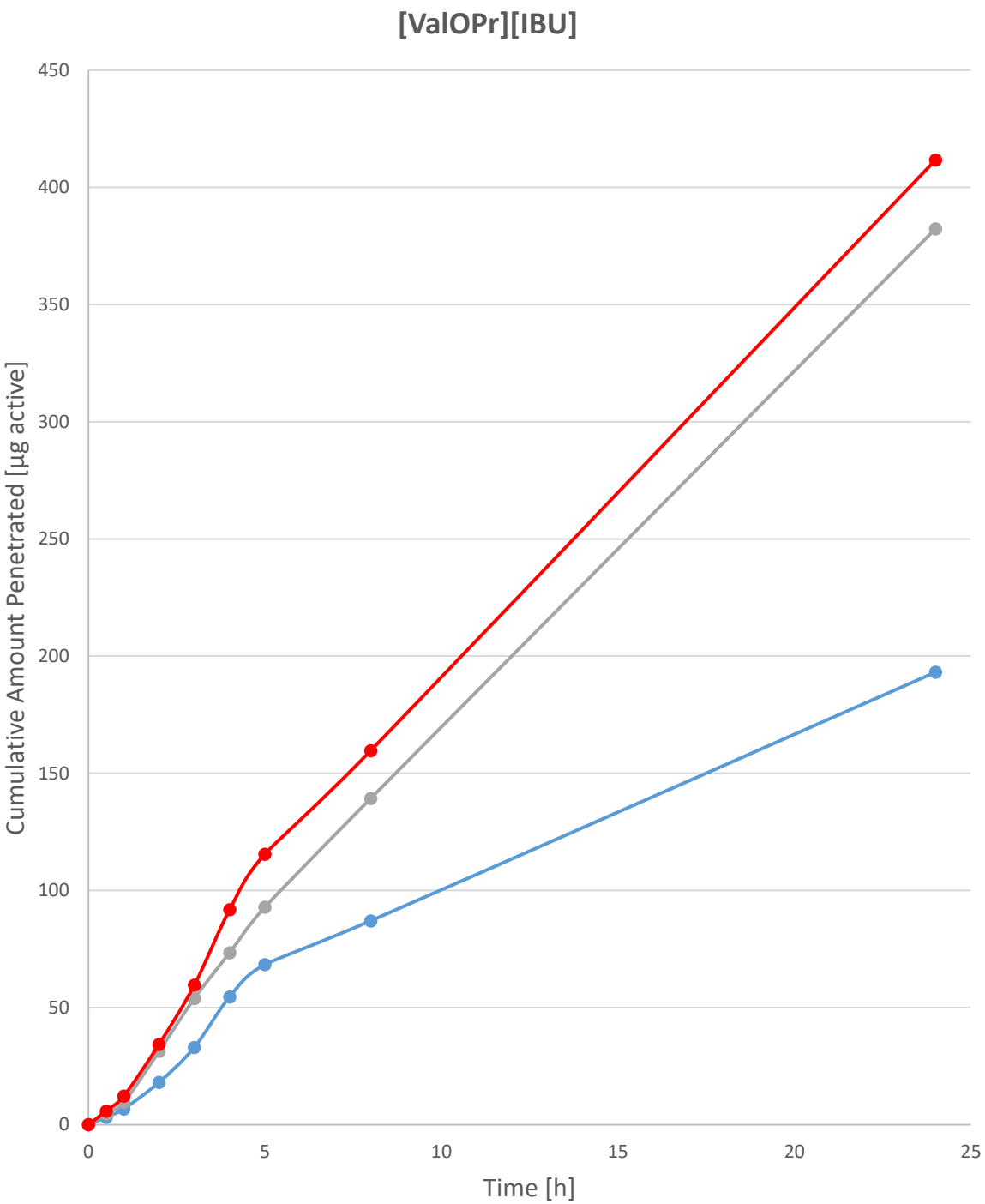

Figure S59. [ValOPr][IBU] diffusing through pig skin from alcoholic solution (blue – methanolic; gray – ethanolic; red – isopropanolic) to acceptor phase with pH 7.4

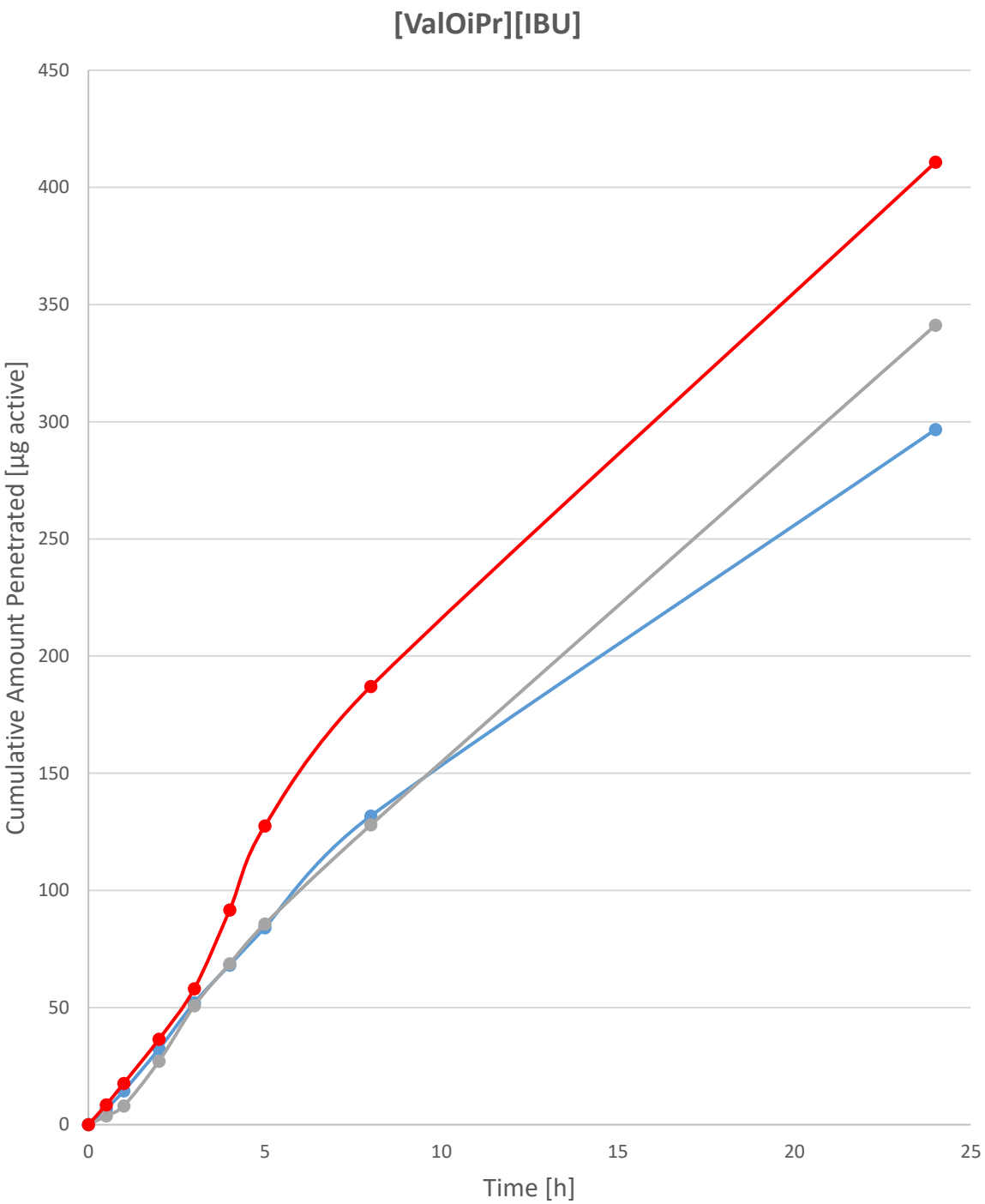

Figure S60. [ValOiPr][IBU] diffusing through pig skin from alcoholic solution (blue – methanolic; gray – ethanolic; red – isopropanolic) to acceptor phase with pH 7.4

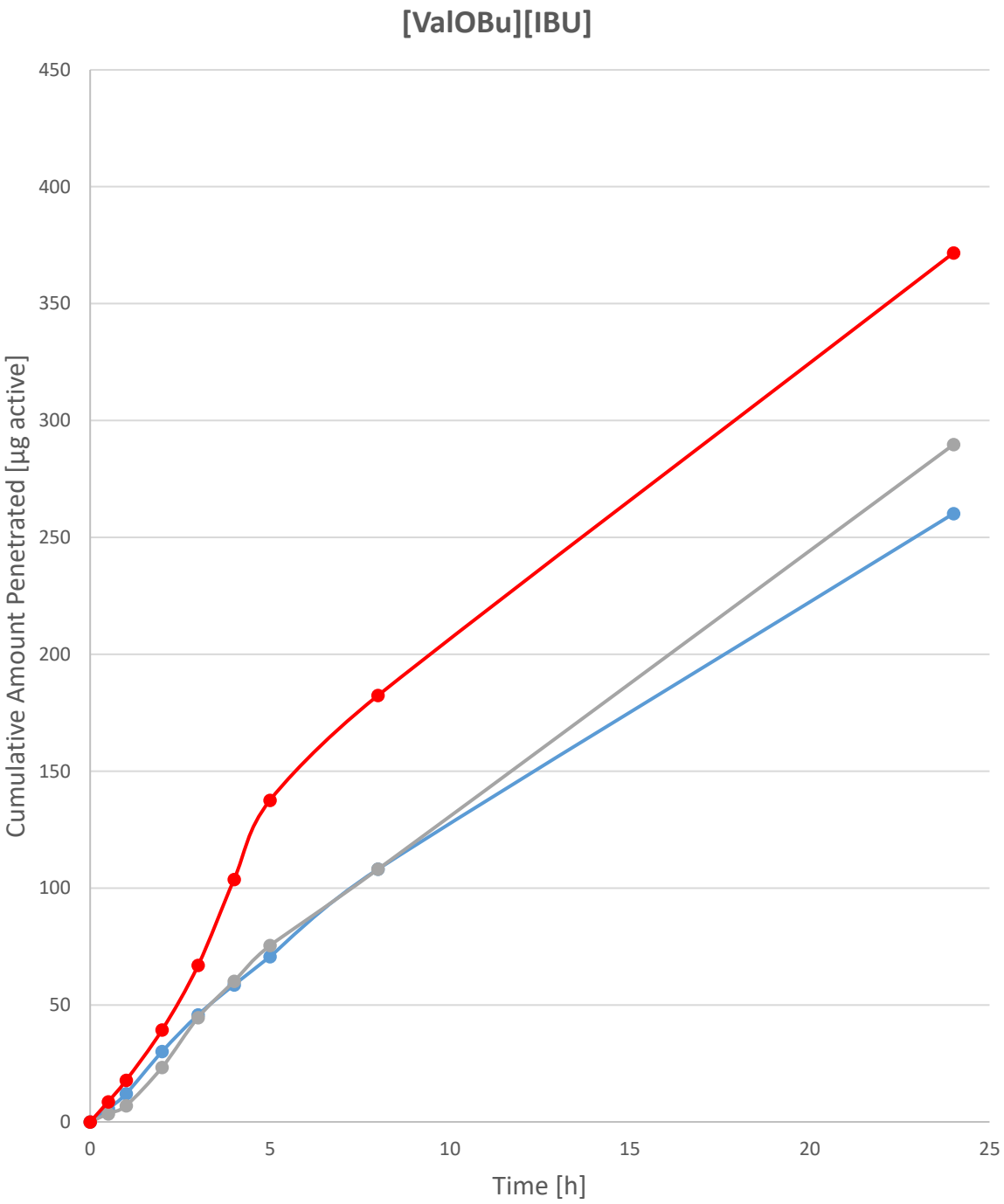

Figure S61. [ValOBu][IBU] diffusing through pig skin from alcoholic solution (blue – methanolic; gray – ethanolic; red – isopropanolic) to acceptor phase with pH 7.4

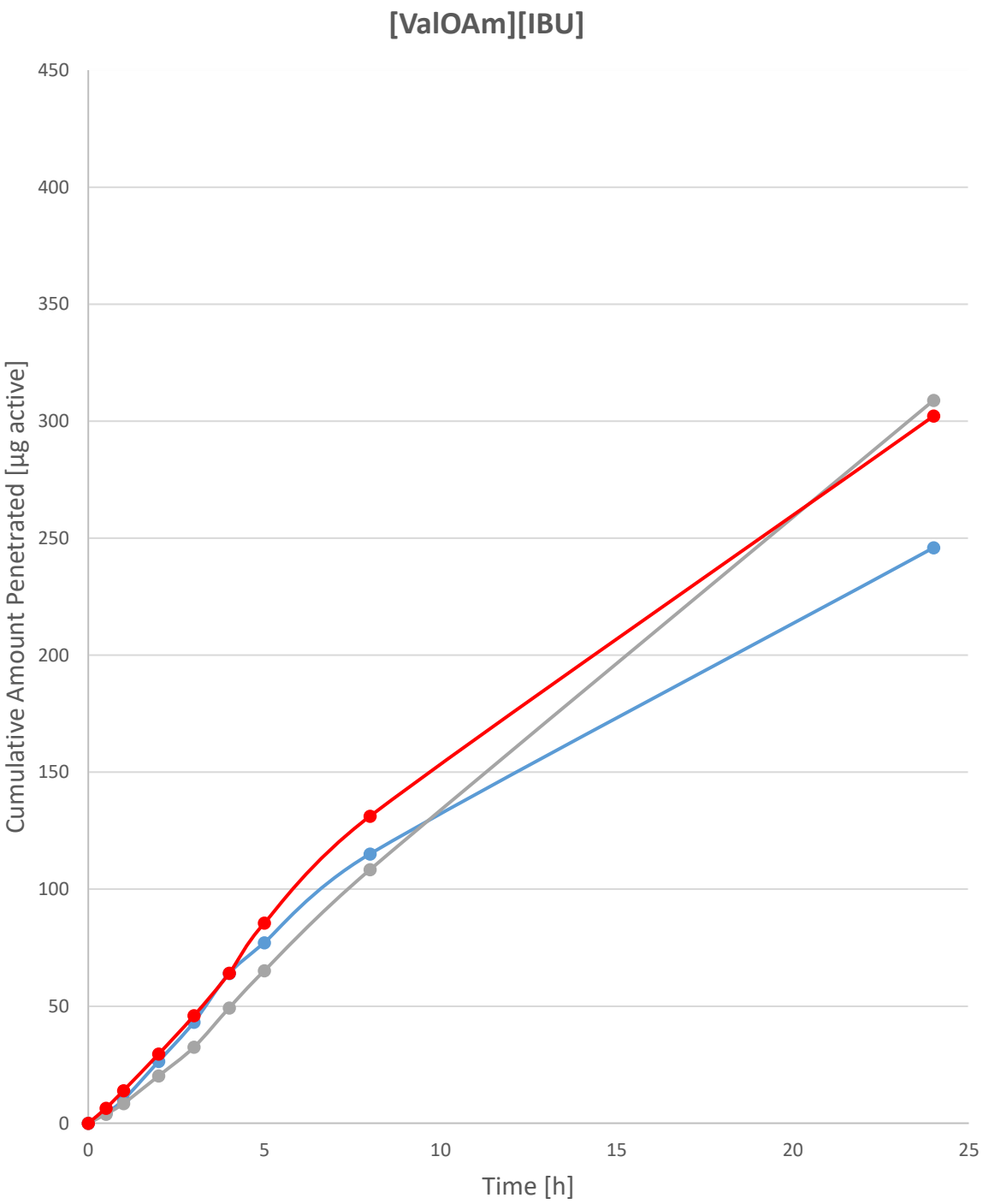

Figure S62. [ValOAm][IBU] diffusing through pig skin from alcoholic solution (blue – methanolic; gray – ethanolic; red – isopropanolic) to acceptor phase with pH 7.4

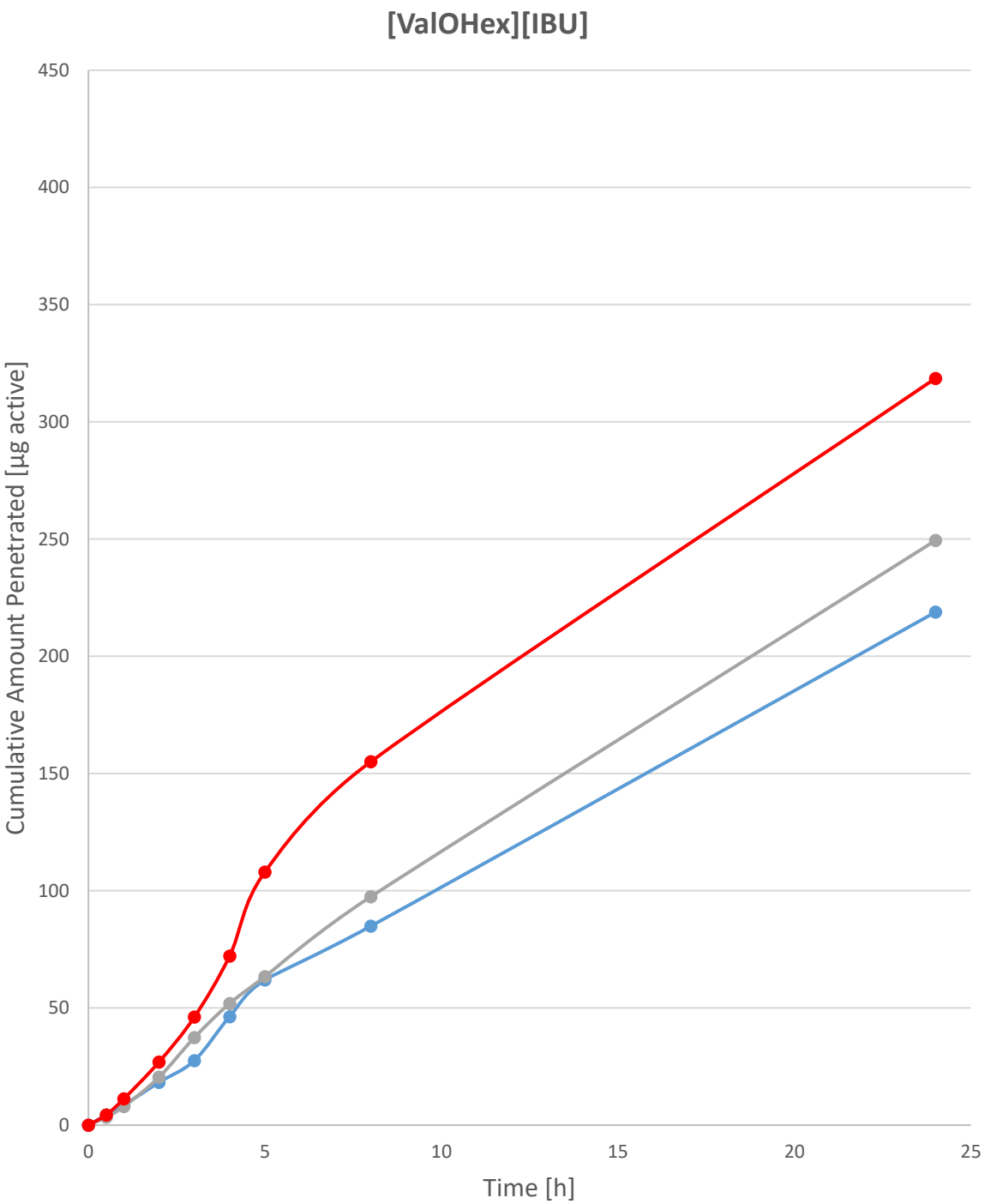

Figure S63. [ValOHex][IBU] diffusing through pig skin from alcoholic solution (blue – methanolic; gray – ethanolic; red – isopropanolic) to acceptor phase with pH 7.4

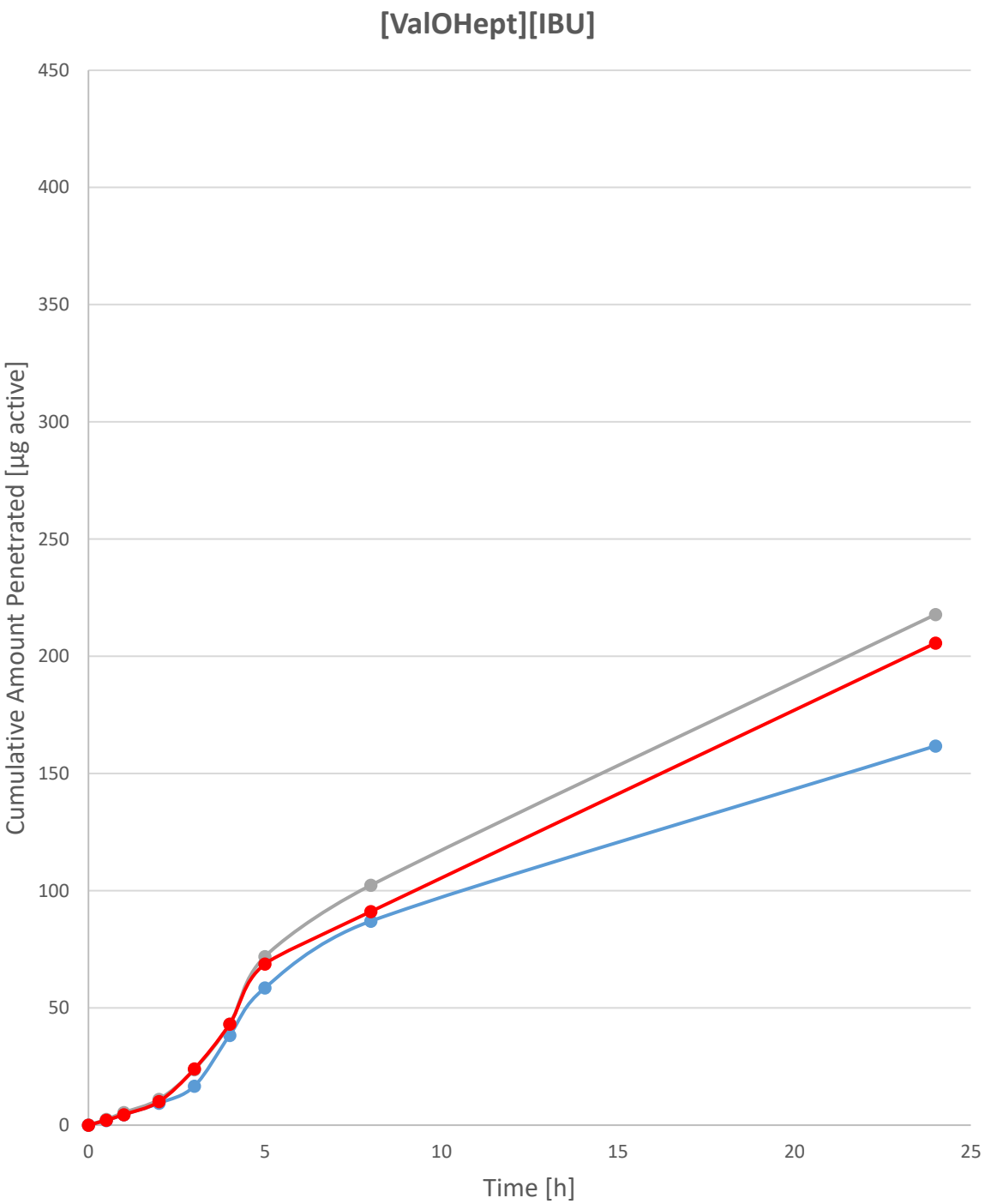

Figure S64. [ValOHept][IBU] diffusing through pig skin from alcoholic solution (blue – methanolic; gray – ethanolic; red – isopropanolic) to acceptor phase with pH 7.4

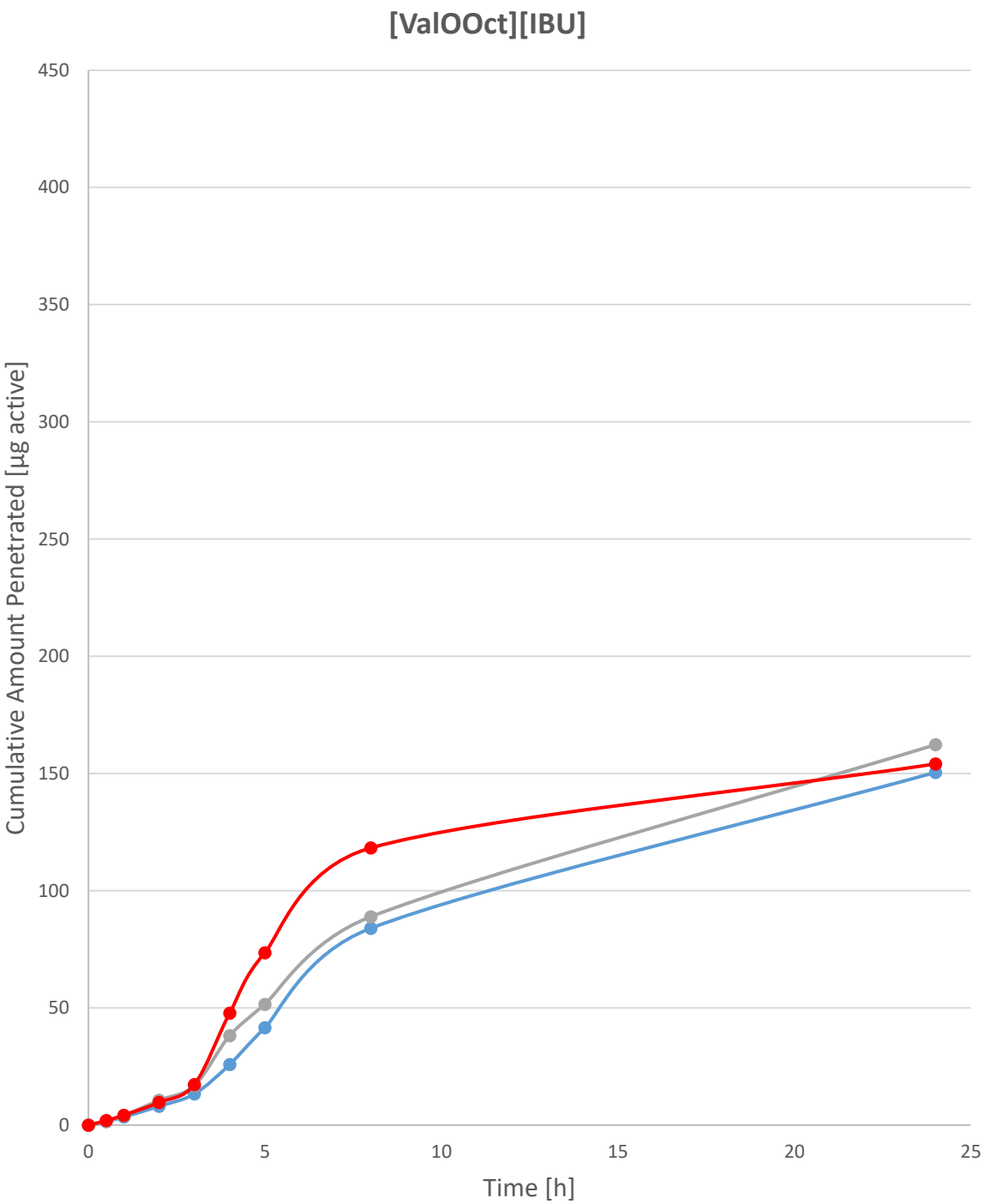

Figure S65. [ValOOct][IBU] diffusing through pig skin from alcoholic solution (blue – methanolic; gray – ethanolic; red – isopropanolic) to acceptor phase with pH 7.4

REFERENCES:

(S1) Janus, E.; Ossowicz, P.; Klebeko, J.; Nowak, A.; Duchnik, W.; Kucharski, Ł.; Klimowicz, A. Enhancement of Ibuprofen Solubility and Skin Permeation by Conjugation with L-Valine Alkyl Esters. *RSC Adv.* **2020**, *10* (13), 7570–7584. https://doi.org/10.1039/D0RA00100G.

(S2) Li, J.; Sha, Y. A Convenient Synthesis of Amino Acid Methyl Esters. *Molecules* **2008**, *13* (5), 1111–1119. https://doi.org/10.3390/molecules13051111.

(S3) *Vogel's Textbook of Quantitative Chemical Analysis*, 5. ed., rev.; Vogel, A. I., Jeffery, G. H., Eds.; Longman: Harlow, 1989.

(S4) Géniès, C.; Jamin, E. L.; Debrauwer, L.; Zalko, D.; Person, E. N.; Eilstein, J.; Grégoire, S.; Schepky, A.; Lange, D.; Ellison, C.; Roe, A.; Salhi, S.; Cubberley, R.; Hewitt, N. J.; Rothe, H.; Klaric, M.; Duplan, H.; Jacques-Jamin, C. Comparison of the Metabolism of 10 Chemicals in Human and Pig Skin Explants. *J Appl Toxicol* **2018**, jat.3730. https://doi.org/10.1002/jat.3730.

(S5) Čuříková, B. A.; Procházková, K.; Filková, B.; Diblíková, P.; Svoboda, J.; Kováčik, A.; Vávrová, K.; Zbytovská, J. Simplified Stratum Corneum Model Membranes for Studying the Effects of Permeation Enhancers. *International Journal of Pharmaceutics* **2017**, *534* (1–2), 287–296. https://doi.org/10.1016/j.ijpharm.2017.10.038.

(S6) Khiao In, M.; Richardson, K. C.; Loewa, A.; Hedtrich, S.; Kaessmeyer, S.; Plendl, J. Histological and Functional Comparisons of Four Anatomical Regions of Porcine Skin with Human Abdominal Skin. *Anat Histol Embryol* **2019**, *48* (3), 207–217. https://doi.org/10.1111/ahe.12425.

(S7) Jacobi, U.; Kaiser, M.; Toll, R.; Mangelsdorf, S.; Audring, H.; Otberg, N.; Sterry, W.; Lademann, J. Porcine Ear Skin: An in Vitro Model for Human Skin. *Skin Res Technol* **2007**, *13* (1), 19–24. https://doi.org/10.1111/j.1600-0846.2006.00179.x.

(S8) Badran, M. M.; Kuntsche, J.; Fahr, A. Skin Penetration Enhancement by a Microneedle Device (Dermaroller®) in Vitro: Dependency on Needle Size and Applied Formulation. *European Journal of Pharmaceutical Sciences* **2009**, *36* (4–5), 511–523. https://doi.org/10.1016/j.ejps.2008.12.008.

(S9) Davies, D. J.; Ward, R. J.; Heylings, J. R. Multi-Species Assessment of Electrical Resistance as a Skin Integrity Marker for in Vitro Percutaneous Absorption Studies. *Toxicology in Vitro* **2004**, *18* (3), 351–358. https://doi.org/10.1016/j.tiv.2003.10.004.

(S10) Haq, A.; Michniak-Kohn, B. Effects of Solvents and Penetration Enhancers on Transdermal Delivery of Thymoquinone: Permeability and Skin Deposition Study. *Drug Delivery* **2018**, *25* (1), 1943–1949. https://doi.org/10.1080/10717544.2018.1523256.

(S11) Kuntsche, J.; Bunjes, H.; Fahr, A.; Pappinen, S.; Rönkkö, S.; Suhonen, M.; Urtti, A. Interaction of Lipid Nanoparticles with Human Epidermis and an Organotypic Cell Culture Model. *International Journal of Pharmaceutics* **2008**, *354* (1–2), 180–195. https://doi.org/10.1016/j.ijpharm.2007.08.028.

(S12) Simon, A.; Amaro, M. I.; Healy, A. M.; Cabral, L. M.; de Sousa, V. P. Comparative Evaluation of Rivastigmine Permeation from a Transdermal System in the Franz Cell Using Synthetic Membranes and Pig Ear Skin with in Vivo-in Vitro Correlation. *International Journal of Pharmaceutics* **2016**, *512* (1), 234–241. https://doi.org/10.1016/j.ijpharm.2016.08.052.

(S13) Kopečná, M.; Macháček, M.; Prchalová, E.; Štěpánek, P.; Drašar, P.; Kotora, M.; Vávrová, K. Galactosyl Pentadecene Reversibly Enhances Transdermal and Topical Drug Delivery. *Pharm Res* **2017**, *34* (10), 2097–2108. https://doi.org/10.1007/s11095-017-2214-3.

(S14) Ahad, A.; Aqil, Mohd.; Ali, A. The Application of Anethole, Menthone, and Eugenol in Transdermal Penetration of Valsartan: Enhancement and Mechanistic Investigation. *Pharmaceutical Biology* **2016**, *54* (6), 1042–1051. https://doi.org/10.3109/13880209.2015.1100639.
(S15) Rozwadowski, Z. Deuterium Isotope Effects on 13C Chemical Shifts of Lithium Salts of Schiff Bases Amino Acids. *Journal of Molecular Structure* **2005**, *753* (1–3), 127–131. https://doi.org/10.1016/j.molstruc.2005.06.005.
(S16) Radeglia, R. Breitmaier, E., Und Voelter, W.: 13C-NMR Spectroscopy, Methods and Applications in Organic Chemistry. 2. Aufl., XIII, 344 S., 93 Abb., 114 Tab., Format. 17×24,3 Cm. Weinheim-New York: Verlag Chemie 1978. (Monographs in Modern Chemistry, Vol. 5). Leinen DM. *J. Prakt. Chem.* **1981**, *323* (6), 1016–1016. https://doi.org/10.1002/prac.19813230630.
(S17) Ossowicz, P.; Janus, E.; Schroeder, G.; Rozwadowski, Z. Spectroscopic Studies of Amino Acid Ionic Liquid-Supported Schiff Bases. *Molecules* **2013**, *18* (5), 4986–5004. https://doi.org/10.3390/molecules18054986.
(S18) Vairam, S.; Premkumar, T.; Govindarajan, S. Trimellitate Complexes of Divalent Transition Metals with Hydrazinium Cation: Thermal and Spectroscopic Studies. *J Therm Anal Calorim* **2010**, *100* (3), 955–960. https://doi.org/10.1007/s10973-009-0459-8.
(S19) *Vogel's Textbook of Practical Organic Chemistry*, New. ed., 5. ed., rev. [Nachdr.].; Furniss, B. S., Vogel, A. I., Eds.; Pearson/Prentice Hall: Harlow, 2009.
(S20) Reichardt, C.; Welton, T. *Solvents and Solvent Effects in Organic Chemistry*, 4th, updated and enl. ed ed.; Wiley-VCH: Weinheim, Germany, 2011.